
The synthesis of α -alkoxy and α -aminostannanes
as precursors to Novel Chromium Fischer Carbenes

A thesis submitted in fulfilment of the
requirements of the degree of

Master of Science

of

Rhodes University

by

Annalene Meyer

April 2011

Abstract

The present study involves the use of main group organometallics: organostannanes and organolithiums as precursors to chromium Fischer carbene complexes. Fischer carbenes are well stabilized by the π -donor substituents such as alkoxy and amino groups and low oxidation state metals such as Group 6 (Chromium, Molybdenum or Tungsten). Carbenes are an important intermediate in the synthesis of a range of compounds through cyclopropanations, insertions, coupling and photochemical reactions.

Synthesis and successful characterisation of three α -alkoxystannanes was achieved *via* nucleophilic addition of tributylstannyl lithium to the respective aldehydes, followed by an immediate MOM protection of the resulting alcohol. Six α -aminostannanes were synthesised, consisting of N-BOC, *N*-acetyl and *N*-ethyl derivatives of pyrrolidine and piperidine, *via* α -lithiation and subsequent tin-lithium transmetalation in the presence of TMEDA. The ^{13}C NMR analysis highlighted an interesting phenomenon of tin-carbon coupling that revealed unique structural information of both types of stannanes. DFT analysis was completed on the series of stannanes; a predicted frequency analysis was obtained which complemented the experimental *Infra-red* data in elucidation of the compounds.

The α -alkoxy and α -aminostannanes provided stable precursors to the organolithiums required for the synthesis of the novel Fischer chromium carbenes. The organolithiums were obtained *via* tin-lithium exchange at low temperatures, followed by the addition of chromium hexacarbonyl to form the acylpentacarbonyl-chromate salt. Alkylation of this intermediate using a Meerwein salt, Me_3OBF_4 , gave rise to the novel Fischer chromium carbene complexes. Fischer chromium carbenes derived from the two isomeric butyl and isobutyl stannanes and the two *N*-ethyl α -aminostannanes were successfully synthesised. The difficulty encountered in the purification of the Fischer carbene complexes hindered the full characterisation, due to the presence of a by-product, tetrabutyltin.

Table of Contents

	Page
Abstract	ii
Table of Contents	iii
List of Figures	vi
List of Schemes	viii
List of Tables	x
List of Abbreviations	xi
Acknowledgements	xiii

Chapter One: General Introduction

1.1	The origins and history of organometallic compounds	2
1.2	The importance of organometallic compounds	3
1.3	Chemistry and characteristics of organometallic compounds	3
1.4	Applications of organometallic compounds	4
1.5	Aims of this thesis	5

Chapter Two: Synthesis of α -alkoxy and α -aminostannanes

2.1	Introduction	7
2.1.1	General use of organostannanes	7
	<i>a) History and scope of organotin compounds</i>	7
	<i>b) Chemistry of tin</i>	7
	<i>c) Catalytic coupling reactions</i>	8
	<i>d) Radical reactions</i>	10
	<i>e) Organostannanes involved in tin-lithium exchange</i>	11

2.1.2	Preparations of organostannanes	13
	<i>a) α-Alkoxytannanes</i>	14
	<i>b) α-Aminostannanes</i>	17
2.2	Results and Discussion	18
2.2.1	α -Alkoxytannanes	18
	<i>a) Synthesis</i>	18
	<i>b) Challenges of synthesis</i>	20
	<i>c) NMR characterisation</i>	23
	<i>d) Infra-red spectroscopy and molecular modelling</i>	29
2.2.2	α -Aminostannanes	32
	<i>a) Synthesis and characterisation</i>	32
	<i>b) Infra-red spectroscopy and molecular modelling</i>	41
2.3	Concluding remarks	43

Chapter Three: Novel Fischer Chromium Carbenes

3.1	Introduction	45
3.1.1	Discovery of carbenes	45
3.1.2	Synthesis of Fischer carbene complexes	48
3.1.3	Applications of Fischer carbenes	51
	<i>a) Cycloaddition reactions</i>	52
	<i>b) Photochemical reactions</i>	53
3.2	Results and Discussion	53
3.2.1	Synthesis of Carbene complexes	53
	<i>a) General synthesis of methyl carbene complex and NMR characterisation</i>	54
	<i>b) Synthesis of carbenes derived from α-alkoxytannanes</i>	56
	<i>c) Synthesis of carbenes derived from α-aminostannanes</i>	57

3.2.2	NMR characterisation of carbenes	64
3.2.3	Molecular modelling and Infra-red spectroscopy	67
3.3	Concluding remarks	71

Chapter Four: Experimental Details

4.1	General Experimental Procedures	73
4.2	Synthesis of stannanes	74
4.2.1	Synthesis of α -alkoxystannanes	74
4.2.2	Synthesis of α -aminostannanes	79
4.3	Synthesis of Fischer Carbenes	84

References		90
-------------------	--	-----------

List of Figures

		Page
Figure 1	Organometallic compounds: Zeise's salt (1), Ferrocene (2), diethylzinc (3) and butylmagnesium bromide (4)	2
Figure 2	Different bonding of cyclopentadienyl anion (7) to a metal (M)	4
Figure 3	The mixture of a trimer (8) and the pentamer (9) that are present Salvarsan	5
Figure 4	Stabilization effect of oxygen on organolithiums	12
Figure 5	Structures of the α -alkoxystannanes 37a-f	19
Figure 6	Expanded region (4.70 – 4.40 ppm) of 400 MHz ^1H NMR spectrum of α -alkoxystannane 37a (A) and 37c (B) showing the effect of solvents on the chemical shift	24
Figure 7	400 MHz ^1H NMR spectrum of α -alkoxystannane 37a in CDCl_3	25
Figure 8	400 MHz COSY spectrum of α -alkoxystannane 37a in CDCl_3	26
Figure 9	400 MHz DEPT135 spectrum of α -alkoxystannane 37a in CDCl_3	27
Figure 10	Expanded region (400 MHz, 70 – 80 ppm) DEPT135 spectrum of α -alkoxystannane 37a in CDCl_3 illustrating the Sn-C coupling at C-1	28
Figure 11	Calculated IR spectrum obtained from model of α -alkoxystannane 37	30
Figure 12	Far IR region (650 to 30 cm^{-1}) of tributyl(1-(methoxymethoxy)propyl)stannane 37a	31
Figure 13	400 MHz ^1H and 100 MHz ^{13}C spectra of <i>tert</i> -butyl pyrrolidine-1-carboxylate 42a in CDCl_3	33
Figure 14	400 MHz ^1H and 100 MHz ^{13}C spectra of α -aminostannane 43a in C_6D_6	35
Figure 15	Conformational equilibrium of α -aminostannane 43a	35
Figure 16	Stacked 100 MHz ^{13}C spectra of α -aminostannanes 43a , 44a and 45a in CDCl_3	38
Figure 17	Conformations of <i>N</i> -methyl piperidine stannane (46) ⁴⁹	39
Figure 18	A region (F1 = δ 1.4 – 3.0 ppm; F2 = δ 20 – 60 ppm) of the HSQC spectrum (400 MHz, CDCl_3) of 45b . The accompanying scheme shows the ring flip between the two chair conformations	41
Figure 19	Calculated IR spectrum (3500 – 0 cm^{-1}) obtained from the molecular model model of <i>N</i> -BOC piperidine stannane 43b	42
Figure 20	Far IR region (700 – 30 cm^{-1}) of <i>N</i> -BOC piperidine stannane 43b	43

Figure 21	Schematic representations of a) σ -donor and π -back bonding in Fischer carbenes and b) covalent bonding in Schrock carbenes	46
Figure 22	Grubb's catalyst (50) and Schrock's catalyst (51) used for alkene metathesis	47
Figure 23	A simplified energy diagram highlighting promotion of electrons that lead to the MLCT and LF bands in the UV-vis spectrum	50
Figure 24	The reactivity pattern of Fischer carbene complexes (B = base, E = electrophile, L = ligand, and Nu = nucleophile)	51
Figure 25	^1H NMR (400 MHz, CDCl_3) and ^{13}C NMR (100 MHz, CDCl_3) spectra of methyl carbene 66	56
Figure 26	^{13}C NMR (100 MHz, C_6DCl_6) spectra of carbene 68b before and after sublimation	62
Figure 27	^{13}C NMR region (100 MHz, C_6DCl_6 250-150 ppm) of isobutyl carbene 68c illustrating the inverted $\text{C}=\text{O}_{\text{trans}}$ signal	64
Figure 28	^{13}C NMR region (100 MHz, C_6DCl_6 380-150 ppm) of isobutyl carbene 68c showing the presence of oxidation products ($\text{C}=\text{O}_{\text{ester}}$) and the decrease in the carbene signal ($\text{Cr}=\text{C}$)	65
Figure 29	A geometry optimised model of (A) butyl carbene 68b and (B) <i>N</i> -ethyl piperidine carbene 70b	68
Figure 30	(A) Mid and (B) Far IR region ($4000\text{-}30\text{ cm}^{-1}$) of <i>N</i> -ethyl piperidine carbene complex 70b	69
Figure 31	Calculated IR spectra for the <i>N</i> -ethyl carbene (70b) and the stannane precursor (45b)	70

List of Schemes

		Page
Scheme 1	An addition reaction of diethyl zinc (3) with catalyst (2 <i>S</i>)-DAIB and benzaldehyde (5) to form the (<i>S</i>)-enantiomer of phenyl-1-propanol (6)	2
Scheme 2	Stille coupling reaction used for a crucial step in synthesis of natural product arcyriacyanin A	8
Scheme 3	Simplified reaction mechanism of palladium catalyzed coupling of stannanes with organic electrophiles (adapted from Espinet <i>et al.</i> ²⁹)	9
Scheme 4	A photocatalytic reaction of 13 carried out with tetrabutyltin as a radical initiator	10
Scheme 5	Cyclization of <i>cis</i> - and <i>trans</i> -stannylpyrrolidines (17 and 18) to afford <i>exo</i> -2-methyl-7-azabicyclo[2.1.1]heptane 19	13
Scheme 6	Preparation of organostannanes (i) S _N 2 at tin (ii) S _N 2 at carbon	14
Scheme 7	New carbon-carbon bond formation <i>via</i> a hydroxyl-substituted carbocation 22 (route i) or <i>via</i> a carbonyl carbanion 23 (route ii)	15
Scheme 8	Conversion of 4-(tributylstannyl)-1,3-dioxane (25) to an alkoxyorganocopper reagent (26) which undergoes conjugate addition with ethyl propiolate to form (27)	16
Scheme 9	Formation of enantiomerically enriched α -alkoxystannanes (30a,b) <i>via</i> the separation of diastereomeric carbamates (29a,b)	17
Scheme 10	Addition Bu ₃ SnLi of <i>tert</i> -butanesulfinimine (31) and subsequent conversion to an enantiomerically enriched N-BOC protected α -aminoorganostannane (34)	18
Scheme 11	Synthesis of α -alkoxystannanes and their respective yields	19
Scheme 12	Reaction of diphenyl acetic acid with nBuLi	20
Scheme 13	Formation of peroxides in THF (i) and a possible mechanism for the formation of radicals (ii) that prevent the formation of Bu ₃ SnLi (iii)	21
Scheme 14	Formation of the N-BOC protected derivatives 42a and 42b	32
Scheme 15	Formation of N-BOC α -aminostannanes 43a and 43b (a: n=1; b: n=2)	34
Scheme 16	Conversion of N-BOC α -aminostannanes to N-ethyl α -aminostannanes (i) TMSI, dry CH ₂ Cl ₂ , (ii) NaOH (2.5M), Acetyl chloride, (iii) LiAlH ₄ in dry Et ₂ O, (iv) MeOH (a: n=1; b: n=2)	36
Scheme 17	Formation of a Schrock carbene 48 from a) Petasis' reagent 47 and b)	46

	Tebbe's reagent 49	
Scheme 18	General Fischer carbene synthetic route	48
Scheme 19	Semmelhack-Hegedus method for the synthesis of alkoxy carbene complexes (53 , route a) and amino carbene complexes (54 , route b)	49
Scheme 20	Reaction pathway for the formation of Gold (I) carbenes from Tungsten carbenes via transmetallation	49
Scheme 21	Benzannulation of phenyl(methoxy)carbene (62) and subsequent oxidation to afford hydroquinone (64)	52
Scheme 22	Synthesis of methyl carbene 66	54
Scheme 23	Metal carbon bonding in the Fischer chromium carbene complex 66	55
Scheme 24	Synthesis of Fischer carbenes from α -alkoxystannanes (i) nBuLi (ii) TMEDA, dry Et ₂ O (iii) Cr(CO) ₆ , CH ₂ Cl ₂ , -40°C and (iv) Me ₃ OBF ₄ , degassed water (R = C ₂ H ₅ , C ₃ H ₇ , CH(CH ₃) ₂)	57
Scheme 25	Synthesis of Fischer carbenes from <i>N</i> -ethyl α -aminostannanes (i) nBuLi (ii) TMEDA, dry Et ₂ O (iii) Cr(CO) ₆ , CH ₂ Cl ₂ , -40°C and (iv) Me ₃ OBF ₄ , degassed water (a : n=1 b : n=2)	58
Scheme 26	Synthesis of Fischer carbenes from <i>N</i> -BOC α -aminostannanes (i) nBuLi (ii) TMEDA, dry Et ₂ O (iii) Cr(CO) ₆ , CH ₂ Cl ₂ , -40°C and (iv) Me ₃ OBF ₄ , degassed water (a : n=1 b : n=2)	58
Scheme 27	Synthesis of the carbene 68c using two alternative methods a) Fischer method ¹¹¹ , b) Lotz method ¹⁴⁹	59

List of Tables

		Page
Table 1	Comparison of ^{13}C chemical shifts (100 MHz) in CDCl_3 of isomers 37b and 37c	27
Table 2	$J_{\text{Sn-C}}$ coupling constants observed in 400 MHz ^{13}C spectra for compounds 37a-c	29
Table 3	A summary of significant vibrational frequencies observed for the α -alkoxystannanes	31
Table 4	$J_{\text{Sn-C}}$ observed in 400 MHz ^{13}C NMR spectra for compounds 43a,b – 45a,b	40
Table 5	A summary of significant frequencies observed for the α -aminostannanes 43a, 43b, 45a and 45b	42
Table 6	A comparison of the synthetic methods used to synthesise Fischer carbenes	60
Table 7	Summary of Fischer Chromium Carbenes synthesised and their characteristics	63
Table 8	^{13}C NMR (C_6D_6 , 100 MHz) acquired for 37c and 68c	66
Table 9	DFT calculated bond lengths of novel chromium Fischer carbenes synthesized in this study	68
Table 10	Frequency analysis of Fischer carbene complexes 68b, 68c, 70a and 70b	71

List of Abbreviations

^{13}C NMR	Carbon-13 Nuclear Magnetic Resonance
1D	One dimensional
^1H NMR	Proton Nuclear Magnetic Resonance
2D	Two dimensional
Ac	Acetyl
AIBN	Azoisobutyronitrile
aq	Aqueous
br	Broad
C_6D_6	Deuterated benzene
CDCl_3	Deuterated chloroform
cm	Centimetre
conc.	Concentrated
COSY	^1H - ^1H Correlation Spectroscopy
d	Doublet
DAIB	Dimethylamino isoborneol
DCM	Dichloromethane
DCN	1,4-dicyanonaphthalene
DEPT	Distortionless Enhancement by Polarisation Transfer
eq	Molar equivalent
Et_2O	Diethyl ether
EtOAc	Ethyl acetate
EtOH	Ethanol
g	Grams
h	Hour(s)
H_2O	Water
HMBC	Heteronuclear Multiple Bond Correlation
HSQC	Heteronuclear Single Quantum Coherence
IR	Infra-red
J	Scalar coupling constant
K_2CO_3	Potassium carbonate
LAH	Lithium aluminium hydride
LDA	Lithium diisopropylamide
LF	Ligand-field
m	Multiplet
M	Molarity
Me_3SiCl	Trimethylsilyl chloride
MeCN	Acetonitrile
MeOH	Methanol
mg	Milligram
MgSO_4	Anhydrous magnesium sulphate
MHz	Megahertz
mL	Millilitre

MLCT	Metal Ligand Charge Transfer
mmol	Millimoles
mol	Moles
MOM	Methoxymethyl
MOMCl	Chloromethylmethyl ether
NaCl	Sodium chloride
NaOH	Sodium hydroxide
N-BOC	<i>t</i> -Butoxycarbonyl on nitrogen
nBuLi	nButyllithium
NCI	National Cancer Institute
NH ₄ Cl	Ammonium chloride
NMR	Nuclear magnetic resonance
°C	Degrees Celsius
OMe	Methyl ether
OTs	4-toluenesulfonic acid
ppm	Parts per million
q	Quartet
RT	Room temperature
s	Singlet
sat.	Saturated
sec-BuLi	sec Butyllithium
t	Triplet
<i>t</i> -BOC	<i>tert</i> -Butoxycarbonyl
<i>t</i> -BuLi	<i>tert</i> Butyllithium
THF	Tetrahydrofuran
TLC	Thin-Layer Chromatography
TMEDA	<i>N,N,N',N'</i> -Tetramethylethylenediamine
TMSI	Trimethylsilyliodide
UV	UltraViolet
δ	Chemical shift (ppm)

Acknowledgements

I would like to sincerely thank my supervisor, Dr Klein for all her guidance and encouragement throughout my postgraduate career, especially during Masters. Her excitement in the progress of my project kept me going even when things looked grim and I appreciate all her effort in making this an incredible and memorable time for me. It's a privilege to work under her supervision.

I would also like to thank Dr Lobb for his help with computer modeling and Prof Kaye for his useful suggestions during group meetings. A big thank you to Mrs Sewry for understanding my passion for outreach, it was so special for me to be a part of the team that went to Bristol, and it has been so rewarding. Thank you to Sunny, not only for his help with my research but also in showing me how to share my love of science with the public.

To present and past members of F22 lab, thank you for sharing the highs and lows in research and making it an interesting experience, especially Matshawe for being helping me get started in the lab and Byron who helped tremendously with air-free techniques. Thanks to the support and technical staff in the Chemistry Department, in particular, Mrs B. Tarr for her ability to help you even when she has a hundred other things on the go, to Mr A. Adriaan and Mr. R. Douglas who have assisted with glassware and other equipment needs.

To my friends, who have made my time at Rhodes an amazing experience thanks and I will always treasure the friendships I have formed here. A special thanks to Candy for her support and encouragement, thanks for being there for me through all the good and bad times.

Thanks to NRF/Thuthuka for financial support.

Most importantly, I would like to thank my family, Sarel, Francis, Dirk and Elmarie as well as Rob who have been a great emotional support and who remind me of the important things in life. Baie dankie Ma en Pa, ek het julle baie lief.

Chapter One: General Introduction

1. General Introduction

1.1. The origins and history of organometallic compounds

The first organometallic compound was synthesised from ethylene and platinum (II) chloride to give a salt known as Zeise's salt $[K(C_2H_4)PtCl_3]$ (**1**, Figure 1).¹ This was carried out by William Zeise in 1825, although it was only much later, in the 1950's, that the correct structure of compound **1** was elucidated. The structure was reported in connection with the structure of ferrocene (**2**) which was studied by two different groups simultaneously and finally confirmed with x-ray diffractions studies to be a sandwich structure (Figure 1). These types of compounds, with the characteristic sandwich structure, are known as metallocenes.^{1,2} Pauson and Kealy incorrectly assigned the structure of ferrocene, which they had synthesised by accident.¹ It was Woodward and Wilkinson who correctly assigned the structure based on its reactivity.³

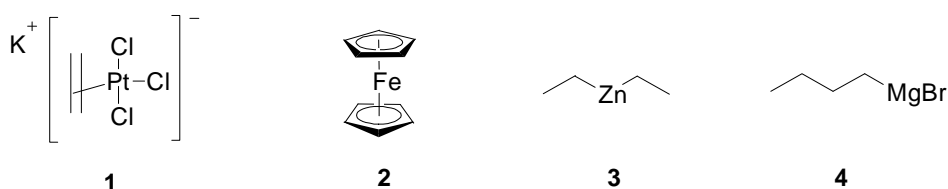
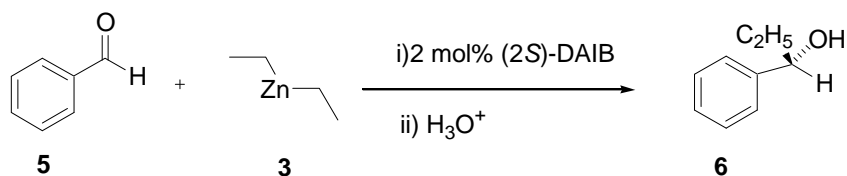


Figure 1: Organometallic compounds: Zeise's salt (**1**), Ferrocene (**2**), diethylzinc (**3**) and butylmagnesium bromide (**4**)

In 1849, Edward Frankland synthesised diethylzinc (**3**) from ethyl iodide and zinc metal. Diethylzinc acts as an ethyl synthon in organic synthesis, and therefore is useful in addition reactions to carbonyls, such as the enantioselective addition of an ethyl group to aldehydes (Scheme 1).⁴



Scheme 1: An addition reaction of diethyl zinc (**3**) with catalyst (2S)-DAIB and benzaldehyde (**5**) to form the (S)-enantiomer of phenyl-1-propanol (**6**)

Another important class of organometallic compounds discovered in 1899 by Victor Grignard was organomagnesium compounds such as butyl magnesium bromide (**4**, Figure 1). These compounds

are more commonly known as Grignard reagents today. Grignard reagents act as strong bases and as nucleophiles in nucleophilic addition reactions to carbonyls forming new carbon-carbon bonds.⁵

1.2. The importance of organometallic compounds

Organometallic compounds have played an important role in catalysis and organic synthesis. This is clear from the number of Nobel Prizes that have been awarded to several chemists relating to their work on different organometallic compounds. The first Nobel Prize in chemistry was awarded in 1912⁶ to Victor Grignard and fellow Frenchman Paul Sabatier for their work on organomagnesium compounds (Grignard reagents), Karl Ziegler and Giulio Natta received their Nobel Prize in 1963⁶ for the discovery of a titanium based catalyst and their work on what became known as the Ziegler-Natta catalyst. This catalyst is used in the synthesis of polymers of α -olefins and still accounts for a large portion of the manufacturing of plastics from alkenes worldwide.⁷ In 1973, the Nobel Prize in chemistry went to Geoffrey Wilkinson and Ernst Otto Fischer for their work on metallocenes, also known as sandwich compounds.⁶ The work by Yves Chauvin, Robert Grubbs and Richard Schrock on alkene metathesis using organometallic catalysts was acknowledged with a Nobel Prize in 2005⁶ and more recently Richard Heck, Ei-ichi Negishi and Akira Suzuki were awarded the Nobel Prize for their work in palladium catalysed coupling reactions in 2010.⁶

1.3. Chemistry and characteristics of organometallic compounds

Organometallic compounds are characterised by a metal carbon bond, which can either be a bond directly between the metal and carbon or a π -complex involving the overlap of metal orbitals with π -orbitals of the ligand.⁸ The bonding is mainly covalent, but there are ionic characteristics found in some compounds. This occurs with very electropositive metals (such as alkali metals), or when the carbon ligand can exist as a resonance stabilized carbanion (such as an aromatic cyclopentadienyl anion **7**), or if the substituents on the carbon are electron withdrawing, (such as the triphenylmethyl anion).⁸ For example, organolithiums are ~90% ionic, stable in solution and undergo many important reactions in organic synthesis.⁹ The bonding in ferrocene (**2**), on the other hand, is almost completely covalent. This particular bonding involves the π -orbitals of the organic ligands which ligate to the metal centre. Other common properties of organometallic compounds include their insolubility in water, high toxicity levels and their ability to be oxidised.

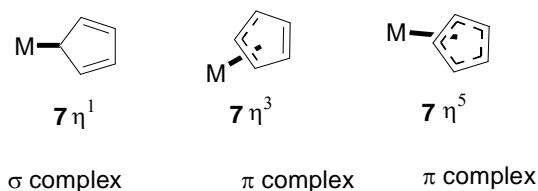


Figure 2: Different bonding of cyclopentadienyl anion (**7**) to a metal (M)

A systematic notation for the naming of organometallic compounds was developed in the 1960's to differentiate between the types of metal bonding, in particular when transition metals are involved.¹⁰ If a normal σ bond between the metal and ligand exists, there is no need to use the 'hapto' (η) notation because the metal is only attached to one carbon, for example a simple Grignard reagent is η^1 since the magnesium is bonded to a single carbon. This is not a useful clarification since there is no alternative and the notation is thus redundant. This notation becomes more important when the metal can be bonded to more than one carbon, as is commonly found in metal π -complexes, where the π -orbitals of the organic ligand are involved as described earlier. The cyclopentadienyl anion (**7**) is a good example, since it can act as a σ ligand (η^1) or an allyl ligand (η^3) or a cyclopentadienyl ligand (η^5) (Figure 2).⁵

The 18-electron rule assists in the prediction of the stability of organometallic compounds. The electrons from the ligands which are involved in bonding as well as the electrons in the d-orbitals of the metal are counted. Once there are 18 electrons, the transition metal centre has the same configuration in the valence shell as a noble gas hence affords stability.⁵

1.4. Applications of organometallic compounds

One of the earliest applications of organometallic compounds was the use of an organoarsenic compound called Salvarsan as a treatment for syphilis in 1909.¹¹ This was first discovered by Paul Ehrlich and thought to have a double bond between the two arsenic atoms. However, it was only in 2005 that the true structure was revealed by mass spectroscopy to be a mixture of cyclic trimers (**8**) and a pentamer (**9**) with the bonds between arsenic being σ bonds (Figure 3).¹¹

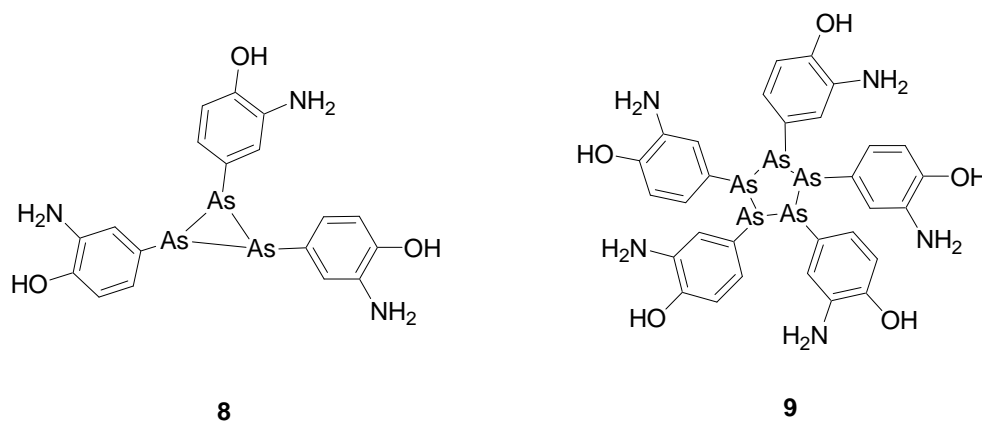


Figure 3: The mixture of a trimer (**8**) and the pentamer (**9**) that are present in Salvarsan¹¹

Tetraethyllead was previously used in petrol as an anti knocking agent, but due to the toxicity of lead, its usage was stopped and it has been replaced by other organometallic compounds such as ferrocene and methylcyclopentadienyl manganese tricarbonyl which are less toxic.¹ Other uses of organometallic compounds are for organic synthesis and catalytic reactions, besides those mentioned above with each of the awards of the Nobel Prize in chemistry. Organolithium, organomagnesium (Grignard reagents) and organoaluminium compounds are very basic and can act as reducing agents. Their use in organic synthesis is important in the synthesis of new carbon-carbon bonds.

1.5. Aims of this thesis

As outlined above, the field of organometallic chemistry is diverse and the applications have made these complexes very important. The present study involves the use of main group organometallics, organostannanes and organolithiums, as precursors to chromium Fischer carbene complexes.

The aims of this project include

- i) Synthesis of α -alkoxy and α -aminostannanes as stable precursors to organolithiums.
- ii) Synthesis of novel chromium Fischer carbenes from the α -alkoxy and α -aminostannanes *via* the organolithiums.
- iii) Molecular modelling studies in order to understand more clearly the vibrational spectroscopy of the newly synthesised chromium Fischer carbene complexes.

Chapter Two: Synthesis of α -alkoxy and α -aminostannanes

2.1. Introduction

2.1.1. General use of organostannanes

a) History and scope of organotin compounds

The scope of organotin chemistry is very broad and has found many applications due to the biological, chemical and physical properties of tin. Numerous applications in industry as well as in synthesis led to further investigations of tin in organometallic chemistry in the late 1940's.¹² Some of the general industrial uses include stabilizers for polyvinylchloride (PVC) piping against heat and light degradation, glass coating for strengthening purposes and the production of poly urethanes.^{13, 14} Organotin compounds have a high degree of toxicity which has led to a decrease in their use as biocides,¹⁵ antifouling paints and wood preservatives,¹⁶ after it was found to have adverse effects on the environment.¹³

b) Chemistry of tin

The characteristics of the tin-carbon bond make it useful in organic synthesis. Tin is a heavy metal in Group 4 on the Periodic Table (the same group as carbon). Common characteristics of elements in this group are a valency of four and the formation of tetrahedral compounds.⁵ The covalent bonds to the tin atom are long, with Sn-C and Sn-H bond lengths at 0.22 nm and 0.17 nm respectively compared with C-C and C-H bond lengths which are 0.15 nm and 0.11 nm.⁵ Tin forms stable organic compounds called stannanes where its formal oxidation state is +4. Its atomic radius is large which explains why the bonds to carbon are longer, and this in turn makes the covalent bonds more easily polarized. The polarity of the bond increases with the electrophilicity of the tin atom and the nucleophilicity of the R group.

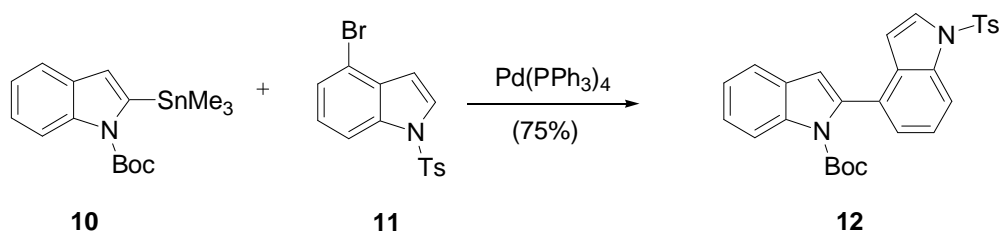
Applications of stannanes in synthesis make use of both the homolytic and heterolytic reactivity of the bonds.^{12, 13} The weakness of the tin-carbon bond allows the transfer of a substituent attached to the tin to another reagent; carbon substituents can be transferred either *via* a radical mechanism or a polar mechanism. For example, Wakabayashi *et al.*¹⁷ described an intramolecular 1,4-aryl migration from tin to a carbon radical which illustrated the transfer of a phenyl group. The reduction of aldehydes by tributyltin hydride is assisted by a Lewis acid or protic acid catalysis which activates

the carbonyl group and allows for the nucleophilic tributyltin hydride to react *via* a polar mechanism.¹⁸

c) Catalytic coupling reactions

The palladium-catalysed cross-coupling of organotin compounds with organic electrophiles such as alkenyl and aryl halides, is an important method of forming new carbon-carbon bonds.^{19,20} Vinylstannanes, commonly used in coupling reactions, are prepared by a hydrostannation reaction of tributyltin hydride with alkynes.²¹ More specifically, the hydrostannation of hindered arylalkynes with two ortho substituents on the same aromatic group gives rise exclusively to α -vinylstannanes.²¹ The products of the hydrostannation have also been shown to be useful substrates for the Negishi coupling between vinyl iodide and organozinc compounds to obtain stereo-defined triarylolefins which have anti-tumour therapeutic interest.²¹⁻²³

The mechanism of the Stille coupling reaction involves the oxidative addition of the organic substrate followed by transfer of ligands between the organotin compound and the palladium (II) species followed by the reductive elimination of the new organic compound.²⁴ It had been used in natural product synthesis, for instance in a crucial step of the synthesis of the slime mould arcyriacyanin A, where the 2-(trimethylstannyl)indole **10** is coupled with the brominated indole **11** in a palladium catalysed reaction to give the bis-indole **12** (Scheme 2).^{25, 26}

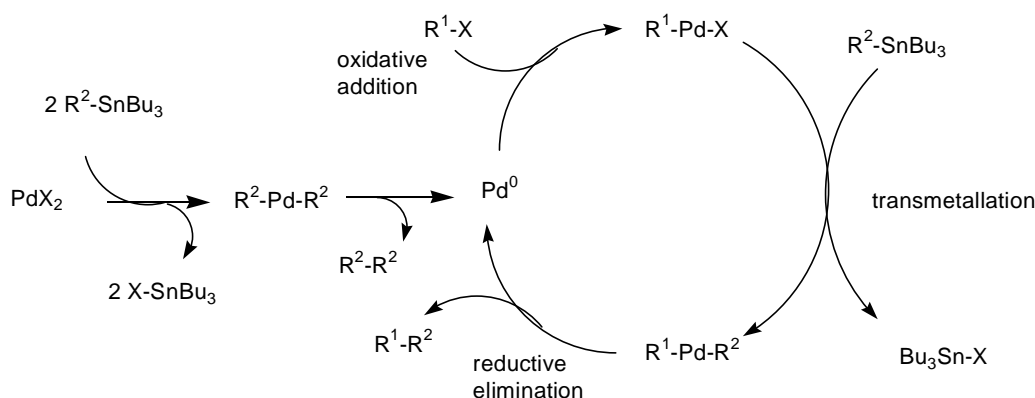


Scheme 2: Stille coupling reaction used for a crucial step in synthesis of natural product arcyriacyanin A

Many aromatic and non-aromatic heterocyclic stannanes have been used in the Stille coupling reaction; however, the Stille reaction is known to use excess organostannane to ensure that the reaction goes to completion.²⁵ Recently di- and tri-functional organotin compounds reacted with iodovinyl acids were investigated to determine how many R-groups were transferred in the reaction. The transfer of multiple R-groups was achieved and the quantity of tin was reduced, making the reactions cleaner.¹⁹ The Stille coupling reaction is generally carried out in organic

solvents; however it was found that when reacting with vinyl epoxides, the presence of water in the organic mixture increased the yields and affected the stereochemistry. The Stille reaction has also been carried out in neat water with a variety of aryl halides.^{20,27}

The Stille reaction mechanism is complex, and the nature of the solvent, the properties of the auxiliary ligand, the type of organostannane and the organic electrophile all affect the reactivity of each step and hence the rate-determining step in a particular example can be any of the stages such as the oxidative addition, the transmetallation or the reductive elimination (Scheme 3).²⁸ The presence of olefins, such as maleic anhydride, during the transmetallation step has been found to play a stabilizing role in the carbon-carbon coupling since the olefin can improve the electrophilicity of the palladium metal centre to which it is coordinated.²⁸ Olefins have also been found to increase the rate of the transmetallation step when using poorly activated vinyl stannanes, reducing the reaction time from as much as a couple of days to approximately 120 minutes.²⁸



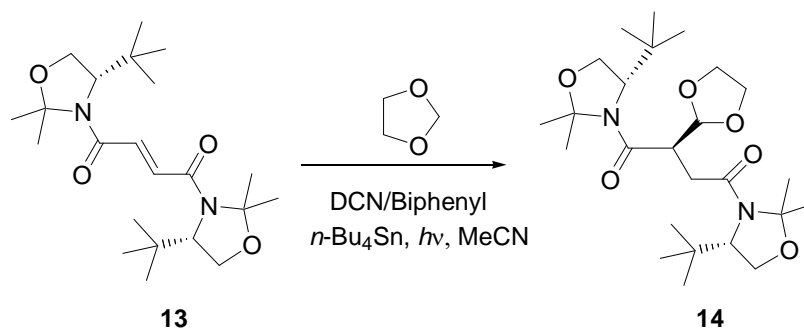
Scheme 3: Simplified reaction mechanism of palladium catalyzed coupling of stannanes with organic electrophiles (adapted from Espinet *et al.*²⁹)

Copper-mediated Stille type coupling reactions have been successfully employed in the synthesis of intricate natural products.^{30, 31} The vinyl stannane was coupled with methyl (*E*)-3-iodopropenoate with the presence of a tin scavenger, tetrabutylammonium diphenylphosphinate, which was needed to obtain a useful yield of the intermediate of formamicin. It is important to note that the reagents were stable under these mild conditions as the reaction failed when the cross coupling was attempted with palladium alone.³² The synthesis of estrogen mimetics has also been achieved using the Stille coupling reaction with copper oxide as the co-reagent,³³ where stannanes derived from benzo[*b*]thiophene and benzaldehyde were coupled with halophenols to produce estradiol mimetics.³³

Stille-type coupling reactions of α -alkoxy and α -aminostannanes with acyl chlorides have been reported by Falck and co-workers, and have proven useful in asymmetric synthesis.^{34, 35} This method is an alternative route to obtain stereospecific α -alkoxy and α -amino ketones with moderate yield when catalysed by palladium and copper (I) salts. This reaction provided a different method to form new carbon-carbon bonds which is similar to the transmetallation of α -alkoxy and α -aminostannanes because it allows access to heteroatom substituted chiral centres.³⁴

d) Radical reactions

Tetraalkylstannanes are known to be effective precursors of alkyl radicals for the formation of carbon-hydrogen and carbon-carbon bonds from various functional groups.³⁶ Tributyltin hydride is a good radical source; the reaction is initiated by reacting it with azoisobutyronitrile (AIBN).⁵ In order for the reaction to proceed, the alkyl starting material must have weak carbon halide bonds (C-X) and the radical trap has to be in a higher concentration, at least ten times the concentration of the tributyltin radical.⁵ In a photocatalysis reaction to form new carbon-carbon bonds, tetrabutylstannane was used as the radical initiator and 1,4-dicyanonaphthalene (DCN)/Biphenyl as the photocatalyst in the reaction of 4-*t*-butyl-2,2-dimethyloxazolidine derivative **13** with 1,3-dioxolane to obtain the dioxolanylsuccinyloxazolidine product **14** in 79% yield. An increased selectivity with respect to alternative thermal alkylations³⁷ was obtained, highlighting the advantage of a photochemical method (Scheme 4).³⁶



Scheme 4: A photocatalytic reaction of **13** carried out with tetrabutyltin as a radical initiator

Another application of organostannanes is in soluble tin functionalised polymer supports for the regioselective benzylation of carbohydrates.³⁸ Purification of the carbohydrate was made simpler, being effected by filtration since the tin was immobilised onto a support. However, the isolated yields were very low at 30% and below. Further investigations were carried out looking into the effectiveness of soluble tin polymer supports and the modified resins were tested by performing a

reduction on 6-bromohexene. Their effectiveness was measured against tributyltin hydride and the supports gave higher yields in comparison.³⁹ The use of polymer supports to remove the tin residues from the desired product has been widely investigated however a few setbacks such as the slow release of tin from the polymer supports often left the products contaminated.⁴⁰ In response to this problem, alternative tin hydride reagents have been synthesised that assist with the removal of tin from the reaction mixtures. These reagents include the use of fluoros tin hydrides,⁴¹ water soluble tin hydrides,⁴² as well as a tin hydride which is unstable under both acidic and basic conditions.⁴³

Allyl and alkyl organotin compounds have been used for reaction with aldehydes and ketones to form allylic alcohols. This reaction is similar to the aldol reaction with high regio- and stereoselective addition. This reaction also allows for further functional group modification at the alkene position.⁴⁴

e) Organostannanes involved in tin-lithium exchange

The conversion of an organostannane to an organolithium provides a more reactive reagent which acts as a nucleophile that can be trapped with many different electrophiles.⁴⁵ Tin-lithium exchange occurs very rapidly, with the mechanism being similar to that of an oxidative insertion reaction between lithium metal and alkyl halides.⁵ A strong nucleophile such as nBuLi reacts at the tin atom, resulting in a 5-coordinate stannate anion. The intermediate is short-lived since the organolithium species is released with tetrabutyltin being formed as the by-product of the reaction.⁵ The organolithium formed is controlled by thermodynamics, hence the greater the stability of the organolithium, the more likely it is to be formed. Vinyl, allyl, aryl and alkenyl lithiums are more stable than alkyl lithiums so the reformation of butyllithium is not favourable.⁵

Tin-lithium exchange also provides a route to form organolithiums that are not accessible from direct lithiation, as is true for α -alkoxy organolithiums and some α -amino organolithiums. These organolithiums cannot be formed by the direct lithiation of the carbon which has oxygen/nitrogen attached to it since the hydrogen atom is not acidic enough to be removed by basic lithiating agents such as nBuLi or even tBuLi.⁵

The first tin-lithium exchange for α -amino organolithiums using (*N,N*-di-methylaminomethyl) tributyltin and nBuLi to form *N,N*-disubstituted aminomethyl lithium was accomplished in 1970 by Peterson.^{46,47} Since then, many studies have been carried out to determine the reaction sequences, configurational stability, and aggregation behaviour.⁴⁸⁻⁵⁰

Both α -alkoxy and α -aminostannanes are used to obtain organolithiums and the relative stability of each of these compounds has been studied extensively.⁹ It is well established that both oxygen and nitrogen play an important role in the stabilization of the respective organolithiums at the α -position.^{51, 52} The type of protecting group also plays a role in stabilizing the organolithium. A carbamate protecting group, for example, was found to stabilize both oxygen atoms and nitrogen atoms due to its electron-withdrawing nature.⁵¹

McGarvey investigated the relative stabilities of organolithiums derived from α -alkoxystannanes and found that there was a destabilizing effect of additional alkyl groups and a stabilizing effect of alkoxy substituents on tetrahedral organolithiums.^{53, 54} The organolithium (**15**) derived stability from the five membered ring lithium-oxygen chelation, however this stability would change with respect to solvent, temperature, and the nature of other groups attached to the oxygen (Figure 4).⁵³ The stability of the adjacent carbon lithium bond arises from the σ -inductive effect of the alkoxy moiety as well as from coordination of the farthest oxygen (Figure 4). The stabilization of the α -lithioamines is due to the chelation of the lithium to the oxygen of the carbamate group (**16**, Figure 4).

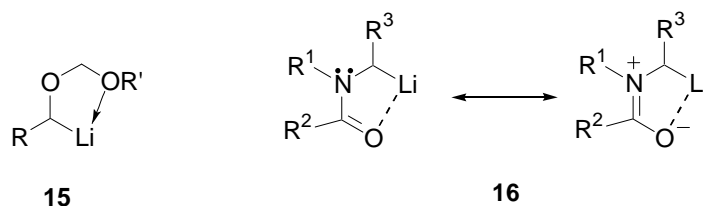
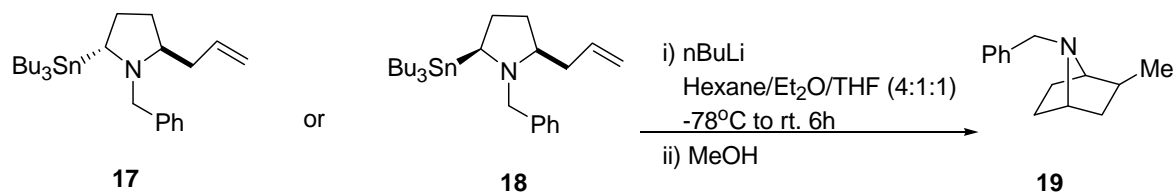


Figure 4: Stabilization effect of oxygen on organolithiums

More recently Sardina investigated a method to quantify the stability provided by oxygen and nitrogen atoms present on the α -carbon of an organostannane.⁵¹ The research group developed a stability scale using thermodynamic stability derived from tin-lithium exchange equilibria. It was found that a carbonyl group as the *O*-substituent on the carbanion is more stabilizing than an alkyl or alkoxyalkyl group.⁵¹ This work helps with the investigation of structure-stability relationships of more complex organolithiums.

Anionic cyclization of α -aminoorganolithiums has been reported by Coldham's group^{55, 56} which is useful for medicinal chemistry for the preparation of nitrogen containing compounds. Bridged bicyclic compounds are commonly found in alkaloids, however the use of organolithiums to obtain these cyclic structures is unusual.⁵⁷ In order for the cyclization onto an unactivated alkene to occur, the lithium coordinates to the π -system, therefore as tin-lithium exchange is known to occur with

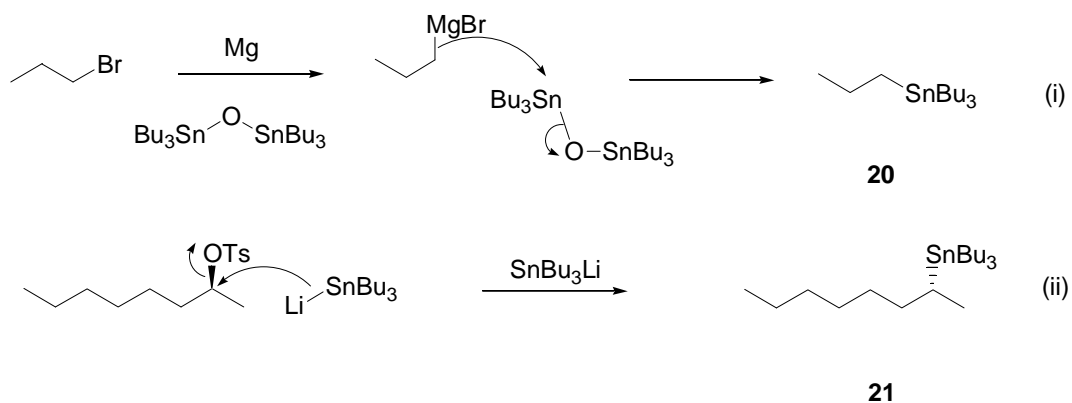
the retention of configuration, it was interesting to notice that both *cis*- and *trans*-stannylpyrrolidines (**17** and **18**) cyclized to afford *exo*-2-methyl-7-azabicyclo[2.1.1]heptane (**19**, Scheme 5). The *endo* isomer was not isolated, suggesting that the organolithium derived from the *trans* isomer epimerised to the *cis* isomer before cyclization took place.⁵⁶



Scheme 5: Cyclization of *cis*- and *trans*-stannylpyrrolidines (**17** and **18**) to afford *exo*-2-methyl-7-azabicyclo[2.1.1]heptane **19**

2.1.2. Preparation of organostannanes

Organostannanes can be prepared in various ways depending on the other functional groups required and the reaction mechanisms they undergo.⁵ An alkyltributyltin can be prepared using a Grignard reagent and an organotin electrophile such as bis(tributyltin) oxide which goes *via* an S_N2 reaction mechanism at the tin atom. The d-orbitals of the tin provide a suitable site for nucleophilic attack and the substitution reaction is facilitated by the long carbon-tin bonds that reduce the steric interactions to form a penta-valent tin anion intermediate (stannate). This intermediate forms slowly and then breaks down quickly with the loss of the tin oxide (Scheme 6, i) to afford tributyl(propyl)stannane (**20**). An alternative method to form an alkyltributyltin is to reverse the polarity of the tin by forming a stannyl lithium complex through the deprotonation of tributyltin hydride or reductive cleavage of a diorganotin with lithium metal. The stannyl lithium adds to organic electrophiles such as alkyl halides or alkanes with good leaving groups such as a tosyl group. For example, (*S*)-octan-2-yl 4-methylbenzenesulfonate reacted with the tributylstannyl lithium to form (*R*)-tributyl(octan-2-yl)stannane (**21**, Scheme 6, ii). This reaction follows an S_N2 reaction at the carbon, which has no analogy to the S_N2 reaction at the tin.⁵



Scheme 6: Preparation of organostannanes (i) S_N2 at tin⁵ (ii) S_N2 at carbon⁵

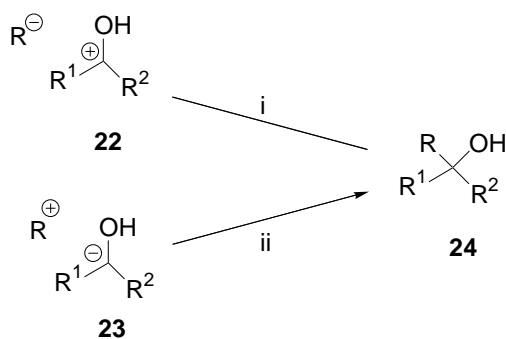
There are many types of organostannanes that can be synthesised and some of their various applications have been briefly outlined. This study focused on the synthesis and application of α -alkoxy and α -aminostannanes specifically. The importance of these stannanes is that they can undergo tin-lithium exchange to form a reactive organolithium species which is required to synthesise Fischer chromium carbenes.

a) α -Alkoxy-stannanes

Still⁵⁴ has shown that an α -alkoxy-stannane can be used as an example of a hydroxymethyl anion equivalent.⁵⁸ Hydroxymethyl anion equivalents can be used as building blocks in the synthesis of complex organic compounds. The synthesis of such an α -alkoxy-stannane involved the nucleophilic attack of an aldehyde with tributylstannyl lithium, which is formed *in situ*.⁵⁸ This is a carbonyl addition reaction which results in the formation of a tributylstannylcarbinol. These species are found to react readily with the elimination of tin and therefore the hydroxyl moiety is protected immediately. Due to the acid sensitive nature of the carbinol intermediate, mild conditions for the protection were used; α -chloromethyl methyl ether together with a base gave the protected derivatives in good yields, above 90%.⁵⁴ The MOM protecting group, known to be easily hydrolyzed under mild acid conditions, has the advantage of being achiral. The inclusion of an additional chiral centre into synthetic intermediates was unwanted since there would be complications with manipulation, analysis and purification of diastereomeric mixtures.⁵⁸

The initial use of α -alkoxy-stannanes as precursors for α -organolithiums via tin-lithium exchange was explored over 30 years ago by W. C. Still.⁵⁴ In general, addition reactions which lead to new carbon-carbon formation occur with the carbonyl acting as a hydroxyl substituted carbocation (**22**).

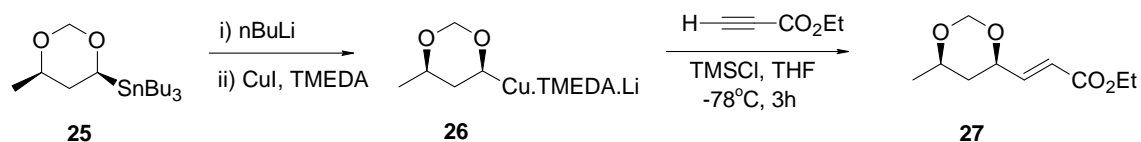
This carbocation then undergoes nucleophilic attack to form the new carbon-carbon bond as shown by route (i) in Scheme 7. However, not many examples of polarity inversion at the carbon centre were known, such that the carbonyl acts as a carbanion (**23**) instead. This approach was uncommon because of the relative unavailability of reagents which form the carbonyl carbanion equivalent. The use of 'umpolung' gave access to the alternative route (ii) through using organolithiums. The alternative route as demonstrated by Still, involved the use of an aldehyde and proceeded *via* an α -alkoxyorganostannane to obtain the carbonyl carbanion equivalent **23** (Scheme 7).⁵⁴



Scheme 7: New carbon-carbon bond formation *via* a hydroxyl-substituted carbocation **22** (route i) or *via* a carbonyl carbanion **23** (route ii)

Later studies showed that this procedure can be used to obtain chiral organostannanes by introducing stereospecificity to the organostannane and separating the desired stereoisomer.⁵⁴ These chiral stannanes are stable precursors to chiral organolithium compounds. The reaction of aldehydes with tributyltinlithium occurs very quickly at low temperatures (-78°C), with high yields obtained when the reaction is quenched at these low temperatures, keeping in mind that the α -hydroxystannanes formed are temperature sensitive and can decompose if they are not handled carefully.⁵⁹

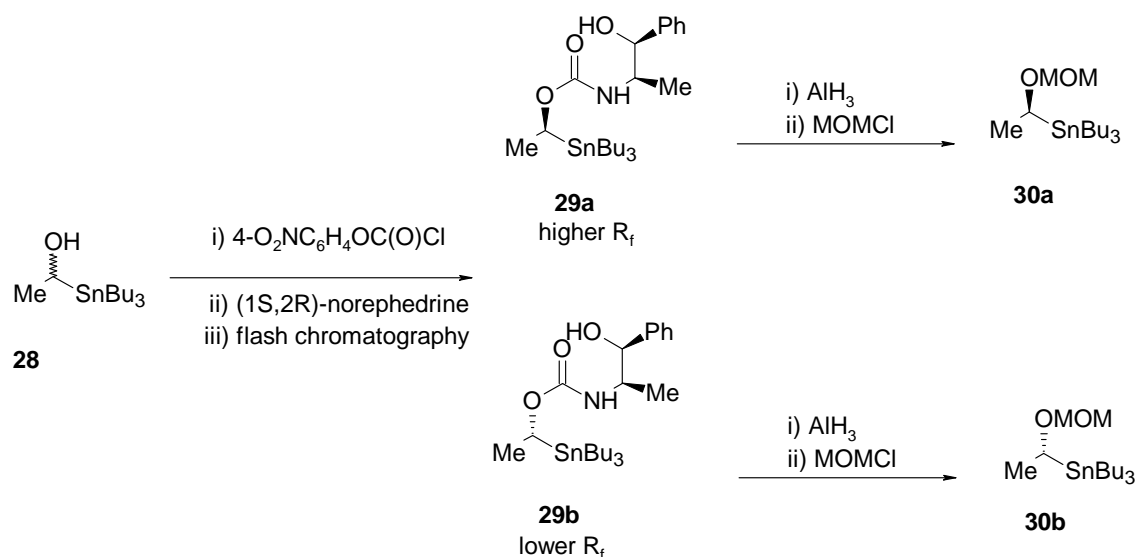
Linderman described the use of 4-(tributylstannyl)-1,3-dioxanes for the synthesis of α -alkoxyorganocopper reagents (Scheme 8).⁶⁰ The α -alkoxyorganocopper reagents were generated using *n*BuLi to form the lithio species and then using a TMEDA copper (I) iodide complex for the lithium/copper transmetalation. Transmetalation of tin-lithium and then lithium/copper was found to occur without racemisation of both enantiopure dioxane stannanes. The α -alkoxyorganocopper reagents were able to undergo conjugate addition reactions to ethyl propiolate with retention of configuration (Scheme 8).⁶⁰



Scheme 8: Conversion of 4-(tributylstannyl)-1,3-dioxane (**25**) to an alkoxyorganocopper reagent (**26**) which undergoes conjugate addition with ethyl propiolate to form (**27**)

Enantiomerically enriched α -alkoxystannanes lead to the synthesis of chiral secondary alcohol derivatives.⁴⁵ α -Hydroxystannanes are easily converted to the α -alkoxystannanes with the protection of the hydroxyl functional group using α -chloromethyl methyl ether.⁵⁸ The preparation of enantiomerically enriched α -hydroxystannanes can be carried out by the separation of the associated diastereomeric Mosher esters⁶¹ or methoxymenthyl ethers which undergo regioselective acetal exchange or acetal group cleavage.⁶² Both methods are expensive and have minimal separation by chromatography therefore an alternative method to reproducibly obtain the enantiomerically enriched α -alkoxystannanes was found to be necessary for the large scale production and high selectivity required.

Chong and co-workers⁴⁵ used norephedrine carbamate derivatives of α -hydroxystannanes (**29a,b**) which were easily separated by column chromatography followed by the reduction of the carbamate group to give rise to the enantiomerically enriched α -alkoxystannanes [Scheme 9 (**30a,b**)]. This method was an improvement as the conversion of racemic α -hydroxystannanes (**28**) to the norephedrine carbamates allowed for the resolution of the enantiomers and the reaction was performed on a multi-gram scale which is better than previous methods described.

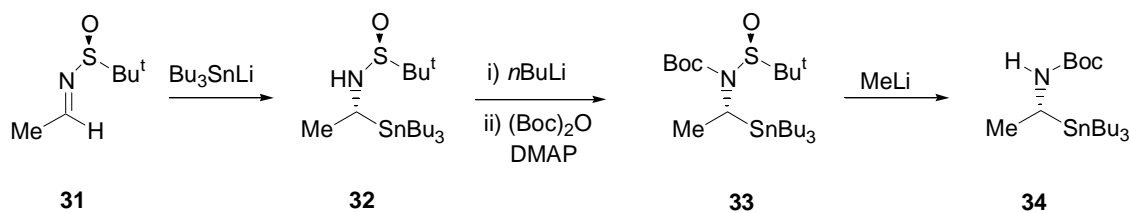


Scheme 9: Formation of enantiomerically enriched α -alkoxystannanes (**30a,b**) *via* the separation of diastereomeric carbamates (**29a,b**)

b) α -Aminostannanes

The synthesis of α -aminostannanes has been explored in depth by Beak,^{52, 63} Gawley^{49, 64, 65} and Quintard⁶⁶⁻⁶⁸ among others. The reaction usually proceeds *via* an electrophilic substitution at the α -position when the amide is reacted with *sec*-BuLi/TMEDA and tributyltin chloride.

Kells *et al.*⁵⁹ described an alternative route using tributylstannyllithium to access α -aminostannanes (Scheme 10). Addition reactions of Bu_3SnLi to aldehydes and ketones has been reported beforehand however, the addition to C=N group was unknown until it was attempted by Chong and co-workers.⁵⁹ The addition of Bu_3SnLi to a range of *tert*-butanesulfinimines (**31**) occurred at the C=N bond at -78°C which resulted in good yields and high diastereoselectivities with less than 1% of the minor enantiomer being detected in most cases of the stannylsulfonamides.⁵⁹ The *tert*-butanesulfinyl group was difficult to remove from the products, and so the stannylsulfonamides (**32**) were deprotonated with *n*BuLi followed by the addition of the well known *t*-BOC group. Finally, the selective removal of the *tert*-butanesulfinyl group with methyllithium gave rise to the *t*-BOC protected α -aminostannanes (**34**).⁵⁹



Scheme 10: Addition Bu₃SnLi of *tert*-butanesulfinimine (**31**) and subsequent conversion to an enantiomerically enriched N-BOC protected α-aminoorganostannane (**34**)

α-Aminostannanes provide useful precursors to organolithiums, in the same way that α-alkoxystannanes do.^{49, 51} α-Aminostannanes can also be used as reagents in various Stille coupling reactions, as shown previously in the synthesis of the natural product arcyriacyanin A (Scheme 2).

2.2. Results and Discussion

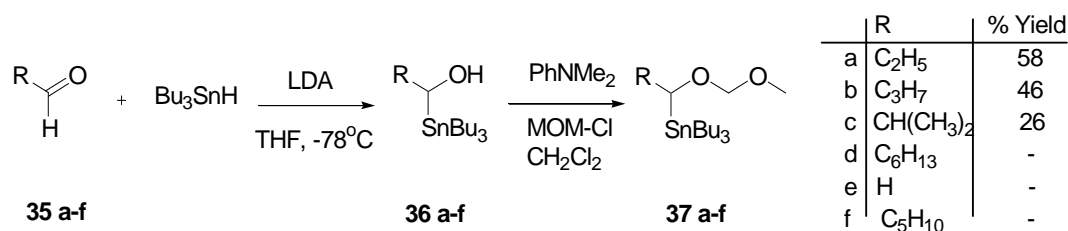
The aim was to synthesise organostannanes which were stable, would be easily purified and could be stored over a period of time. The two types of α-hetero substituted organostannanes were synthesised differently: the α-alkoxystannanes were obtained via a nucleophilic addition reaction while the α-aminostannanes were obtained by an electrophilic substitution reaction. The synthesis of α-alkoxy and α-aminostannanes provided stable intermediates for the respective organolithiums which were subsequently used in the synthesis of novel Fischer chromium carbenes after undergoing tin-lithium exchange. The synthesis of the Fischer chromium carbenes will be discussed in more detail in the next chapter.

2.2.1. α-Alkoxystannanes

a) Synthesis

In this study the synthesis of α-alkoxystannanes was accomplished according to the method developed by Still.⁵⁴ The use of a range of aldehydes gave rise to stannanes with varying chain length. Tributylstannyl lithium was formed *in situ* by the deprotonation of tributyltin hydride with LDA. This carbanion equivalent then acted as a nucleophile, attacking the carbonyl (for example, propanal, **35a** Scheme 11). According to Still,⁵⁴ it was found that alkyl lithiums and Grignard reagents were less effective bases in the deprotonation step. The lithium diisopropylamide (LDA) is a very

strong base,⁶⁹ which is readily quenched by water and therefore precautions were necessary to remove all water from the reaction system. The reactions were thus performed using Schlenk techniques⁷⁰ and anhydrous solvents. Nucleophilic addition resulted in the formation of the stannous alcohol, **36**. These compounds are relatively unstable and react readily, eliminating the tin moiety, and therefore the hydroxyl moiety was protected immediately. Due to the acid sensitive nature, mild conditions for the protection were used; α -chloromethyl methyl ether together with a base such as dimethyl aniline gave the protected derivatives **37a-f** (Scheme 11).⁵⁴



Scheme 11: Synthesis of α -alkoxystannanes and their respective yields

The MOM protecting group is known to be easily hydrolyzed under mild acid conditions. The MOM protection group provided stability to the stannane **37a**, which was purified using column chromatography to afford the pure compound in 58% yield.

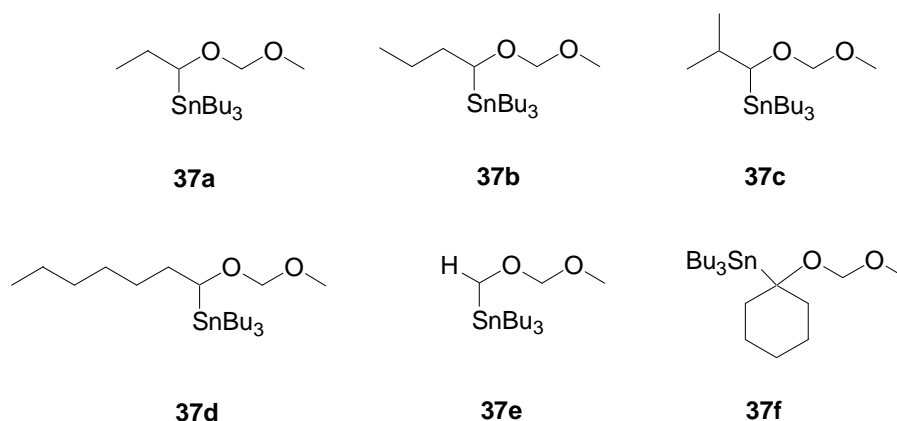


Figure 5: Structures of the α -alkoxystannanes **37a-f**

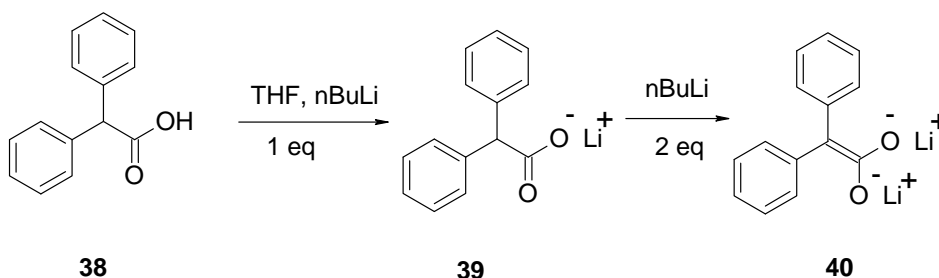
The α -alkoxystannanes **37a-f** were synthesized using tributylstannyllithium, and the products **37a-c** were fully characterized by spectroscopic analysis, including 1- and 2-dimensional NMR and IR. Three stannanes (**37d-f**) were not isolated due to challenges which are explained in detail at a later stage.

There is a distinct variation in the yields obtained following the same reaction scheme (Scheme 11). This can be explained by various factors such as the unreliable concentration of the nBuLi used to synthesise the tributylstanyllithium and the difficulty encountered in the purification methods used for the stannanes.

b) Challenges of synthesis

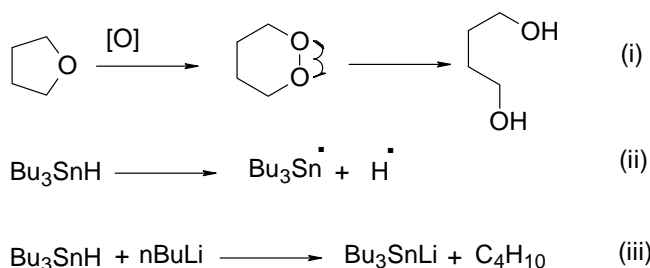
Our earliest attempts at making the α -alkoxystannanes gave little or no yield, and prompted an investigation of all the reagents and reaction conditions. The nBuLi, for example, had been used according to the manufacturer specified concentration. However, since the solution contained a precipitate of lithium hydroxide or lithium hydride, presumably formed on exposure to moisture, it was evident that the concentration of nBuLi was probably lower than stated, and efforts were made to find a practical and routine method to measure the concentration of the nBuLi. A decoupled nondeuterated solvent NMR experiment was attempted to measure the concentration of the organolithium.⁷¹ This experiment did not work due to instability in the magnetic field, and a titration was then used to determine the concentration according to a method developed by Lipton *et al.*⁷²

The method recommended the use of 1,5-diphenylacetone *p*-tosylhydrazone. Unfortunately, this reagent was not readily available, and diphenyl acetic acid (**38**) was used as a substitute (Scheme 12). The titration was carried out at 0°C in dry THF. The mono-anion (**39**), formed by the addition of one equivalent of nBuLi, is colourless, and a sharp colour change to the bright orange of the di-anion (**40**) was observed immediately after the addition of the first equivalent. It was thus found that a solution presumed to be 2.5 M was in fact only 2.0 M. Thereafter the concentration of the organolithium was regularly checked before each synthesis was attempted.



Scheme 12: Reaction of diphenyl acetic acid with nBuLi

Another possible source of difficulty was that the tributyltinlithium did not form *in situ* as expected. This could have been due to the presence of small amounts of peroxides in THF, which then would easily form radicals and hence induce radical reactions [equations (i) and (ii)] instead of nucleophilic addition reaction [Scheme 13, equation (iii)]. The side products formed in this way were not identified.



Scheme 13: Formation of peroxides in THF (i) and a possible mechanism for the formation of radicals (ii) that prevent the formation of Bu_3SnLi (iii)

Organolithiums have been known to react with solvents depending on the temperature at which they are used; THF is decomposed by butyllithium at a fast rate if left at room temperature *via* a reverse cycloaddition reaction to form ethylene and a lithium enolate of acetaldehyde.⁹ This may also have played a role in the failed transmetallation reaction, if the temperature was not maintained below 0°C.

Heptaldehyde (**35d**) was used to synthesise the alkoxytannane **37d**. The long aliphatic chain may have hindered the attack of tributylstannyl lithium at the carbonyl carbon and thus reduced the formation of the corresponding stannous alcohol. TLC analysis of the crude mixture appeared to show evidence of the characteristic spot of the product **37d** as well as numerous side products such as tetrabutyltin, and reagents including heptaldehyde and dimethyl aniline. The crude mixture was purified on a silica column using 10% ethyl acetate in hexane as the solvent system. 1D NMR analysis of the appropriate fraction exhibited signals apparently belonging to the protected stannous alcohol **37d** as well as several impurities. The mixture was therefore purified further by radial chromatography using 10% dichloromethane in hexane. This served to slow down the movement of the product and enable better separation from the unwanted side products. The first compound eluted was tetrabutyltin, as is characteristic of all the stannanes in the purification step. The second compound, presumed to be the product, was eluted as a mixture. 1D NMR analysis of this particular fraction confirmed that the product had decomposed on the chromatotron plate and was therefore not isolated. The reason for its decomposition may be because of its instability during storage or the

affinity of the product for tetrabutyltin due to their shared lipophilicity and the resulting difficulty in separating the two components.

The synthesis of α -alkoxystannanes derived from paraformaldehyde (**35e**) and cyclohexanone (**35f**) were previously reported by Sawyer *et al.*,⁵³ where the method was adapted from Still.⁵⁴ Paraformaldehyde is not very soluble in organic solvents and hence it was suspended in dry THF (5 mL) and the solution of tributyltinlithium was added to the reaction flask. Upon the addition of the tributyltinlithium, a colour change occurred from a pale yellow to a dark brown. This is not typical for the series of α -alkoxystannanes synthesized, as the rest of the organolithiums are pale yellow in colour.⁵³ After the suggested reaction time of 5 hours, there was still a white solid present, presumed to be unreacted paraformaldehyde. ¹H and ¹³C NMR analysis of the fractions showed the presence of the protected α -alkoxystannane **37e**. However, upon further purification using the ChromatotronTM, the product **37e** decomposed and was not isolated.

In this study, the use of cyclohexanone, a ketone, was unusual but the same synthetic approach was used and the reaction was expected to follow the same mechanism as for the aldehydes. The reaction mixture was left stirring for a longer time, 16 hours as opposed to the 5 hours which was used for compounds **37a-e**, in an attempt to ensure nucleophilic attack on the carbonyl carbon. This was not a problem for Sawyer *et al.*⁵³ as they achieved a 60% yield within 15 minutes. The crude mixture was a dark yellow oil, and on purification with column chromatography the compound **37f** was not isolated. It is possible that the mixture was left to stir for an excessive period of time, during which decomposition of the intermediate stannous alcohol took place. The decomposition of organostannanes has been previously reported by Behling *et al.*,⁷³ where destannylation was the most common route for decomposition of organostannanes.

Purification of the organostannanes was difficult. Fractional distillation was not considered to be a viable route because the compounds are viscous oils and consequently have high boiling points.^{45, 74} Chromatography was chosen as the preferred option although organostannanes have been found to elute very quickly on silica gel even when using hexane as the eluent, unless they contain very polar substituents.⁷⁴ In this study the protection of the hydroxyl moiety makes the α -alkoxystannane less polar and thus confers on it a high R_f value. Purification of the compounds **37a-f** proved difficult as the side products such as tetrabutyltin and unreacted starting materials such as the respective aldehydes had very close R_f values. In a solvent system of 10% ethyl acetate in hexane, compound **37a** had an R_f value of 0.73, whilst the tetrabutyltin was 0.85 and the next compound after the

product eluted with an R_f value of 0.61. In earlier attempts to purify this compound, much of **37a** was lost in other fractions because the product and side products co-eluted and the silica gel may have caused destannylation due to its acidic nature.⁷³

Farina used a reverse phase procedure with C-18 to purify organostannanes.⁷⁴ This procedure eliminated the decomposition of the organostannane and used dichloromethane and acetonitrile as the solvent system. Although the effective purification was comparable with that developed by Still,⁷⁵ for this work, a C-18 support was not available. However, when dichloromethane was used as a 10% solution in hexane on silica gel, most of the components, including the product **37a** had a lower retention factor ($R_f = 0.26$), which facilitated the easy removal of the major impurity, tetrabutyltin, which still maintained an R_f value of 0.85. The solvent system was then changed to elute the α -alkoxystannane using 10% ethyl acetate in hexane solution with minimal loss on the column. A slower flow rate was also found to be advantageous for the good separation of the range of compounds which previously co-eluted with the product.

c) NMR characterisation

The characterization of the α -alkoxystannane products was at first hindered and then facilitated by some unexpected behaviour. The ^1H NMR spectrum of the α -alkoxystannane **37a** revealed two doublets at 4.61 ppm and 4.55 ppm respectively (Figure 6). The signals correspond to the diastereotopic protons of the methylene between the oxygen atoms of the MOM group. These protons are not in the same chemical environment because they are near to a chiral centre, and thus they resonate at different frequencies, and couple to each other with a geminal coupling constant of 6.7 Hz.

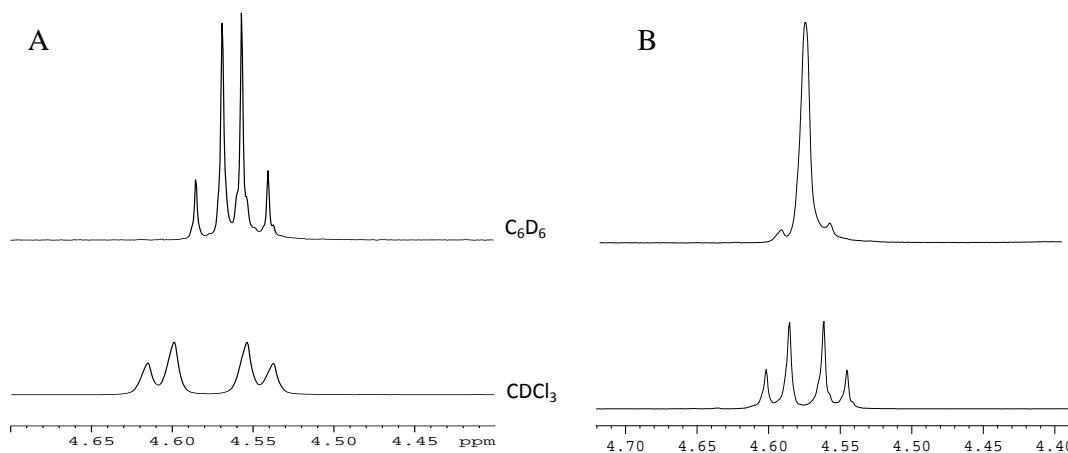


Figure 6: Expanded region (4.70 – 4.40 ppm) of 400 MHz ^1H NMR spectrum of α -alkoxystannane **37a** (A) and **37c** (B) showing the effect of solvents on the chemical shift

In different solvents (deuterated chloroform and deuterated benzene) these protons resonate at different frequencies. As a result, in chloroform, where the difference in chemical shift (17 Hz) is much greater than the coupling constant, the two signals appear as slightly distorted doublets. In benzene on the other hand the difference in chemical shift (4.8 Hz) is smaller than the coupling constant and the two signals appear as a distorted quartet. The COSY spectrum (Figure 8) showed that the signal is not a quartet since there is no coupling to any other nuclei. This same effect is seen in the remaining α -alkoxystannanes **37b** and **37c** with a similar spectrum observed in chloroform and benzene (Figure 6). In the spectrum of the α -alkoxystannane **37c** the two diastereotopic proton signals appear as two doublets in chloroform and then as a singlet (with satellites) in deuterated benzene, where the difference in chemical shift becomes much smaller than the coupling constant. This further illustrates the effect of the solvent on the chemical shift.

Not all the diastereotopic protons can be observed in the ^1H NMR, for example, if the difference in chemical shift is zero it will appear as a singlet. A general guide is that the methylene protons closer to the stereogenic centre are more likely to be observed as separate signals than those further away. Furthermore the protons in a more rigid environment are more likely to show obvious differences than those in a flexible, freely rotating part of the molecule.⁵

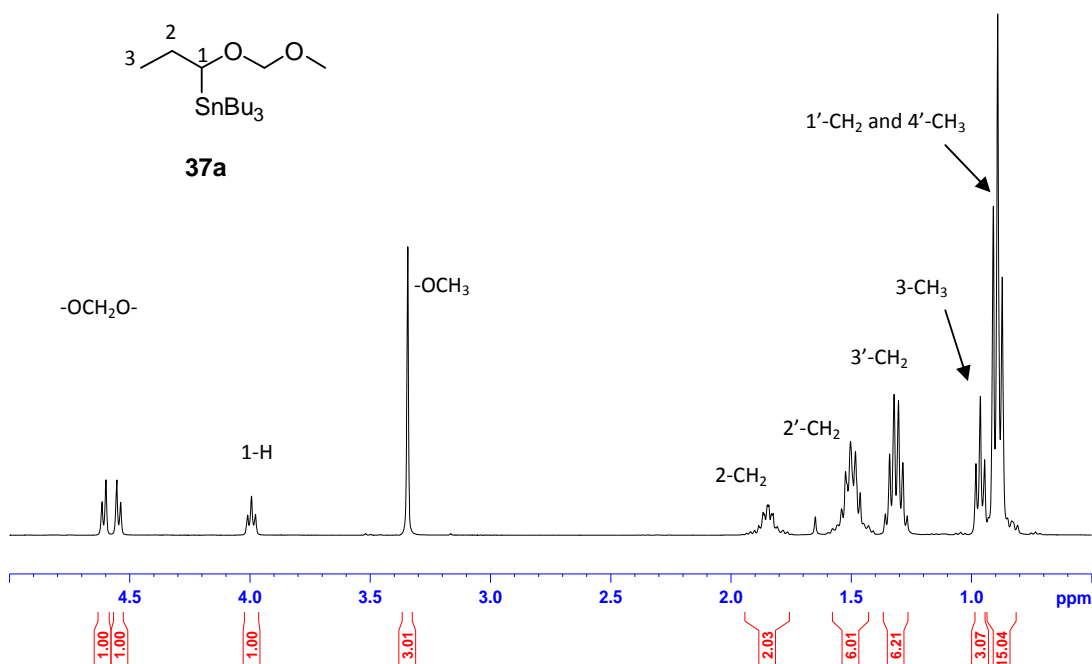


Figure 7: 400 MHz ^1H NMR spectrum of α -alkoxystannane **37a** in CDCl_3

The remainder of the spectrum of each stannane was relatively simple to assign, as described for **37a** (Figure 7). The triplet at 3.99 ppm corresponds to the methine proton at the chiral centre, while the methoxy of the MOM protecting group resonates at 3.34 ppm with evidence of ^{13}C satellites (Figure 7). The $^1J_{\text{C,H}}$ coupling constant is 70 Hz, and is caused by the 1.1% of carbon atoms that have a ^{13}C nucleus.⁷⁶ The protons of the methoxy group couple to the ^{13}C nucleus and give rise to a doublet in the ^1H spectrum, which appear as satellites with an intensity of 0.5% of the main peak.⁷⁶ The multiplet at 1.84 ppm corresponds to the 2-methylene protons. The splitting pattern is complex due to the tin-proton coupling ($^3J_{\text{H,Sn}}$) and proton-proton ($^3J_{\text{H,H}}$) coupling with the adjacent 3-methyl protons and the 1-methine proton. The multiplet at 1.41-1.60 ppm corresponds to the 2'-methylene protons on the butyl chain. There are three butyl chains attached to the tin centre, nonetheless the protons experience the same chemical environment and appear as one signal. The splitting pattern shows that the protons are coupled to four adjacent protons and these correspond to the methylene protons on C-1' and C-3'. The triplet at 0.96 ppm with a coupling constant of 7.2 Hz corresponds with the terminal methyl group at C-3, these protons are chemically equivalent and couple to the methylene protons on C-2. These correlations were confirmed by a COSY spectrum. (Figure 8)

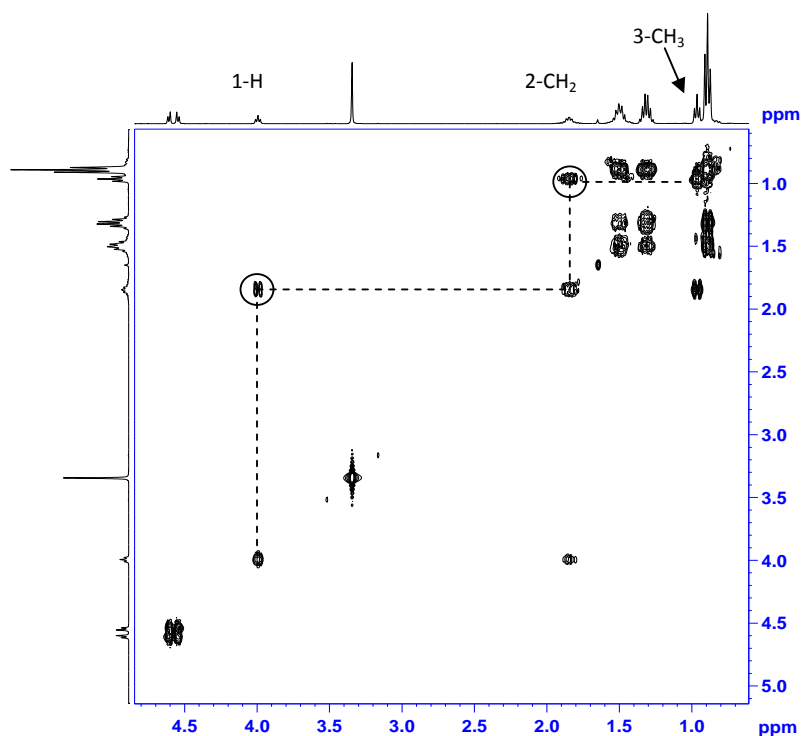


Figure 8: 400 MHz COSY spectrum of α -alkoxystannane **37a** in CDCl_3

The DEPT135 spectrum (Figure 9) shows 9 signals which correspond to the 17 proton bearing carbons in the compound **37a**. The three butyl chains of the tributyltin moiety are chemically equivalent hence only 4 signals are observed and the remaining signals are accounted for. The methylene carbon of the MOM protecting group, resonating at 96.4 ppm, the chiral carbon at 75.7 ppm, and the methoxy carbon at 55.3 ppm accounted for the oxygenated carbons. The methylene carbons of C-2', C-2 and C-3' resonated at 29.2, 27.9, and 27.5 ppm respectively. The methyl carbons of C-4' and C-3 appeared at 13.6 and 12.3 ppm respectively and the methylene carbon of C-1' resonated at 9.2 ppm. The DEPT135 spectrum confirmed the presence of five methylene signals and assisted with the correct assignment of the carbons. Satellites observed in this spectrum are due to the $^{117/119}\text{Sn}$ - ^{13}C coupling (Figure 9).

α -Alkoxystannanes **37b** and **37c** are constitutional isomers with the same chemical formula ($\text{C}_{18}\text{H}_{40}\text{O}_2\text{Sn}$) but have different structures, hence they have different chemical and physical properties.⁵ This is observed in the ^{13}C NMR spectra of the two isomers, with a slight change in chemical shift for the corresponding carbons (Table 1). The major differences in chemical shifts are found for the carbons closer to the tin centre, namely C-1, C-2 and C-1' as well as the terminal carbon, C-4.

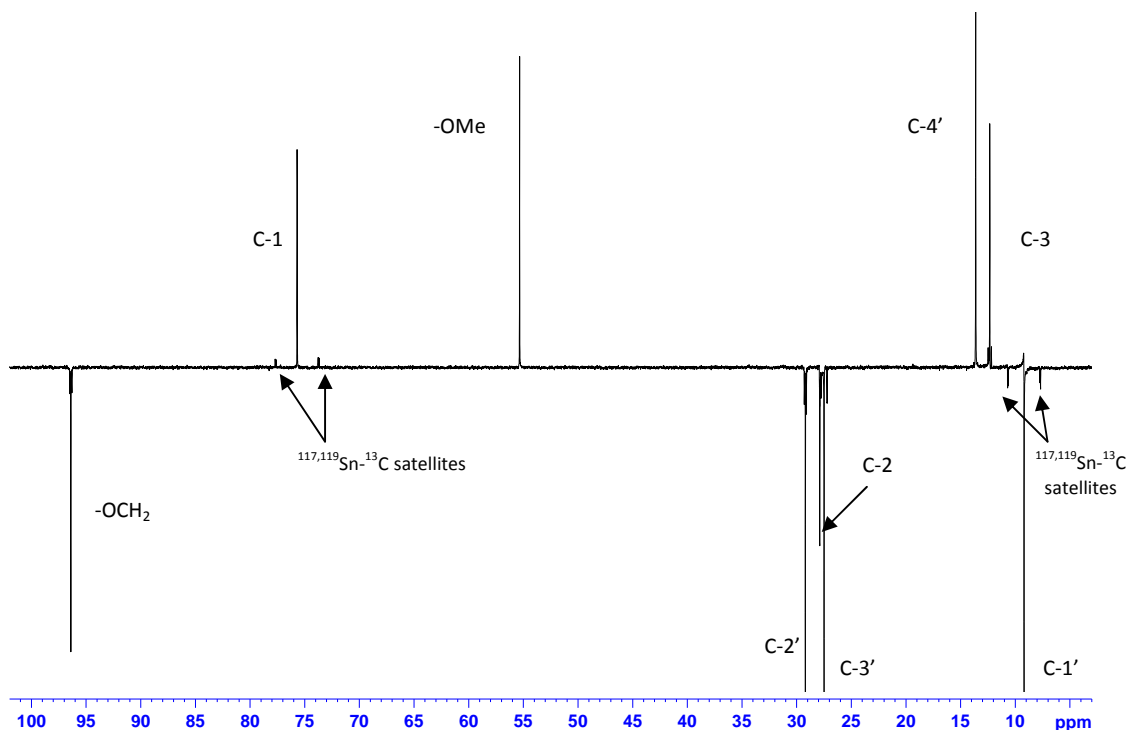


Figure 9: 400 MHz DEPT135 spectrum of α -alkoxystannane **37a** in CDCl_3

The α -alkoxystannane **37c** the isopropyl chain should have the methyl carbons (C-3 and C-4) which resonate with the same chemical shift as they appear to be in the same chemical environment. However, C-3 and C-4 of the isomer **37c** are diastereotopic as a result of being next to the chiral centre, and therefore they have different chemical shifts of 21.5 ppm and 20.2 ppm (Table 1).

Table 1: Comparison of ^{13}C chemical shifts (100 MHz) in CDCl_3 of isomers **37b** and **37c**

Carbon	37b δ_{C} ppm	37c δ_{C} ppm
OCH_2	96.9	97.3
OCH_3	55.4	55.4
C-1	74.1	82.4
C-2	38.1	33.3
C-3	21.8	21.5
C-4	14.4	20.2
C-1'	9.7	10.4
C-2'	29.9	29.7
C-3'	28.1	28.0
C-4'	13.9	13.9

Tin has ten naturally occurring isotopes, three of which (^{115}Sn , ^{117}Sn and ^{119}Sn) have a nuclear spin $\frac{1}{2}$, which makes them suitable for NMR studies.¹³ Their relative abundances are 0.35, 7.61 and 8.58% respectively. The relative abundance is much greater than the ^{13}C isotope (1.108%) and this makes tin more sensitive and explains why the effects of the coupling are observed in the 1-D spectra (Figure 10). The low relative abundance of ^{115}Sn and its gyromagnetic ratio of -8.801 ($10^7 \text{ rad T}^{-1} \text{ s}^{-1}$), means that it does not contribute to the observable effects in the NMR spectra. The $^1J(^{119}\text{Sn}-^{13}\text{C})$ coupling constant of 404 Hz, which is larger than the $^1J(^{117}\text{Sn}-^{13}\text{C})$ coupling constant of 386 Hz. The size of the coupling constant is proportional to the gyromagnetic ratio of each isotope. The ratios are -10.014 and -9.589 ($10^7 \text{ rad T}^{-1} \text{ s}^{-1}$) for the ^{119}Sn and ^{117}Sn isotopes, and hence the ^{119}Sn isotope will have a larger coupling constant in comparison with the ^{117}Sn isotope in the ^{13}C spectrum (Figure 10). The ratio of $J(\text{Sn}^{119})/J(\text{Sn}^{117})$ observed from the spectrum of **37a** is 1.0466 which is in agreement with literature,^{13, 77, 78} with 1.0462 referenced as the appropriate value (Table 2). The intensities of the satellites are proportional to the relative abundances of each isotope.⁷⁷

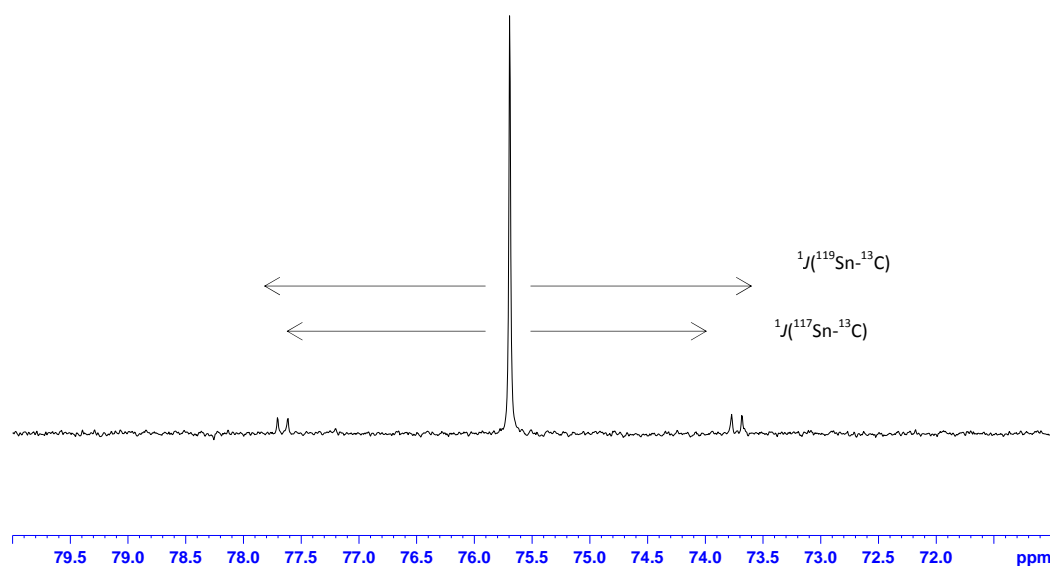


Figure 10: Expanded region (400 MHz, 70 – 80 ppm) DEPT135 spectrum of α -alkoxystannane **37a** in CDCl_3 illustrating the Sn-C coupling at C-1

An interesting pattern develops in the coupling constants between tin and carbon. The closer the carbon is to the tin atom, the larger the coupling constant observed and the carbon which is four bonds away has no coupling present. This fits the trend found in similar organotin compounds studied by Kuivila and co workers⁷⁹, as well as Al-Allaf.⁸⁰ A summary of the coupling constants found for the three α -alkoxystannanes **37a-c** is shown in Table 2. Not all of the carbons exhibit satellites, because there is a four bond distance which does not allow for strong coupling to take place

between the carbon and tin nucleus. For the direct one bond coupling constants, two sets of satellites are observed correlating to the two isotopes ^{117}Sn and ^{119}Sn . For the two bond ($^2J_{\text{Sn-C}}$) and three bond ($^3J_{\text{Sn-C}}$) coupling, the satellites overlap hence appear as only one pair of doublets but the satellites represent both the doublets from isotopes ^{117}Sn and ^{119}Sn . The direct coupling constants ($^1J_{\text{Sn-C}}$) are large because the carbon and tin are directly bonded with a large orbital overlap of the sigma bond and so there is a closer interaction between the magnetic moments of each nuclei.^{76, 79}

Table 2: $J_{\text{Sn-C}}$ coupling constants observed in 400 MHz ^{13}C spectra for compounds **37a-c**

Stannane	$J_{\text{Sn-C}}/\text{Hz}$	C-1 ^a	C-3	OCH ₂	C-1' ^a	C-2'	C-3'
37a (CDCl ₃)		386.4, 404.4	31.0	19.8	291.0, 304.4	19.6	54.4
	Sn ¹¹⁹ /Sn ¹¹⁷ ratio	1.0466			1.0461		
37b (C ₆ D ₆)		396.8, 413.0	31.8	20.4	287.8, 301.4	20.0	53.2
	Sn ¹¹⁹ /Sn ¹¹⁷ ratio	1.0408			1.0473		
37c (C ₆ D ₆)		397.2, 413.8	30.6	20.4	286.2, 299.2	20.4	54.2
	Sn ¹¹⁹ /Sn ¹¹⁷ ratio	1.0418			1.0454		

^a Where two coupling constants are given, the smaller refers to $^1J(^{117}\text{Sn}-^{13}\text{C})$ and the larger to $^1J(^{119}\text{Sn}-^{13}\text{C})$

The magnitude of $^nJ(^{119}\text{Sn}-^{13}\text{C})$ depends on the solvent used, in more polar solvents such as CDCl₃ a decrease in magnitude as compared to C₆D₆ has been observed.^{80, 81} This is illustrated in Table 2 where the α -alkoxystannane **37a** in CDCl₃ has a coupling constant $^1J(^{119}\text{Sn}-^{13}\text{C})$ for C-1 of 404.4 Hz while the α -alkoxystannanes **37b** and **37c** in C₆D₆ have a larger coupling constant $^1J(^{119}\text{Sn}-^{13}\text{C})$ for C-1 at 413.0 and 413.8 Hz respectively. As expected, the size of the coupling constants varied as follows: $^1J > ^3J > ^2J$.⁸¹

d) Infra-red spectroscopy and Molecular modelling

Infra-red spectroscopy was another technique used to fully characterize the α -alkoxystannanes **37a-c**. Mid IR as well as far IR were carried out in order to observe the C-Sn vibrations/stretching which characteristically occur in the region of 700 - 50 cm⁻¹. Although there is in depth data of the mid IR region available for most organotin compounds from literature,^{53, 54} the far IR region was less well documented. In this study DFT calculated spectra were used in order to assist in the assignment of the IR data and helped to identify the specific frequencies associated with the Sn-C vibrations.

Calculations were carried out using the Gaussian 03 program.⁸² The level of theory used was Density Functional Theory (DFT) and mixed basis sets B3LYP/gen were used to accommodate the heavy tin atom. Basis sets are functions that describe the atomic orbitals. For heavy atoms such as tin, core electrons are not important and relativistic effects play a role, and hence core electrons are modelled as a function, only treating the valence electrons explicitly. This is known as effective core potential (ECP).^{83, 84} Full geometry optimizations and complete vibrational analyses were done to give the expected IR spectrum (Figure 11).

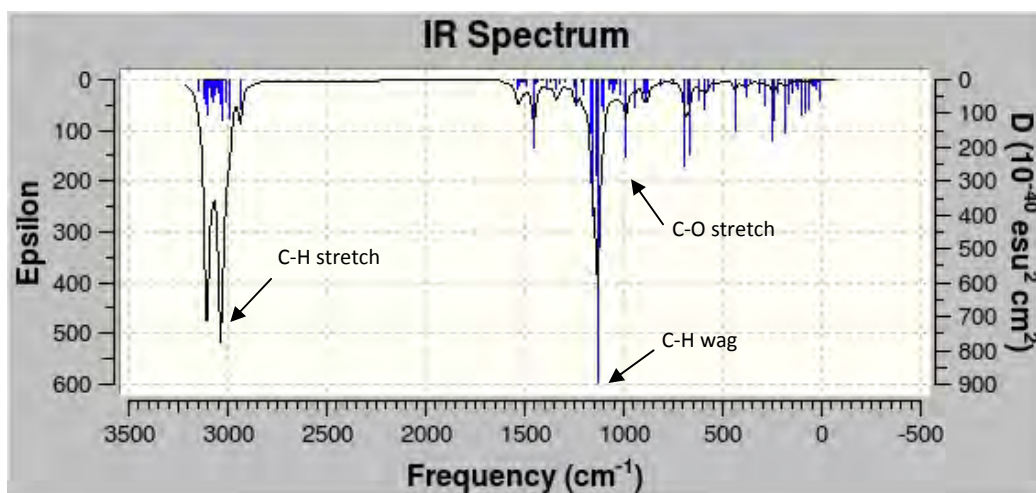


Figure 11: Calculated IR spectrum obtained from model of α -alkoxystannane **37a**

This is a model essentially in a vacuum, with no experimental considerations factored into the calculation. This is evident when comparing the theoretical spectrum with the actual IR spectrum obtained for tributyl(1-(methoxymethoxy)propyl)stannane **37a**. Figure 11 shows the calculated IR spectrum with two bands around 3100 and 3030 cm^{-1} which correspond to the C-H stretches, and the band around 1131 cm^{-1} which corresponds to the wagging of the methylene and methyl groups of the propyl chain. The weak band at 988 cm^{-1} represents the C-O stretch of the MOM protecting group. The spectrum shows that the relative intensities in the far IR region are very weak. However, with comparison to experimental data (Figure 12), it was possible to assign frequencies for the Sn-C vibrational modes.

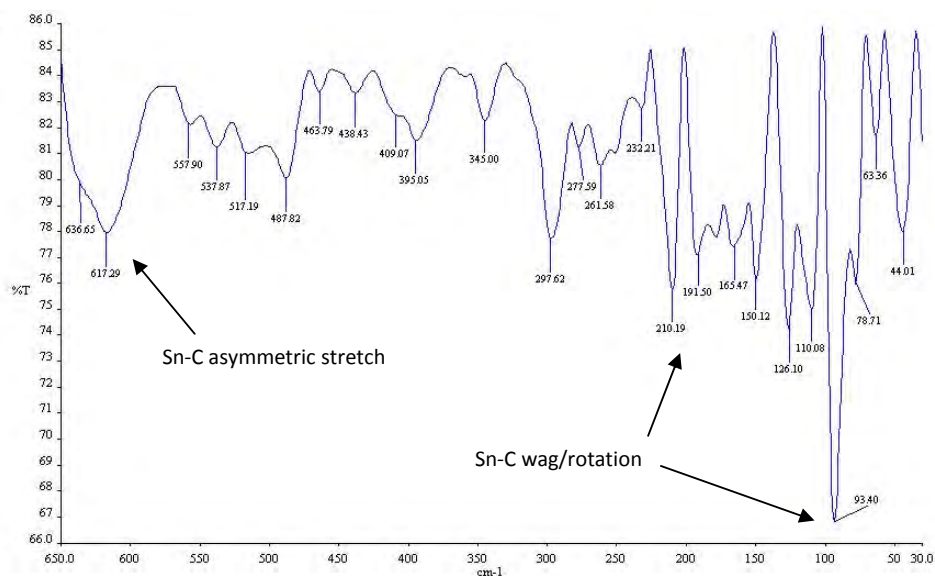


Figure 12: Far IR region (650 to 30 cm^{-1}) of tributyl(1-(methoxymethoxy)propyl)stannane **37a**

The energy optimised structures of the remaining α -alkoxystannanes, **37b** and **37c** were also calculated and the frequency analysis was used to obtain the expected IR spectra. This was then compared with the experimental data obtained to fully assign the vibrational modes. In all cases there was a good correlation between calculated and experimental data for key frequencies (Table 3). An anomaly is noted for the C-Sn bond frequency of stannane **37a** which has a calculated frequency of 596 cm^{-1} ; however the experimental frequency recorded is 617 cm^{-1} . No apparent reason can be deduced, however the signal is very broad and this may account for the difference (Figure 12).

Table 3: A summary of significant vibrational frequencies observed for the α -alkoxystannanes

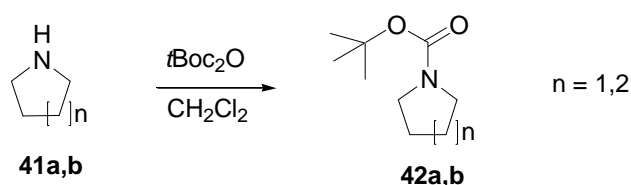
Bond	37a / cm^{-1}		37b / cm^{-1}		37c / cm^{-1}	
	Calc.	Exp	Calc.	Exp	Calc.	Exp
C-O	988.18	1358.05	984.44	1378.42	1133.43	1070.00
C-H _{stretch}	3031.58	2956.04	3027.18	2957.71	3030.19	2956.04
C-H _{bend}	1455.05	1462.30	1458.49	1463.03	1456.01	1462.30
C-Sn	596.00	617.29	595.88	593.93	594.02	593.27

2.2.2. α -Aminostannanes

a) Synthesis and characterisation

The aim of this project was to synthesise a series of α -aminostannanes derived from pyrrolidine (**41a**) and piperidine (**41b**). The stannanes were synthesised according to the method described by Beak *et al.*,^{63,85} using *sec*-BuLi·TMEDA as the lithiating base.

The reaction differs from that described for the α -alkoxystannanes as it is an α -directed deprotonation/lithiation and subsequent electrophilic substitution reaction. In order to achieve the α -directed deprotonation the pyrrolidine (**41a**) was reacted with di-*tert*-butyl dicarbonate to form the carbamate protected derivative, *tert*-butyl pyrrolidine-1-carboxylate (**42a**, Scheme 14). The *tert*-butoxycarbonyl (*t*-BOC) group is an activating group that has a dipole stabilizing function for the α -lithiation and electrophilic substitution next to the nitrogen.^{85, 86} The use of the *t*-BOC group is convenient and very useful for secondary amines, and a more suitable option compared with a formamide group that was used previously by Meyers and co-workers.⁸⁷



Scheme 14: Formation of the N-BOC protected derivatives **42a** and **42b**

The ¹H NMR spectrum of N-BOC pyrrolidine **42a** (Figure 13) showed a broad multiplet at 3.28 – 3.33 ppm which corresponds to the methylene protons, 2-CH₂ and 5-CH₂ adjacent to the nitrogen. The protons are shifted downfield due to the interaction with the adjacent electronegative nitrogen atom. The resonance is broad because of the restricted rotation about the amide bond of the carbamate group, causing the two methylenes to experience different environments.⁷⁶ The frequency of the rotation is temperature dependant and at higher temperatures the rotation is faster hence the protons will appear as a singlet. However, at lower temperatures the hindered rotation plays a role in the chemical environment of the protons and they appear as two signals. The restricted rotation is caused by the delocalization of the electrons from the lone pair of the nitrogen and the carbonyl π -bond (Figure 13).⁷⁶

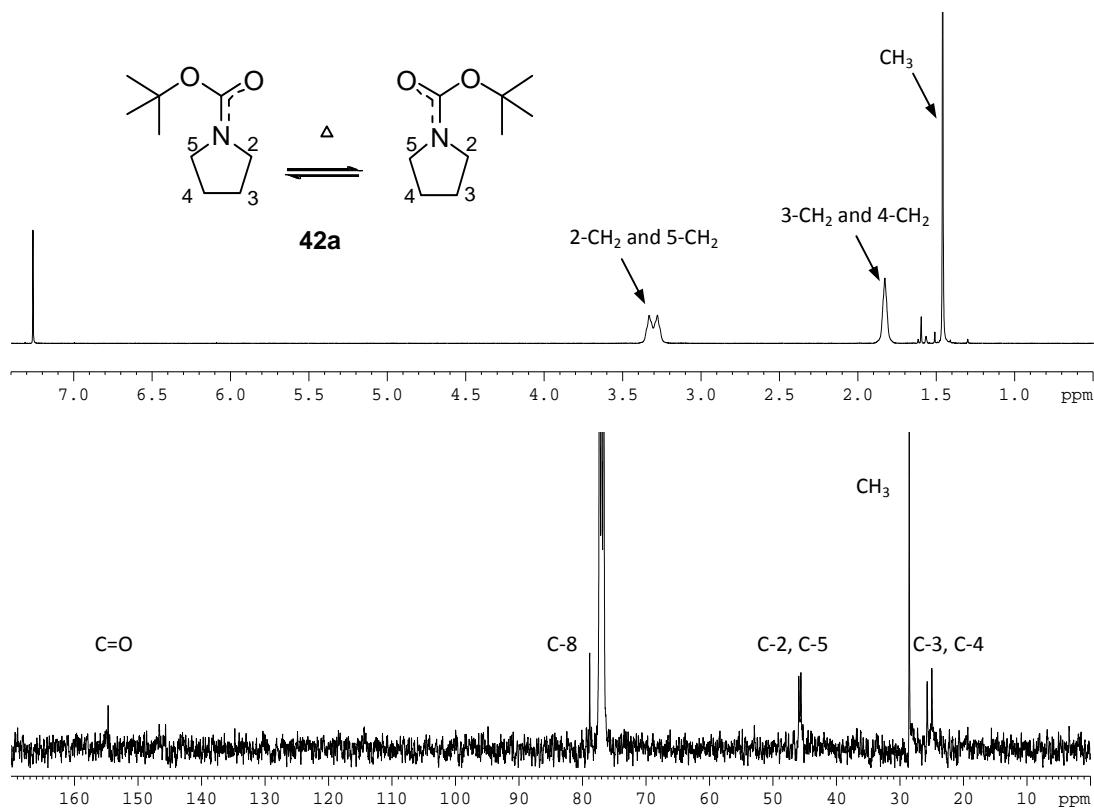
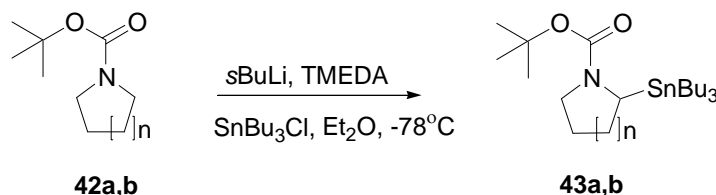


Figure 13: 400 MHz ^1H and 100 MHz ^{13}C spectra of *tert*-butyl pyrrolidine-1-carboxylate **42a** in CDCl_3

The ^{13}C spectrum of *N*-BOC pyrrolidine **42a** (Figure 13) shows the expected seven signals. The two quaternary signals which represent the carbonyl and *tert*-butyl carbon appear at 154.7 and 78.9 ppm respectively. The methylene carbons C-2 and C-5 resonate very close together at 45.9 and 45.6 ppm and appear as broad signals due to the restricted rotation described earlier. The methyl carbons resonate at 28.6 ppm while the remaining methylene carbons, C-3 and C-4, resonate at 25.8 and 25.0 ppm respectively. The DEPT135 spectrum confirmed these assignments. The broad singlet at 1.83 ppm corresponds to the methylene protons, 3- CH_2 and 4- CH_2 and the nine methyl protons of the *tert*-butyl group resonate at 1.46 ppm as a singlet.

A cyclohexane solution of *sec*-BuLi was used for the α -lithiation reaction (Scheme 15). This organolithium is known to have a higher degree of association in solution than *n*BuLi and therefore a bifunctional Lewis base additive, TMEDA, is added. It coordinates with the lithium and thus decreases the degree of association, thereby increasing the basicity of the *sec*-BuLi.⁸⁸ The addition of tributyltin chloride to the cold mixture allowed for the substitution to take place, and the α -aminostannane, **43** was obtained in 46% and 61% yield for the pyrrolidine and piperidine derivatives respectively. The lithiation of the *N*-BOC piperidine analogue **42b** takes longer than for

N-BOC pyrrolidine **42a** as found by Beak *et al.*,⁸⁵ (6 h for N-BOC piperidine and 4 h for N-BOC pyrrolidine).



Scheme 15: Formation of N-BOC α -aminostannanes **43a** and **43b** (a: n=1; b: n=2)

The ^1H spectrum for the N-BOC α -aminostannane **43a** (Figure 14) gave a more complex spectrum where the splitting pattern of the methylene protons in the ring were significantly changed. This resulted from addition of the tributyltin group at C-2. The methine at this position resonates at 3.15-3.11 ppm as confirmed by ^1H - ^{13}C correlation spectroscopy (HSQC). The signals for the protons on C-5 have separated and appear on either side of H-2 at 3.27-3.21 and 3.07-3.01 ppm, which suggested a pseudo-axial and equatorial arrangement of the protons in the 5-membered ring structure. The remaining ^1H signals were assigned from the HSQC (heteronuclear single quantum coherence) spectrum since the signals were overlapping. From the HSQC spectrum it was also possible to assign the methylene protons on C-4 which are concealed under the resonance of the C-2' methylene protons in the region of 1.74-1.56 ppm. The methylene protons on C-3 resonate more downfield as a result of being closer to the tin atom and the shift is due to the 'heavy atom effect'.⁷⁶ The signal appears as a multiplet in the range of 1.89-1.78 ppm.

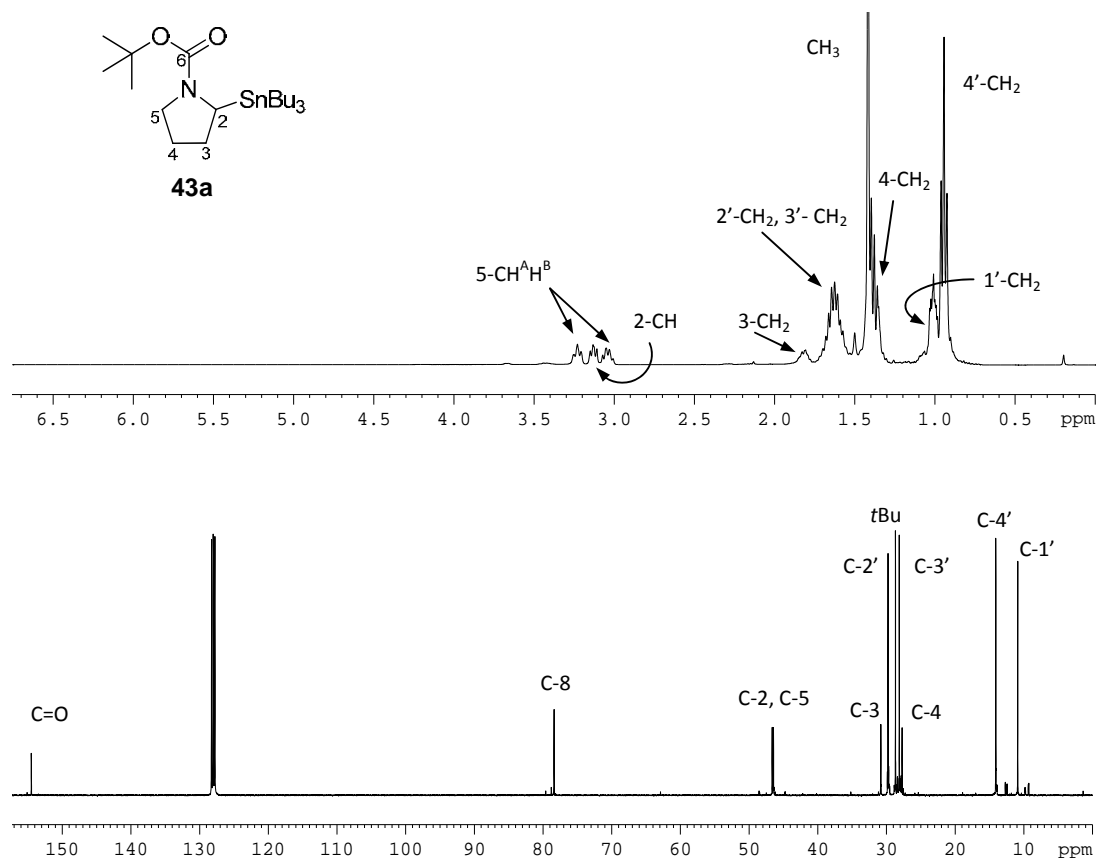


Figure 14: 400 MHz ^1H and 100 MHz ^{13}C spectra of α -aminostannane **43a** in C_6D_6

The proton signals are very broad, since, as discussed earlier, the restricted rotation about the amide bond will play a role as will the ring inversion. The 5-membered ring can exist in two envelope conformations which interconvert and thus exchange the environment that the protons are in. This process results in broader signals when the rate of exchange is close to the frequency difference of the two signals (Figure 15).⁷⁶

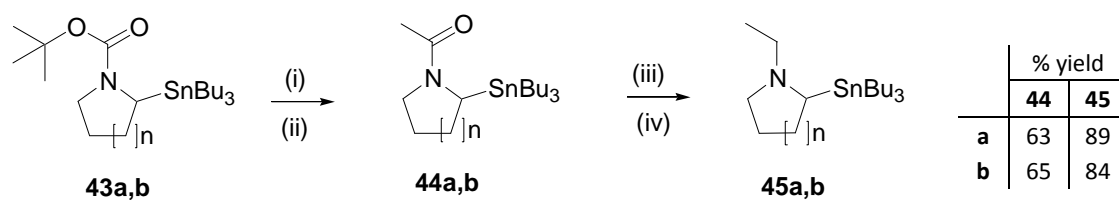


Figure 15: Conformational equilibrium of N-BOC α -aminostannane **43a**

The ^{13}C spectrum (Figure 14) of N-BOC α -aminostannane **43a** showed all the same signals as for the N-BOC pyrrolidine **42a** with four additional signals corresponding to three butyl chains. The relative intensity of the four signals is similar to the three methyl carbons of the *tert*-butyl group. The methylene carbons of the tributyl chain resonate at 29.8 and 28.1 and 10.9 ppm for the C-2', C-3'

and C-1' carbons while the methyl carbon, C-4' has a resonance of 14.1 ppm. The methyl carbons of the carbamate group resonate at 28.7 ppm. The quaternary carbons of the carbamate group shifted only slightly in comparison to the spectrum of N-BOC pyrrolidine **42a** (Figure 13), with the carbonyl at 154.5 ppm and the *tert*-butyl carbon at 78.4 ppm. The methylene carbons C-2 and C-5 resonate at 46.7 and 46.5 ppm respectively while the other two methylene carbons, C-3 and C-4 shifted a considerable amount to 30.8 and 27.7 ppm respectively. The chemical shifts of the tributyltin chain in the ^1H and ^{13}C spectra of α -aminostannane **43a**, are similar to those found in the α -alkoxystannanes and this helped in the elucidation of the 1-D NMR spectra. The distinctive $J(^{119}\text{Sn}-^{13}\text{C})$ also varied according to the trends for direct, two bond or three bond coupling.

The N-BOC α -aminostannane **43a** and **43b** was converted to the N-ethyl α -aminostannane **45a** and **45b** via the acetyl derivative **44a** and **44b** (Scheme 16). To remove the N-BOC group, the isolation of the hydroiodide salt was attempted. The procedure was followed according to Gawley *et al.*,⁶⁵ with the aim to isolate white crystals as described. However, the hydroiodide salt was not formed and the crude product mixture was a dark yellow oil. Consequently, a decision was made to continue to the acetyl derivative by the addition of NaOH (2.5 M) and acetyl chloride in a water/dichloromethane mixture. After the work up, TLC of the crude mixture showed that a series of side products were obtained with no trace of product.



Scheme 16: Conversion of N-Boc α -aminostannanes to N-ethyl α -aminostannanes (i) TMSI, dry CH_2Cl_2 , (ii) NaOH (2.5M), Acetyl chloride, (iii) LiAlH_4 in dry Et_2O , (iv) MeOH (a: n=1; b: n=2)

In a second attempt, TMSI was again used to remove the N-BOC group.⁶⁵ The solution turned yellow initially although the colour dissipated within 30 minutes. The addition of NaOH (2.5 M) and acetyl chloride was carried out without an intervening workup according to the method by Ashweek *et al.*⁵⁰ and the subsequent reduction of the acetyl group with lithium aluminium anhydride under anhydrous conditions gave rise to the unstabilized α -aminoorganolithium precursor, N-ethyl-2-(tributylstannyl)pyrrolidine **45a** in good yield (89%).

The changes in the compounds from the N-BOC derivative to the *N*-ethyl derivative can be observed in the ^{13}C spectra (Figure 16). *N*-acetyl-2-tributylstannylpyrrolidine **44a** has a carbonyl resonance which has shifted more downfield to 167.2 ppm, the *tert*-butyl carbon at 78.4 ppm has disappeared and the terminal carbon of the acetyl group resonates at 21.9 ppm while the methylene carbons, C-2 and C-5 have shifted slightly with a greater chemical shift difference between them at 46.7 and 47.9 ppm respectively. What is interesting is that the resonances for the methylene carbons, C-4 and C-3' are coincidentally isochronous at 27.5 ppm, as confirmed by the HSQC spectrum.

The ^{13}C spectrum of *N*-ethyl-2-(tributylstannyl)pyrrolidine **45a** highlighted the disappearance of the carbonyl resonance. The methylene carbon, C-6, emerged at 50.8 ppm, downfield from the C-4 and C-3 as a result of the interaction of the electronegative amine nitrogen. The resonances for the methylene carbons, C-4 and C-3' shifted to 24.3 and 27.5 ppm respectively, with the resonance of the methyl carbon at 14.2 ppm. The isolated yields of both the pyrrolidine and piperidine derivatives (recorded in Scheme 16) highlight the efficient conversion from the N-BOC derivatives to the *N*-ethyl stannanes.

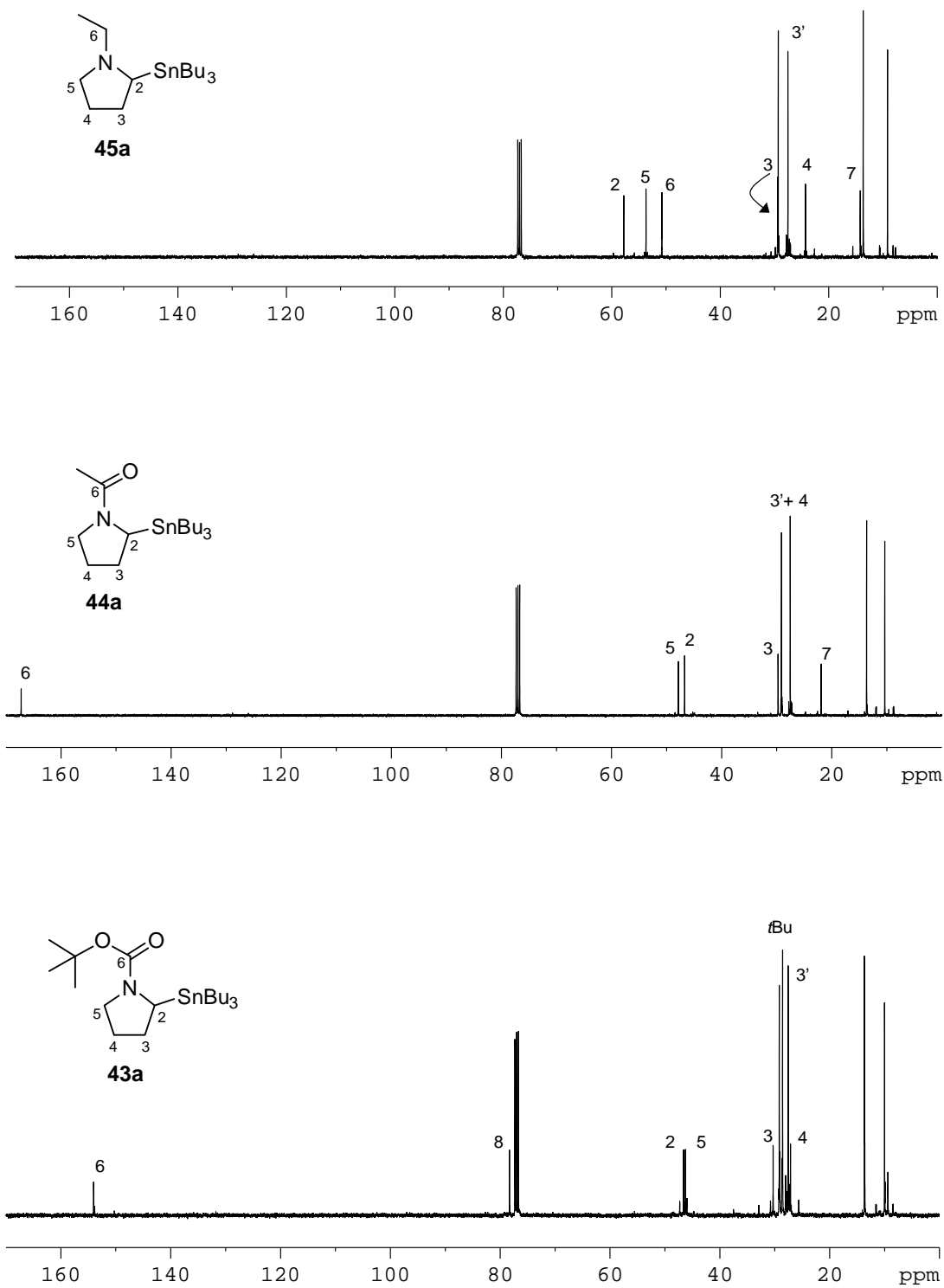


Figure 16: Stacked 100 MHz ^{13}C spectra of α -aminostannanes **43a**, **44a** and **45a** in CDCl_3

The *N*-acetyl and *N*-ethyl aminostannanes derived from the *N*-BOC piperidine α -aminostannane **43b** gave similar changes in the 1-D and 2-D NMR spectra. The coupling constants associated with the $^{117/119}\text{Sn}$ isotopes for each of the α -aminostannanes are recorded below (Table 4). Kitching and co-workers,^{89, 90} observed a Karplus type relationship between the *Sn*-C-C-C torsion angle and the ^{119}Sn - ^{13}C coupling constants. The Karplus relationship has been well established for proton coupling constants and the corresponding dihedral angle.⁵ The coupling is the largest at 180° when the orbitals of the two C-H bonds are parallel, at 90° there is no coupling and at 0° the coupling is very large again as the orbitals are in the same plane but not parallel. This relationship is useful to establish the conformation in cyclic systems.⁵

The Karplus- Kitching relationship can be described according to an equation with error limits of $\pm 3.75 \text{ Hz } (\pm 5^\circ)$ ⁸⁹ : $^3J_{\text{Sn-C}} = 30.4 - 7.6 \cos \theta + 25.2 \cos 2\theta$

This equation and the torsion angles calculated using MM2 force fields enabled Gawley and co-workers to determine the unusual half chair conformation of *N*-methyl piperidine α -aminostannane (**46**) when the tributylstannyl group is in an “equatorial” configuration.⁴⁹ The coupling constant ($^3J_{\text{Sn-C}}$) of the carbon (C-6) adjacent to the nitrogen was 49.2 Hz, while the coupling constant for the same carbon was 47.2 Hz when the tributylstannyl group was in an axial position, with an overall chair conformation.⁴⁹ The coupling constants of the piperidine α -aminostannanes **43b** – **45b** (Table 4) are smaller than 49.2 Hz for C-6 and more in the region of 23.6 Hz suggesting that the configuration is a general chair conformation for all three stannanes (Figure 17).

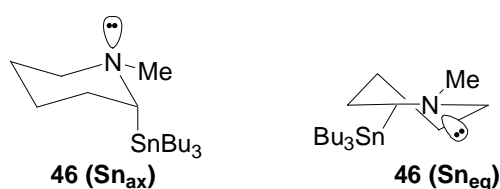


Figure 17: Conformations of *N*-methyl piperidine stannane (**46**)⁴⁹

Table 4: $J_{\text{Sn-C}}$ observed in 400 MHz ^{13}C NMR spectra for compounds **43a,b** – **45a,b**

	$J_{\text{Sn-C}} / \text{Hz}$	C-2 ^a	C-3	C-4	C-5	C-1' ^a	C-2'	C-3'
43a (C_6D_6)		367.6, 383.4	8.8	37.0	13.0	309.8, 323.6	19.8	54.8
	$\text{Sn}^{119}/\text{Sn}^{117}$ ratio	1.0429				1.0445		
44a (CDCl_3)		347.2, 362.8	6.4	29.6	10.4	309.6, 324.6	19.4	55.4
	$\text{Sn}^{119}/\text{Sn}^{117}$ ratio	1.0449				1.0485		
45a (CDCl_3)		376.8, 393.4	-	41.6	52.2	282.2, 296.2	19.8	54.8
	$\text{Sn}^{119}/\text{Sn}^{117}$ ratio	1.0441				1.0492		
	$J_{\text{Sn-C}} / \text{Hz}$	C-2 ^a	C-3	C-4	C-6	C-1' ^a	C-2'	C-3'
43b (C_6D_6)		366.8, 382.8	16.4		17.8	321.4, 336.4	19.6	56.2
	$\text{Sn}^{119}/\text{Sn}^{117}$ ratio	1.0436				1.0467		
44b (CDCl_3)		343.0 360.2	-	32.6	15.0	316.2, 331.6	20.2	36.8
	$\text{Sn}^{119}/\text{Sn}^{117}$ ratio	1.0501				1.0487		
45b (CDCl_3)		307.6, 321.2	-	27.0	26.8	251.2, 261.8	19.4	55.2
	$\text{Sn}^{119}/\text{Sn}^{117}$ ratio	1.0442				1.0422		

^a Where two coupling constants are given, the smaller refers to $^1J(^{117}\text{Sn}-^{13}\text{C})$ and the larger to $^1J(^{119}\text{Sn}-^{13}\text{C})$

It was noted that the heteroatom lone pairs which were close to or involved in the vicinal coupling may affect the size of the coupling constants.⁴⁹ Gawley and co-workers observed that the small coupling constants for *N*-methyl piperidine stannanes (**46**), between the tin and the *N*-methyl group were all less than 18 Hz.⁴⁹ This suggested a torsion angle around 90° which makes the lone pair of electrons of the nitrogen almost eclipsed with the C(2)-Sn bond if it was in a half chair conformation, while the lone pair of electrons of the nitrogen are antiperiplanar to the C-2 and tin bond in the standard chair conformation (Figure 17). This corroborates the experimental data found for the *N*-ethyl aminostannanes **45a** and **45b** which have a coupling constant of 9.0 Hz and 18.2 Hz for the methylenes of the *N*-ethyl group of both **45a** and **45b** respectively.

The ^1H spectra of the piperidine stannanes have very broad signals which may be due to the ring flip of the chair conformation.⁷⁶ The assignment of the protons for *N*-ethyl piperidine stannane **45b** was complex, although that was overcome by elucidation of the HSQC spectrum (Figure 18). The broad signals made it difficult to observe the splitting patterns effectively but the correlations to the carbons assisted in revealing the assignment of the protons attached to the carbons adjacent to the nitrogen atom (C-6 and C-7). The protons attached to C-6 are diastereotopic and so, while the first proton resonates at 2.62 – 2.65 ppm, the other proton resonates at 1.95 – 2.09 ppm which is

overlapping with the resonance of one diastereotopic proton on C-3. The two methylene protons which form part of the *N*-ethyl group (C-7) resonate in between the resonances of the methylene protons attached to C-6 (Figure 18). These proton signals appear sharper as there is more free rotation in the *N*-ethyl group than in the ring conformation.

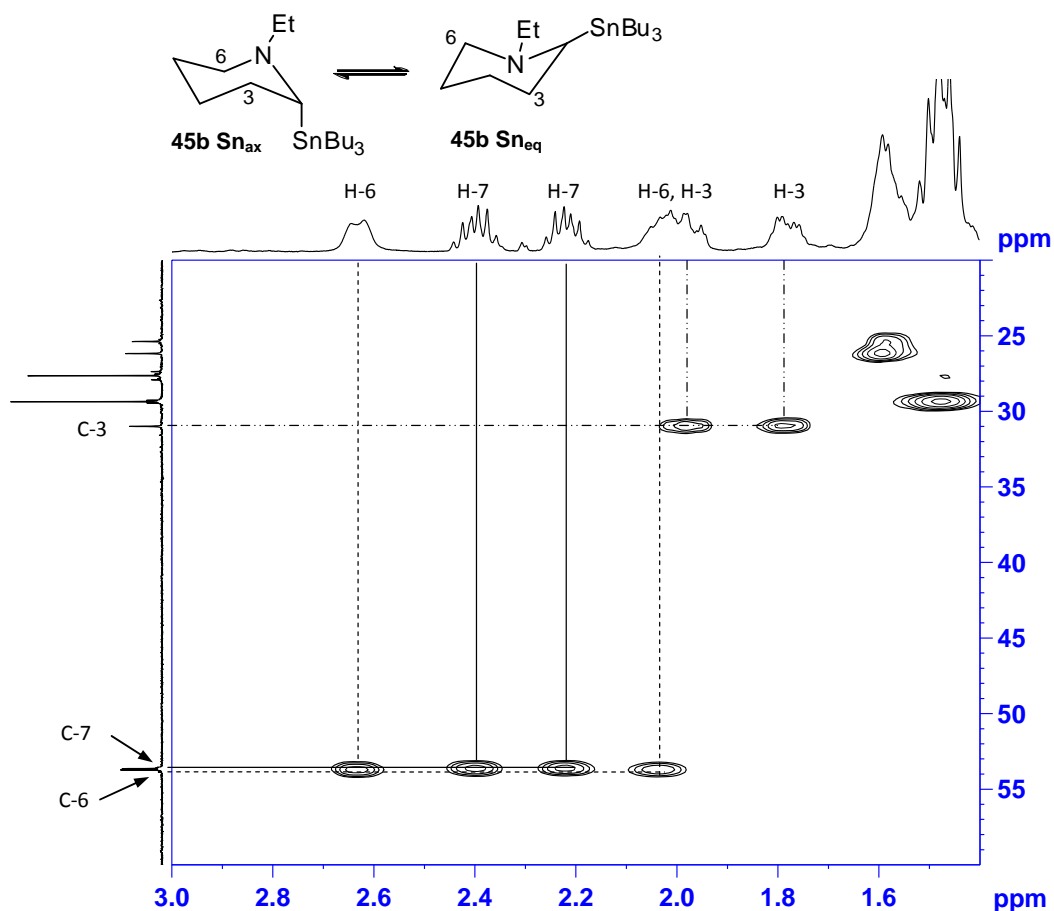


Figure 18: A region (F1 = δ 1.4 – 3.0 ppm; F2 = δ 20 – 60 ppm) of the HSQC spectrum (400 MHz, CDCl_3) of **45b**. The accompanying scheme shows the ring flip between the two chair conformations

b) Infra-red spectroscopy and Molecular modelling

Molecular modelling carried out on all the α -aminostannanes, entailed an energy minimization and frequency analysis using DFT with mixed basis sets B3LYP/gen⁸², as discussed for the α -alkoxystannanes. These calculations in each case resulted in imaginary frequencies, which implied the calculation of a stable transition state for each of the structures. This was not useful for the theoretical calculation of the vibrational spectrum. In order to overcome this challenge, a conformational search was done using a freeware program, VEGA ZZ.^{91, 92} The torsion angles were

optimised which then were used to recalculate the energy optimisation and frequency analysis. The predicted IR spectrum was thus obtained for N-BOC piperidine **43b**, showing the C-H stretches and bends in the region of 3500 to 0 cm^{-1} .

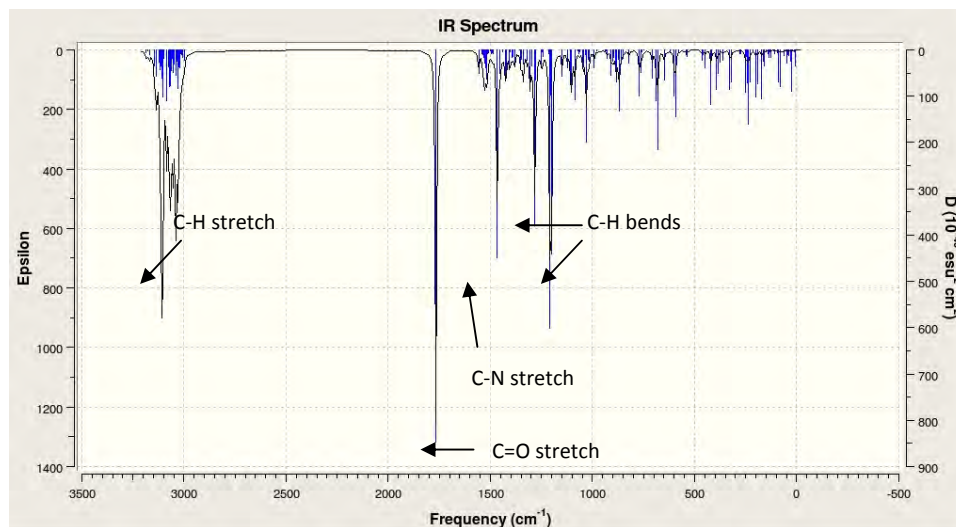


Figure 19: Calculated IR spectrum (3500 – 0 cm^{-1}) obtained from the molecular model of N-BOC piperidine stannane **43b**

The IR spectrum (Figure 19) shows that the carbonyl stretch of the N-BOC group is calculated at 1766.52 cm^{-1} and this fits reasonably well with experimental data of the carbonyl (Table 5). There is a good correlation between the calculated and experimental data for all the α -aminostannanes.

Table 5: A summary of significant frequencies observed for the α -aminostannanes **43a**, **43b**, **45a** and **45b**

Bond	43a / cm^{-1}		43b / cm^{-1}		45a / cm^{-1}		45b / cm^{-1}	
	Calc.	Exp	Calc.	Exp	Calc.	Exp	Calc.	Exp
C-Sn	595.50	592.01	593.61	595.42	592.38	602.82	692.63	674.95
C-N	1433.16	1390.97	1466.21	1421.15	1225.80	1377.05	1258.78	1377.62
C-H	3034.79	2978.02	3029.56	2934.06	3033.63	2958.76	3075.77	2950.54
C-H Et chain	-	-	-	-	1433.12	1463.82	1439.40	1461.81
C-O	1292.05	1253.80	1283.39	1267.52	-	-	-	-
C=O	1769.95	1695.48	1766.52	1692.74	-	-	-	-

The far IR spectrum (Figure 20) of the N-BOC piperidine stannane **43b** highlights the characteristic Sn-C vibrations which include the symmetric and asymmetric stretches at 595.42, 560.80 and 542.05 cm^{-1} .

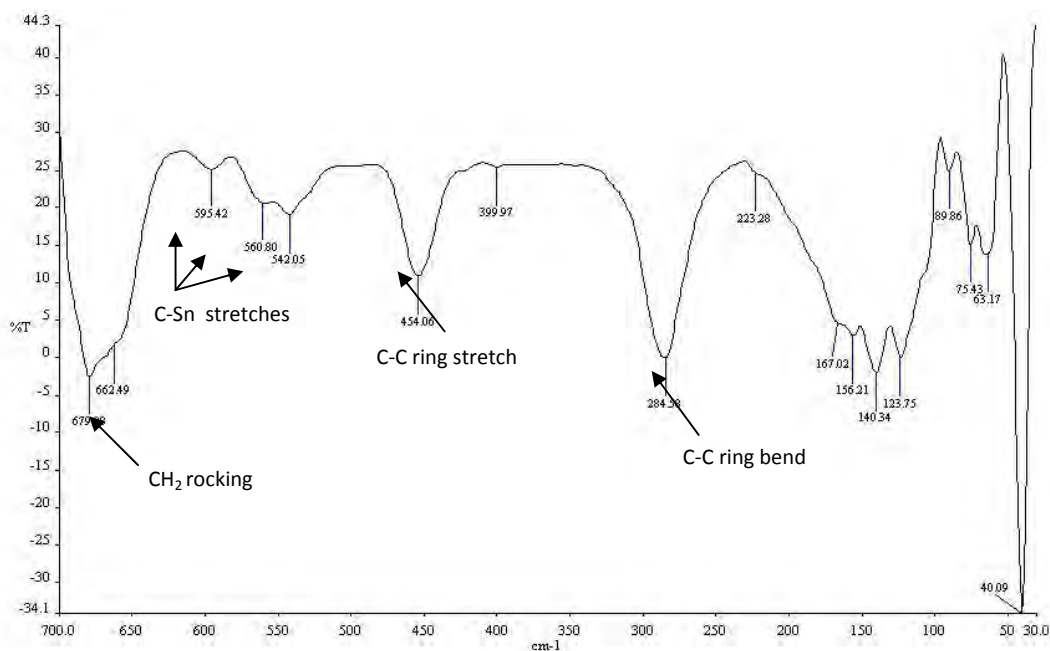


Figure 20: Far IR region (700 – 30 cm⁻¹) of N-BOC piperidine stannane **43b**

2.3. Concluding remarks

The synthesis of α -alkoxystannanes was achieved for three compounds **37a-c** from the respective aldehydes. Six α -aminostannanes were synthesised, three stannanes had a pyrrolidine framework, while the remaining three stannanes consisted of a piperidine framework. The ¹³C NMR analysis highlighted an interesting phenomenon of tin-carbon coupling, which was investigated in depth and revealed unique information regarding the structure of the α -alkoxystannanes and the α -aminostannanes. The theoretical study completed on the series of both α -alkoxy and α -aminostannanes was carried out using DFT analysis on Gaussian 03 program. Frequency analyses were carried out and a predicted IR spectrum was obtained for each of the stannanes. The calculated frequency analysis was consistent with the experimental data recorded, and in agreement with earlier theoretical studies. Future work will include an NMR study of the organolithiums formed *in situ* to probe the reactivity of the organolithiums derived from the α -alkoxy and α -aminostannanes. The aggregation of the organolithiums will be investigated since it is known to influence the reactivity.

Chapter Three: Fischer Chromium Carbenes

3.1. Introduction

3.1.1. Discovery of Carbenes

Organometallic carbenes differ from free carbenes in their reactivity as well as in the generation of the carbene complexes. Metal carbene complexes are made from transition metals and the reactivity and stability of various carbenes have been well documented over the years with a number of reviews being published on this topic.⁹³⁻⁹⁷ The discovery of the first metal carbene was not accredited to Chugaev and co-workers who synthesised a metal carbene in 1915, because the required spectroscopic techniques to reveal the structure were not available until much later.⁹⁵ The structure of the hydrazine-bridged platinum complexes that Chugaev's group synthesised was finally elucidated by X-ray crystal diffraction and NMR techniques in 1973 after further investigations of a possible carbene structure with hydrazines and platinum was explored by Enemark and co-workers.⁹⁸ The first carbene complex to be unmistakably characterised was reported in 1964 by Fischer and Maasböl.⁹⁹ The synthesis of this carbene, methoxyphenylmethylene tungsten (0) pentacarbonyl, was followed by synthesis of carbenes containing chromium (0), iron (0) and manganese (0) and bearing alkoxy and alkyl substituents. At the same time, Wanzlick worked on diaminocarbenes (NHC's) which he thought would be stable due to the presence of the amino substituents,⁹³ however, he was unable to isolate a carbene and only obtained the corresponding enetetramine¹⁰⁰ He later reported an NHC-metal complex¹⁰¹ more than 20 years before the first NHC was isolated by Arduengo.¹⁰² In 1974, the first Schrock type carbene was synthesised from the precursor tri(2,2-dimethylpropyl)methyl tantalum(V) dichloride to obtain the first alkylidene – metal (d^0) complex.¹⁰³

The types of carbenes are classified according to their reactivity, and give rise to three categories. These carbenes are known as Fischer carbenes, Schrock carbenes and *N*-heterocyclic carbenes (NHC's). Fischer carbenes are named after Ernst Otto Fischer who first characterised one of these types of carbenes in the 1960's. They are generally more electrophilic at the carbene carbon centre, contain low oxidation state metals such as tungsten, molybdenum and chromium from Group 6 and commonly have π -donor substituents such as alkoxy and alkylated amino groups which stabilize the complex. These are singlet carbenes as there is a large gap between their singlet and triplet ground states. The carbon metal bond is associated with carbene-metal σ -donor bonding and metal-carbene π -back bonding (Figure 21).⁹³

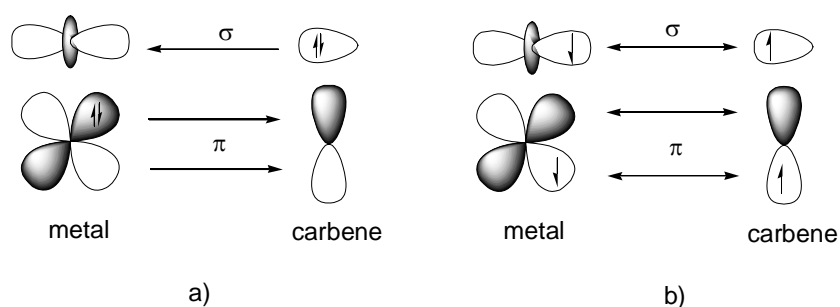
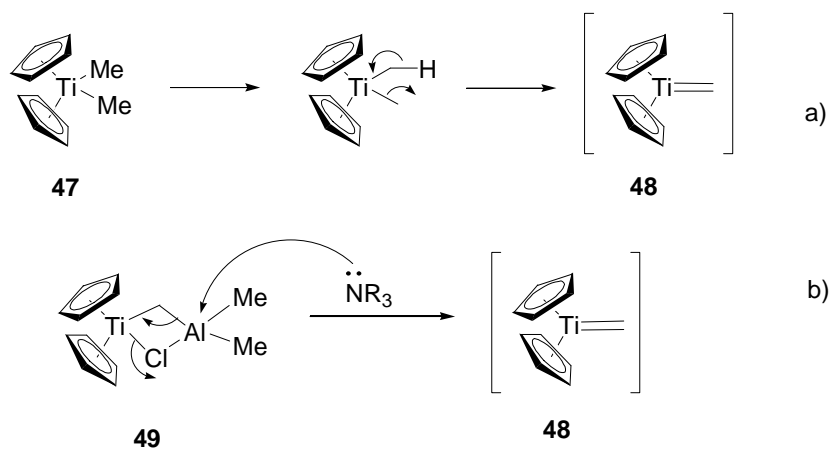


Figure 21: Schematic representations of a) σ -donor and π -back bonding in Fischer carbenes and b) covalent bonding in Schrock carbenes

The Schrock carbenes are named after Richard R. Schrock who first synthesised such carbenes in 1974.¹⁰³ They are more nucleophilic at the carbene carbon centre, and are poorly stabilized as they have a small gap between their singlet and triplet states. The metal and carbene carbon are covalently bonded with the fragments in their triplet ground state (Figure 21). Early transition metals in high oxidation states are used to form these carbene complexes with alkyl substituents.¹⁰³ Synthetic applications of Schrock carbenes include olefination and alkene metathesis. Petasis reagent (**47**) and Tebbe's reagent (**49**), titanium complexes, are used for the olefination of many substrates; a wider range of substrates than can be achieved by the Wittig reaction¹⁰⁴ (Scheme 17). Both Petasis and Tebbe's reagents form a carbene intermediate (**48**) that reacts with the substrate and then releases the terminal alkene product. A major disadvantage is that only a methylene group can be transferred, with the transfer of any larger group being very difficult to achieve.¹⁰⁴⁻¹⁰⁷



Scheme 17: Formation of a Schrock carbene **48** from a) Petasis' reagent **47** and b) Tebbe's reagent **49**^{105, 107}

Grubbs' catalyst (**50**) or Schrock's catalyst (**51**) is used for ring-opening metathesis polymerisation (ROMP) and ring-closing metathesis (RCM) (Figure 22).⁹⁴ Schrock's catalyst is efficient with terminal

and internal alkenes while Grubbs' catalyst is less reactive and has a slow reaction rate with internal alkenes. This is related to the central metal: molybdenum is only stable under inert conditions, while ruthenium is stable in air.

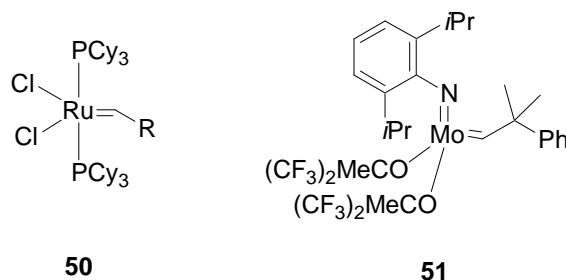


Figure 22: Grubbs' catalyst (**50**) and Schrock's catalyst (**51**) used for alkene metathesis

Metal carbene complexes which fit the description of both Fischer and Schrock carbenes to a certain extent are classified in between. These carbenes are commonly referred to as alkylidenes and benzylidenes, with the type of metal and its oxidation state being inconsequential. A better name for the compounds are alkyl- and phenylcarbenes as the names previously stated have been used to describe some Schrock carbenes.^{95, 108} These complexes are not stabilized by heteroatoms and late-transition metals are used as well as low oxidation states of early transition metals, and are electrophilic at the metal.⁹⁵

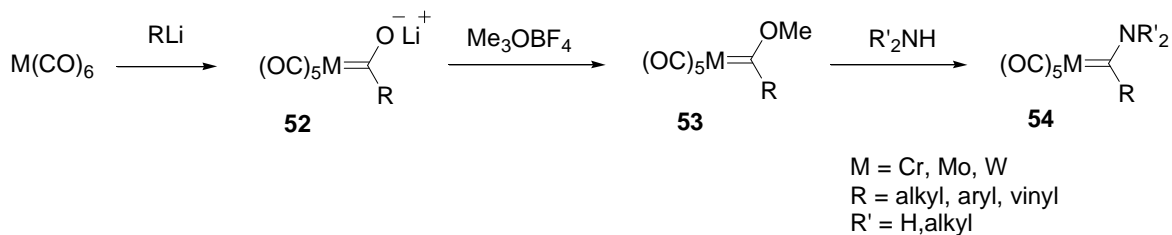
N-Heterocyclic carbenes became more popular after Arduengo was able to isolate a stable carbene, 1,3-bis(adamantyl)imidazole-2-ylidene.¹⁰² These carbenes are diaminocarbenes, with slight changes to the structures having a remarkable effect on the electronic donor properties of the carbene moiety.⁹⁵ One of the limitations of these carbenes is that they are susceptible to dimerization to form enetetramines, and this is the reason proposed for why these carbenes were not isolated by Wanzlick in the 1960's. The mechanism of dimerization involves the attack of an occupied σ lone pair of one carbene centre on the vacant p orbital of the other carbene.¹⁰⁹ Extensive studies of NHC's as ligands for analogues to the Grubbs' catalyst has been carried out since these ligands overcome some of the limitations of the phosphine ligands for use in catalytic metathesis of alkenes.^{94, 95, 110}

Thus the scope of metal coordinated complexes is extensive. The specific focus of this study is Fischer carbene complexes, which will be discussed in depth in the sections which follow.

3.1.2. Synthesis of Fischer Carbenes

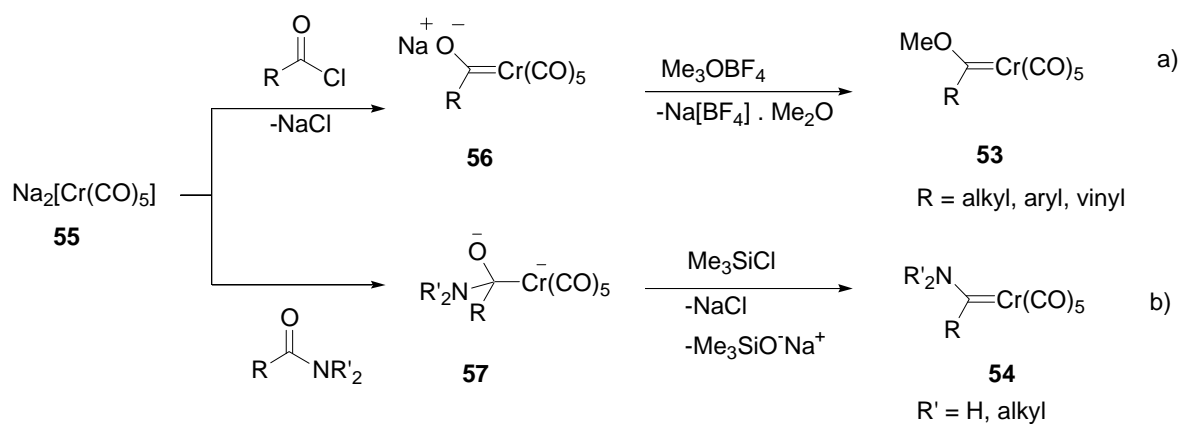
Two types of Fischer carbenes are synthetically accessible, namely alkoxy carbenes and amino carbenes, which refer to the stabilizing substituents on the carbene carbon. A brief overview of the syntheses of both types will be dealt with; focussing primarily on the Fischer synthetic approach for alkoxy carbenes.

There are two general routes to the synthesis of chromium carbene complexes. The first is the well known Fischer route¹¹¹ and the other was developed by Semmelhack and Hegedus in the late 1980's.^{112, 113} The first method leads to the formation of alkoxy carbenes, *via* organolithium compounds which react with a metal carbonyl such as chromium hexacarbonyl (Scheme 18). The resultant product, an acyl metalate **52**, then undergoes alkylation to form the alkoxy carbene complex **53**.^{111, 114} This alkoxy carbene **53** can subsequently be converted to the amino carbene by reacting it with an amine nucleophile to afford the amino carbene complex **54** (Scheme 18).¹¹⁴ In the alkylation step of the Fischer synthesis route many alkylating agents can be used. These include trialkyloxonium tetrafluoroborates, alkyl fluorosulfonates and alkyl trifluoromethanesulfonates^{96, 114} Another method of alkylation is described by Matsuyama *et al.*¹¹⁵ where alkyldiphenylsulfonium salts are used to form a variety of functionalised alkyl groups.



Scheme 18: General Fischer carbene synthetic route

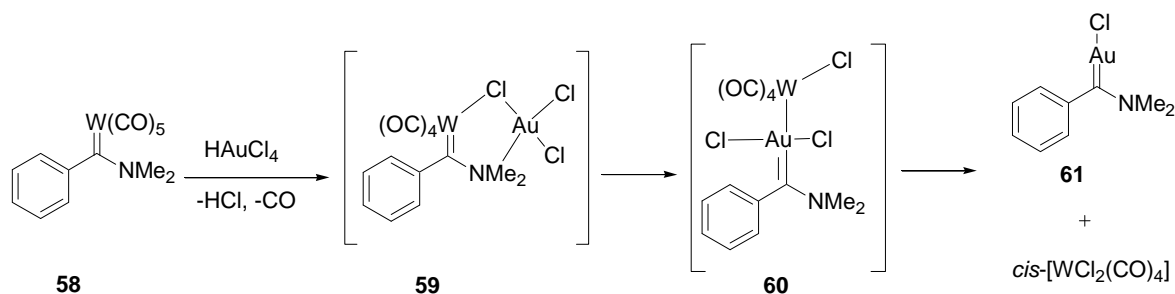
The Semmelhack-Hegedus method involves a pentacarbonylchromate dianion reacted with acyl chlorides or amides. This dianion can be formed by the reduction of chromium hexacarbonyl with sodium naphthalenide. The reactions with acyl chlorides lead to the formation of alkoxy carbenes [Scheme 19, (a)], while the addition of amides leads to the synthesis of aminocarbenes [Scheme 19, (b)]. The alkylation of acyl metalate **56** gives rise to the alkoxy carbene (**53**). The tetrahedral intermediate of the amide derivative (**57**) is reacted with TMSCl to afford the aminocarbene complex **54**.^{112, 114}



Scheme 19: Semmelhack-Hegedus method for the synthesis of alkoxy carbene complexes (**53**, route a) and amino carbene complexes (**54**, route b)

Other methods used to synthesise aminocarbenes include the reaction of isocyanide-metal complexes with nucleophiles such as primary and secondary amines to yield aminocarbene complexes.¹¹⁶ The use of Vilsmeier salts in the presence of a tertiary amine leads to the deprotonation of the iminium salt forming the unstable amino carbenes. A stabilized amino carbene is formed when the Vilsmeier salt is reacted with an electron-rich metal such as platinum (IV).¹¹⁷

Alkoxy carbenes can also be formed from diazirines¹¹⁸ or by transmetallation and carbene transfer. Transfer of a carbene ligand was first reported in 1970.¹¹⁹ The transmetallation occurs between the two metal centres, and thus Group 6 metal complexes have been converted to late transition metal complexes such as rhodium, palladium, copper and gold carbene complexes.⁹⁵ A tungsten Fischer dimethylaminocarbene (**58**) was reacted with gold (V) tetrachloride hydride with the possible reaction pathway (Scheme 20) proceeding *via* a chloride-bridged dinuclear species (**59**). The formation of the gold (I) carbene (**61**) occurs at low temperature (0°C) and is stable at room temperature.¹²⁰



Scheme 20: Reaction pathway for the formation of Gold (I) carbenes from Tungsten carbenes *via* transmetallation

Carbene complexes have varied reactivity which is dependent on the substituents such as the alkoxy and amino groups, as well as on the metal centre involved.^{121, 122} The electronic characteristics of Fischer carbenes allow for a wide application of photochemical methods in the preparation of organic compounds.¹²² Fischer chromium carbenes are generally brightly coloured, ranging from pale yellow to dark red due to the different substituents and the associated electronic characteristics of each substituent.¹²¹ Amino groups are strong π -donors and give rise to pale yellow complexes, while alkoxy groups are soft π -donors, resulting in a darker yellow colour. Alkyl groups which are π -donors cause a blue shift in the electromagnetic spectrum and π -acceptor substituents such as phenyl groups cause a red shift in the electromagnetic spectrum and so yield dark red (or brown) compounds.¹²¹ The UV-vis spectra of the carbene complexes illustrate three absorption bands; a spin-forbidden metal-ligand charge transfer (MLCT) absorption around 500 nm, a spin-allowed ligand-field (LF) absorption with a moderate intensity between 350-450 nm, followed by a more intense LF absorption in the range of 300-350 nm.¹²² Previously, the MLCT band has been assigned to the promotion of an electron from the non-bonding metal-centred HOMO orbital to the carbene carbon p-orbital centred LUMO (Figure 23).¹²² The ligand field band is attributed to the promotion of an electron to the more energetic population of the metal-centred LUMO+1.^{122, 123} However, recent DFT calculations suggest that the MLCT band results from the promotion of an electron characteristic of the metal-centred HOMO-1 \rightarrow LUMO transition. This involves a p-orbital of the carbene carbon. The LF band is characteristic of the HOMO-3 \rightarrow LUMO transition which involves the π -system of the carbene ligand, in this case an aryl group, hence it is a π - π^* transition (Figure 23).¹²¹

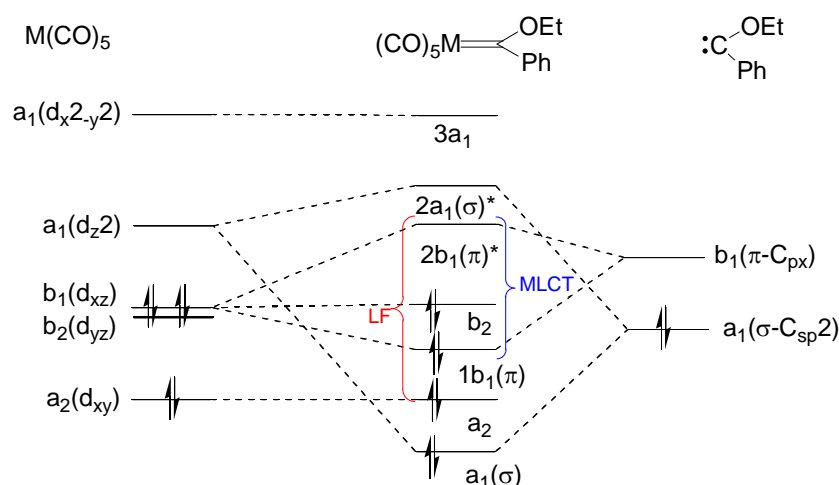


Figure 23: A simplified energy diagram highlighting promotion of electrons that lead to the MLCT and LF bands in the UV-vis spectrum

Taylor and Hall¹²⁴ examined the theoretical aspects of the bonding found in Fischer carbenes. The use of several techniques including dissociation energies, molecular orbital diagrams and fragment analysis of molecular orbitals enabled them to determine the difference in bonding between Fischer carbenes and Schrock carbenes. This work greatly influenced the theoretical work that followed as they originally suggested that heteroatom substituents stabilize the singlet Fischer carbene.^{124, 125} Many groups, including Ziegler and co-workers,¹⁰⁹ and Sierra and co-workers^{121, 126-128} have continued to use theoretical studies to achieve a better understanding of the electronic properties of Fischer carbenes and how they influence the reaction mechanisms Fischer carbenes undergo.

3.1.3. Applications of Fischer Carbenes

The reactivity and therefore the type of reactions that Fischer carbene complexes can undergo is illustrated in Figure 24. The reactivity can be divided into two parts: the ligand based reactivity and the metal-centred reactivity. Addition of nucleophiles, bond formation *via* metal carbene anions, transformations of metal carbenes to metal carbynes, and cycloaddition reactions (including Diels-Alder reactions) are ligand-centred. Annulations and olefination reactions are some of the reactions involved with the metal-centred reactivity. Ligand displacement and substitution also take place at the metal centre.

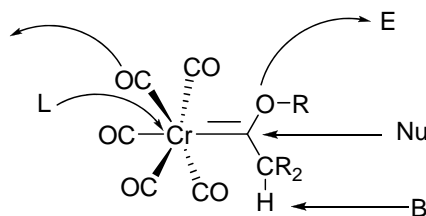


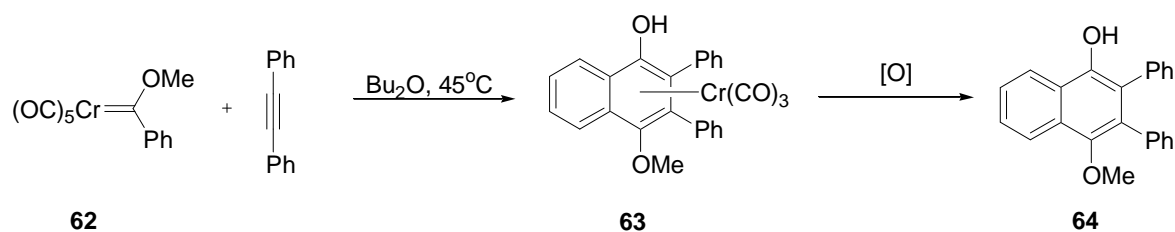
Figure 24: The reactivity pattern of Fischer carbene complexes (B = base, E = electrophile, L = ligand, and Nu = nucleophile)

The carbene carbon is electrophilic due to the electron withdrawing nature of the pentacarbonyl metal moiety.⁹⁶ Hence the carbene carbon can easily undergo nucleophilic attack from nucleophiles such as organolithiums, enolates and amides.¹²⁹ The addition of aryl substituents to Fischer carbenes mainly occurred at the carbene carbon atom following a 1,2-addition mechanism, however when a bulky alkoxy substituent is present, 1,4- and 1,6-additions were noted in some cases.¹²⁹ For (alkoxy)(alkenyl) carbene complexes, the products were either formed *via* 1,2- or 1,4-addition depending on the steric environment of both the metal carbene complex and the nucleophile taking part.¹²⁹ Electrophiles can add to the alkoxy substituent which then leads to the transformation of metal carbenes to carbynes.¹³⁰

The methylene groups at the α -position are acidic as a result of the electrophilic carbene carbon, which allows for their deprotonation by strong bases to form metal carbene anions. These anions can then undergo many transformations, including C-C bond formation such as alkylations,¹³¹ Michael-type reactions,¹³² and aldol reactions.¹³³ Part of the ligand-centred reactivity is the ability of the carbene complexes to undergo cycloaddition reactions, specifically those with alkenyl and alkynyl substituents.⁹⁶

a) Cycloaddition reactions

An example of a non-classical cycloaddition reaction is the benzannulation reaction.¹¹⁴ There are very few reliable methods to synthesise substituted benzenes and the Dötz benzannulation reaction is able to achieve this. Pentacarbonyl chromium complexes with aryl- or alkenyl(alkoxy)carbene ligands react with alkynes and yield highly substituted arenes which remain coordinated to the metal fragment $[\text{Cr}(\text{CO})_3]$.^{96, 134} Subsequent oxidation generates the hydroquinone derivative.¹³⁴ The benzannulation of phenyl(methoxy) carbene **62** produces a naphthohydroquinoid chromium tricarbonyl **63**, followed by oxidation in air yields the hydroquinone derivative **64** (Scheme 21).



Scheme 21: Benzannulation of phenyl(methoxy)carbene (**62**) and subsequent oxidation to afford hydroquinone (**64**)

The chromium metal allows for increased chemo- and stereo selectivity under mild conditions as compared with other metals.^{96, 114} Tungsten and molybdenum react to form indenenes and furans as the major products, not the desired product in this case. Other metals other than Group 6 metals have been used, such as manganese and ruthenium, but these metals have performed poorly in the benzannulation reaction.⁹⁶ This reaction provides an effective route to access the densely substituted arenes which has found many applications in the synthesis of biologically active compounds. For example, the benzannulation reaction was a key step in the total synthesis of fredericamycin A, an antibiotic and antitumor agent.¹³⁵ This is also an important example of an asymmetric synthesis in which Fischer carbene complexes play a valuable role.⁹⁶ Fischer carbene complexes have also been used in reactions with olefins. Ruthenium centred Fischer carbene

complexes work more efficiently than any of the other carbene complexes, however they are still not as effective as catalysts such as the Grubbs' catalyst.¹³⁶

b) Photochemical reactions

Hegedus and McGuire¹³⁷ made the important discovery of the photochemical reaction of Fischer carbene complexes with imines that lead to the formation of β -lactams. UV radiation of the MLCT band in chromium carbene complexes causes the insertion of a carbonyl (CO) into the metal-carbene bond and generates a ketene-like species.^{121, 137, 138} The species can then be trapped by nucleophiles in a [2+2] cycloaddition reaction. The insertion reaction occurs more readily with chromium carbenes as opposed to tungsten and molybdenum analogues.¹³⁹

More recent developments have seen Fischer carbenes being used as building blocks for multi-component reactions.^{97, 140} These types of reactions have a higher atom economy and can be applied in combinatorial chemistry.¹⁴⁰ The role of the Fischer carbene is to incorporate carbonyl ligands along the reaction pathway depending on the reaction conditions applied. Hence up to five components react in a sequential manner. This can lead to the formation of up to nine new carbon-carbon bonds which is of high value in the synthesis of complex compounds.¹⁴⁰

3.2. Results and Discussion

3.2.1. Synthesis of Carbene complexes

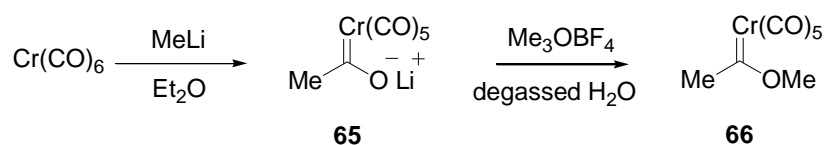
As discussed above, carbenes have been found to be very useful in organic synthesis. Due to the good balance between reactivity and relative stability, extensive applications of Fischer chromium carbene complexes have been exploited.⁹⁶ Since the first report in 1964 by E.O. Fischer,⁹⁹ many groups have studied these metal complexes and the challenges associated with them, such as the sensitivity to light and oxygen. There are many advantages of using Fischer carbenes in synthesis. For example, carbenes can act as nucleophiles which take part in alkylation,¹³¹ aldol and Michael- type reactions.⁹⁶ Extensive studies have also been carried out on cycloaddition reactions such as the Dötz benzannulation reaction.¹¹⁴

Various syntheses of Fischer carbenes have been outlined earlier, with the Fischer synthesis and the Semmelhack-Hegedus synthesis being the two most commonly used methods. The classical Fischer

synthesis¹¹¹ was used in this project to form alkoxycarbenes *via* α -alkoxy and α -aminostannanes which provide stable precursors to the organolithiums required.

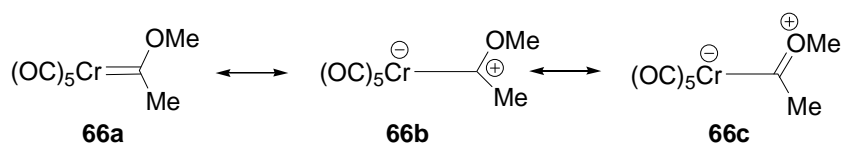
a) General synthesis of methyl carbene complex and NMR characterisation

A simple methyl carbene (**66**) was made from methyllithium as a trial compound before using the organolithiums accessed from the stannanes (Scheme 22). It is important to eliminate air from the reaction system and use Schlenk techniques effectively for the synthesis of carbenes since they are sensitive to oxidation.¹⁴¹ The methyllithium was added drop wise to a solution of chromium hexacarbonyl in dry Et₂O, the methyl carbanion adding to a carbonyl carbon *via* a nucleophilic addition mechanism to form an acylpentacarbonyl-chromate salt (**65**). A Meerwein salt such as trimethyloxonium tetrafluoroborate was used for the *O*-alkylation step. It is necessary to carry out the alkylation step in degassed water as the acylpentacarbonyl-chromate salt is water soluble, although it is sensitive to oxidation by oxygen present in the water. The carbene was then extracted with dry Et₂O and the solvent removed under reduced pressure to afford **66** as bright yellow crystals in a yield of 56%.



Scheme 22: Synthesis of methyl carbene **66**

The 1-D NMR analysis of the methyl carbene **66** was comparable to that found by Nandi *et al.*¹⁴² The ¹H spectrum (Figure 25) shows the distinctive methoxy resonance at 4.73 ppm and the methyl resonance at 2.96 ppm. The methoxy signal is further downfield because of the electronegative effect of the oxygen, and appears very broad. The broadness of the signal is due to the stabilizing effect of the methoxy group involved in π -back donation to the carbene carbon bond which is very electrophilic, hence a delocalisation of electrons occurs over the two bonds.⁹⁵ This results in the partial loss of double bond character and there is more free rotation about the metal carbon bond (Scheme 23 **66b** and **66c**).⁹⁵ If the rotation about the bond is slow the substituents could be in different chemical environments hence have different chemical shifts and lead to the broadness observed in an NMR spectrum. However, this is not likely as the pentacarbonyl moiety is symmetrical and does not provide a different chemical environment for the substituents if they rotate, thus proving that the broad signal is due to the stabilizing effect of the methoxy group.



Scheme 23: Metal carbon bonding in the Fischer chromium carbene complex **66**

The ^{13}C spectrum illustrates the resonances of the expected five carbons (Figure 25). The electrophilic nature of the carbene carbon is apparent from its low field ^{13}C NMR shifts commonly in the range of 350 – 400 ppm.⁹⁶ The resonance at 360.5 ppm confirms the presence of the carbene and the two signals at 223.3 ppm and 216.4 ppm correlate with the carbonyl carbons. One carbonyl is in the *trans* position at 223.3 ppm while the remaining four carbonyls are all in the *cis* position, and hence have the same chemical shift at 216.4 ppm. The ratio of carbonyls is also indicated by the intensity of each resonance. The methoxy and methyl carbons resonate at 67.5 and 49.8 ppm respectively. They appear as very broad signals with very weak intensities.

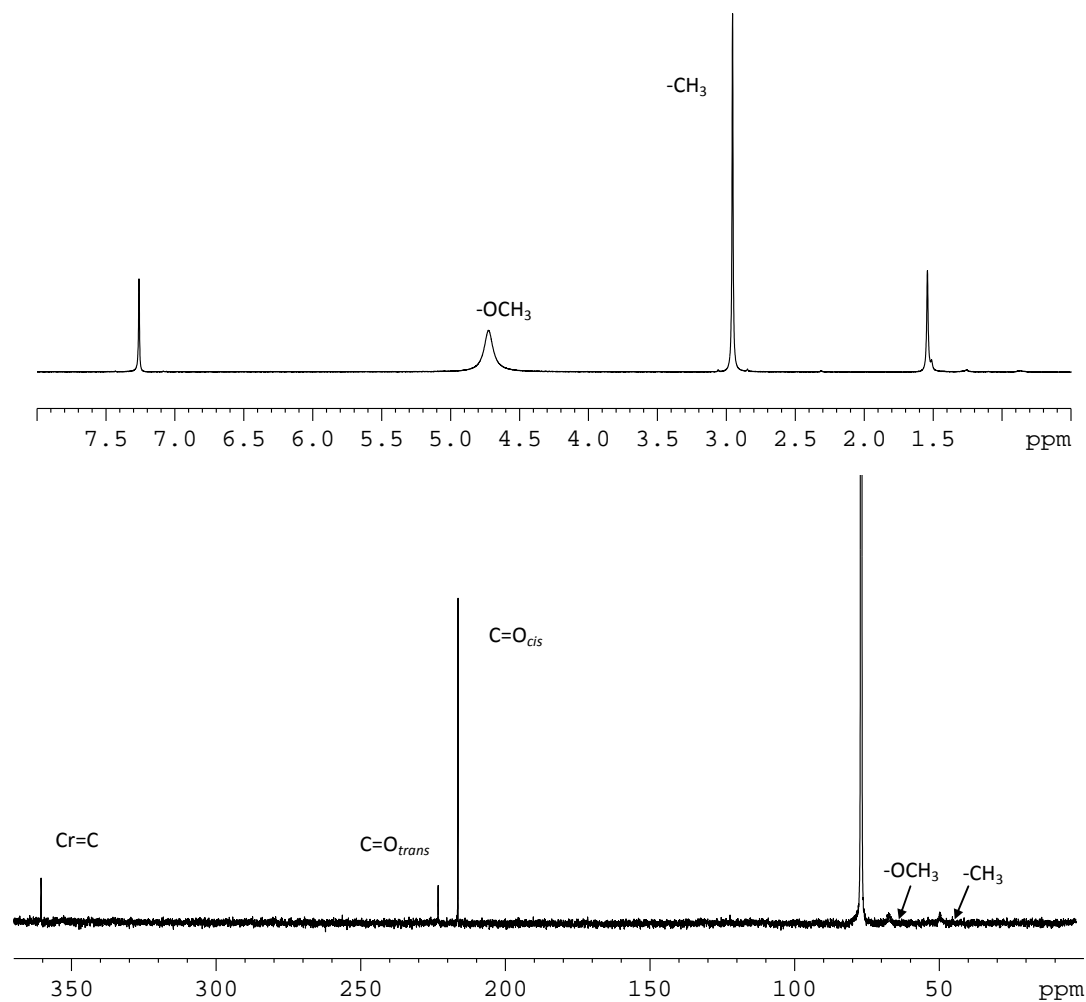
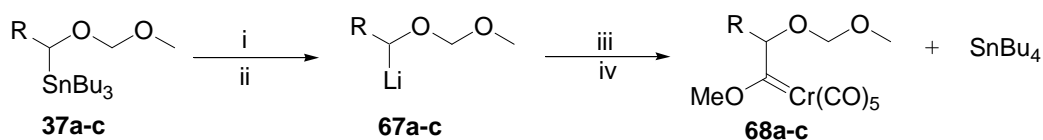


Figure 25: ^1H NMR (400 MHz, CDCl_3) and ^{13}C NMR (100 MHz, CDCl_3) spectra of methyl carbene **66**

b) Synthesis of carbenes derived from α -alkoxystannanes

Three α -alkoxystannanes (**37a-c**) were used to synthesise novel chromium Fischer carbenes. The formation of the organolithium (**67a-c**) *via* tinlithium exchange was noted by a colour change to pale yellow at a temperature of 0°C . It was then reacted with chromium hexacarbonyl to form the acylpentacarbonyl-chromate salt. After 1 h not all of the chromium hexacarbonyl had dissolved as was evident from a white solid observed at the bottom of the Schlenk flask, an indication that not all of the chromium hexacarbonyl had reacted with the organolithium in the nucleophilic addition step. The mixture had turned from a pale yellow to dark brown, and so the alkylation step was carried out using a Meerwein salt (Me_3OBF_4) in degassed water. The Fischer carbene (**68a-c**) was obtained along with a side product of tetrabutyltin (SnBu_4). Once the alkylation step was complete, the yellow carbene was extracted with dry Et_2O . The ether turned bright yellow and the aqueous layer became more pale yellow and then almost colourless as more of the carbene product was extracted (Scheme

24). The solvent was removed under reduced pressure to give the crude carbene product as a yellow solid residue.

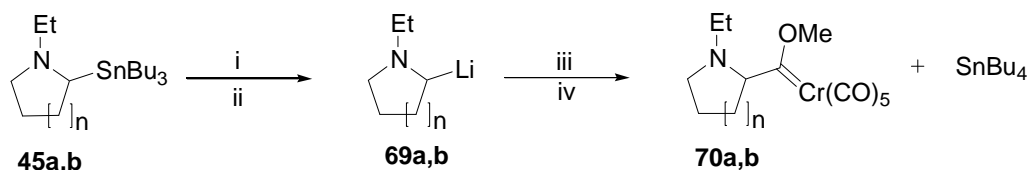


Scheme 24: Synthesis of Fischer carbenes from α -alkoxystannanes (i) $n\text{BuLi}$ (ii) TMEDA, dry Et_2O (iii) Cr(CO)_6 , CH_2Cl_2 , -40°C and (iv) Me_3OBF_4 , degassed water ($\text{R} = \text{C}_2\text{H}_5$, C_3H_7 , $\text{CH}(\text{CH}_3)_2$)

The two carbenes synthesised from the structural isomers, butyl and isobutyl α -alkoxystannanes (**37b** and **37c**) were successfully characterised using NMR and IR analysis, with characteristic ^{13}C chemical shifts for the carbene carbon and the carbonyls summarised in Table 7. The carbene synthesised from the propyl α -alkoxystannane (**37a**) was not formed as demonstrated by the lack of evidence of the chemical shifts in the ^{13}C NMR spectrum associated with the carbene carbon and the $\text{C}=\text{O}_{cis}$ and $\text{C}=\text{O}_{trans}$ from the pentacarbonyl moiety. In all cases, isolated yields were not obtained since the crude carbene product contained tetrabutyltin as a side product of the reaction. The tetrabutyltin was difficult to remove without causing the decomposition of the carbene product. The presence of a resonance around 167 ppm (Table 7), which is characteristic of carbonyls in ester linkages,⁵ suggested that the carbene was being oxidised in the air to the related ester. The carbene complex is known to be an ester equivalent and the oxidation of these complexes can be accomplished with oxygen,¹⁴³ pyridine *N*-oxide,¹⁴⁴ fluoride anions,¹⁴⁵ ceric ammonium nitrate (CAN)¹⁴⁶ and sodium hypochlorite with tetrabutylammonium sulphate as a phase transfer catalyst¹⁴⁷ to give the ester in high yields.

c) Synthesis of carbenes derived from α -aminostannanes

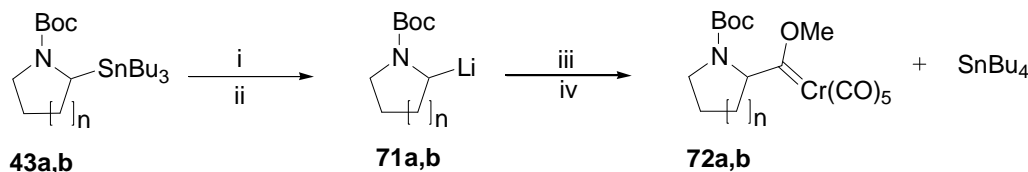
Four α -aminostannanes, two derived from pyrrolidine and another two derived from piperidine were used to synthesise the related Fischer chromium carbenes (Scheme 25). The *N*-ethyl derivatives (**45a** and **45b**) were successfully converted to the carbenes (**70a** and **70b**) and fully characterised with ^{13}C NMR and IR analysis.



Scheme 25: Synthesis of Fischer carbenes from *N*-ethyl α -aminostannanes (i) *n*BuLi (ii) TMEDA, dry Et₂O (iii) Cr(CO)₆, CH₂Cl₂, -40°C and (iv) Me₃OBF₄, degassed water (**a**: *n*=1 **b**: *n*=2)

The syntheses of the carbenes using the α -aminostannanes were carried out in the same manner as the α -alkoxystannanes (Scheme 24). The *N*-ethyl derivatives gave rise to dark brown acylpentacarbonyl-chromate salts, and the colour dissipated during the alkylation step. The solution turned slightly green while stirring in the degassed water, nevertheless the carbene was bright yellow when extracted with several portions of Et₂O. The aqueous layer remained a slight green/yellow colour. The crude products of the *N*-ethyl carbenes were yellow solid residues, and the isolated yields were not calculated due to the difficulty in purifying the carbene without decomposition taking place as mentioned for the carbenes derived from α -alkoxystannanes.

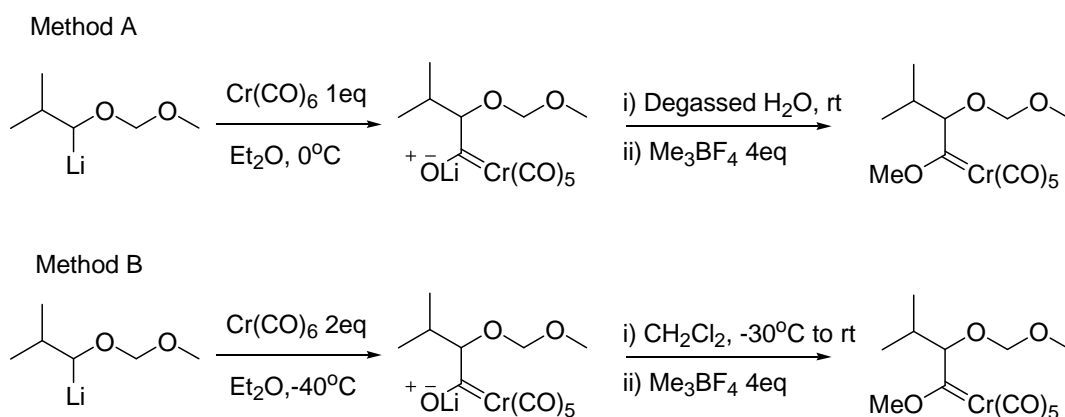
Isolation of the *N*-BOC derivatives gave rise to several challenges in both the synthesis and isolation steps (Scheme 26). The carbenes (**72a** and **72b**) were not fully characterised since significant signals such as the carbene carbon and the carbonyls were not observed in the ¹³C NMR spectra obtained for the *N*-BOC derivatives. The crude products from the *N*-BOC derivatives were yellow oils, which suggested the carbenes had formed but this could not be confirmed by spectral analysis. Not all the carbenes were isolated, and difficulties encountered during the synthesis using the method as outlined by Fischer,¹¹¹ prompted us to investigate alternative synthetic routes which we hoped would lead to improved yields.



Scheme 26: Synthesis of Fischer carbenes from *N*-BOC α -aminostannanes (i) *n*BuLi (ii) TMEDA, dry Et₂O (iii) Cr(CO)₆, CH₂Cl₂, -40°C and (iv) Me₃OBF₄, degassed water (**a**: *n*=1 **b**: *n*=2)

A review of the literature showed that the preferred method to synthesise Fischer carbenes is the Semmelhack-Hegedus method^{112, 113} because it is more versatile and does not have the limiting factor of finding a suitable organolithium. Nevertheless, both methods are still used.⁹⁶ Lotz and co-

workers¹⁴⁸ used both methods to synthesise biscarbene complexes, with the alkylation step being of particular interest since it was carried out in a different manner to the Fischer synthesis method.^{148, 149} The procedure was the same as the Fischer route up to the formation of the acylpentacarbonyl-chromate salt in dichloromethane (Scheme 27). The alkylation step was carried out in the dichloromethane with the addition of the Meerwein salt, triethyloxonium tetrafluoroborate (Et_3OBF_4) to the solution mixture (Scheme 27, Method B). The Fischer method (Scheme 27, Method A) removed the diethylether under reduced pressure and added degassed water followed by the Meerwein salt, Me_3OBF_4 at room temperature. The Meerwein salts used in these syntheses were analogous. The reagent equivalents were different, particularly the amount of chromium hexacarbonyl in relation to the amount of organolithium added, which was increased two fold in method B.



Scheme 27: Synthesis of the carbene **68c** using two alternative methods (A) Fischer method,¹¹¹ and (B) Lotz method¹⁴⁹

Temperature plays an important role in the synthesis of these carbenes. Both the generation of the organolithium (*via* tin-lithium exchange) and the addition of the chromium hexacarbonyl are carried out under conditions of careful temperature control. The use of temperature also differs between the two methods (Scheme 27): Method A has a temperature of 0°C for the addition of the chromium hexacarbonyl while the temperature is lowered to -40°C for the initial addition of chromium hexacarbonyl in method B and then allowed to warm up to room temperature. The variations of equivalents used for the three different approaches as well as the carbenes attempted using those methods are detailed below (Table 6). The first method is a Fischer synthesis route (Method A), the second is derived from Lotz and co-workers¹⁴⁹ (Method B) and the third method is a combination of the two (Method C).

Table 6: A comparison of the synthetic methods used to synthesise Fischer carbenes.

Compound	68c , 72a and 72b	68a, 68c and 72a	68b, 70a, 70b, 72a and 72b
Method	A ¹¹¹	B ¹⁴⁹	C ^{111, 149}
Stannane	1	1	1
nBuLi	1	2	1
Cr(CO) ₆	0.9	2	1
Me ₃ OBF ₄	4	2.5	3
TMEDA	1	2	1

A cheaper and less toxic alternative to Meerwein salts for the alkylation of the lithium acylmetalate are alkyl iodides which allow for a greater variety of substituents that can be included as part of the carbene's alkoxy substituent. This procedure requires the use of a phase transfer catalyst such as a tetraalkylammonium salt (in this case *n*-Bu₄NBr).¹⁵⁰ The strong ion pairing of the lithium acylmetalate needs to be disrupted in order to produce a species that is sufficiently nucleophilic to take part in the alkylation step, and *n*-Bu₄NBr enables that to happen.¹⁵⁰ More recently Nandi *et al.*¹⁴² described an improved method based on the use of alkyl iodides. It was found that the temperature of 55°C gave higher yields than when the reaction was carried out at room temperature. The mechanism for the reaction was confirmed to take place *via* S_N2 pathway as previously suggested by Hoye.^{71, 142} At 55°C there was no decomposition of the carbene complex, although at higher temperatures the yield was adversely affected, possibly due to decarbonylation.¹⁴² The alkylation step using a Meerwein salt may also be affected by temperature as discussed earlier. No further investigation on the effect of temperature was carried out to obtain conclusive results. In this study, the complexity of the carbene alkoxy substituent was not of great importance, while the effect of the alkyl moiety derived from the respective stannanes was the focus of the study.

The improvement in yield for the carbene complexes (**68a**, **68c** and **72a**) was not possible to determine since clean products were not isolated from the syntheses using Method B. The alkylation step in DCM did not appear to work efficiently; the crude mixtures were greener in colour compared with the carbenes prepared from method A. This observation of colour was also noted by Nandi *et al.*¹⁴² when the alkylation step was performed in a range of organic solvents such as DCM, DMF and THF, while an increase in the number of side products formed was also observed. In order to obtain cleaner products a filtration of the acylmetalate was carried out to remove any impurities, including unreacted chromium hexacarbonyl, prior to the alkylation step with alkyl iodides.¹⁴² A similar approach with the synthesis of the remainder of the carbenes was expected to allow for a similar improvement.

As mentioned earlier, Fischer carbenes are readily oxidised to give carbonyl analogues. The synthesis of the carbenes could be confirmed by analogy to the carbonyl analogues which were assumed to be more easily separated and purified. Therefore an oxidation of these carbenes was attempted using a method adapted from Perdicchia *et al.*¹⁴⁷ using household bleach (sodium hypochlorite solution) and tetrabutylammonium bromide (Bu₄NBr) in an ethyl acetate/water mixture. The crude mixtures turned green, which indicated the change in the oxidation state of the chromium; however the ester could not be isolated from the resulting intractable mixture containing several components.

The carbene (**68b**) derived from the butyl α -alkoxystannane and the two *N*-ethyl derivatives (**70a** and **70b**) were successfully synthesised using Method C, but with no definite improvement in the yield, using method C. The compounds were synthesised using the equivalents as stated in Table 6, similar to that used in method A except for using three equivalents of Meerwein salt instead of four. The chromium hexacarbonyl was crushed into a fine powder before adding it to the organolithium at low temperature. The Meerwein salt was also added at low temperature, in contrast with previous syntheses where the addition of the Meerwein salt was carried out at room temperature. The formation of the carbenes from *N*-BOC derivatives (**72a** and **72b**) were not successful since no characteristic signals were observed in the 1-D NMR analysis.

Different purification techniques, including sublimation and chromatography, were attempted to remove the impurities from the carbene complexes without decomposition or oxidation taking place. Although sublimation is normally only considered when the desired product is a solid, it was difficult to establish whether the complexes in question were in fact solids since the tetrabutyltin by-product remained as a solvent, rendering all samples as oils.

In order to remove the tetrabutyltin from the crude product of carbene (**68b**) derived from the butyl α -alkoxystannane, a cold finger sublimation was attempted and successfully executed. The tetrabutyltin was not completely removed but the intensity of the resonances were minimised and thus the elucidation of the carbene was made easier. The carbene signal was not clearly visible in the ¹³C NMR spectrum of the sublimed product, most likely due to the relatively low concentration of carbene present in the sample (Figure 26). The signal at 211.5 ppm is from the unreacted chromium hexacarbonyl, which because of its symmetry shows one resonance for all six carbonyls. The presence of white crystals in the crude product of **68b** was confirmed by ¹³C NMR to be unreacted chromium hexacarbonyl [Cr(CO)₆].

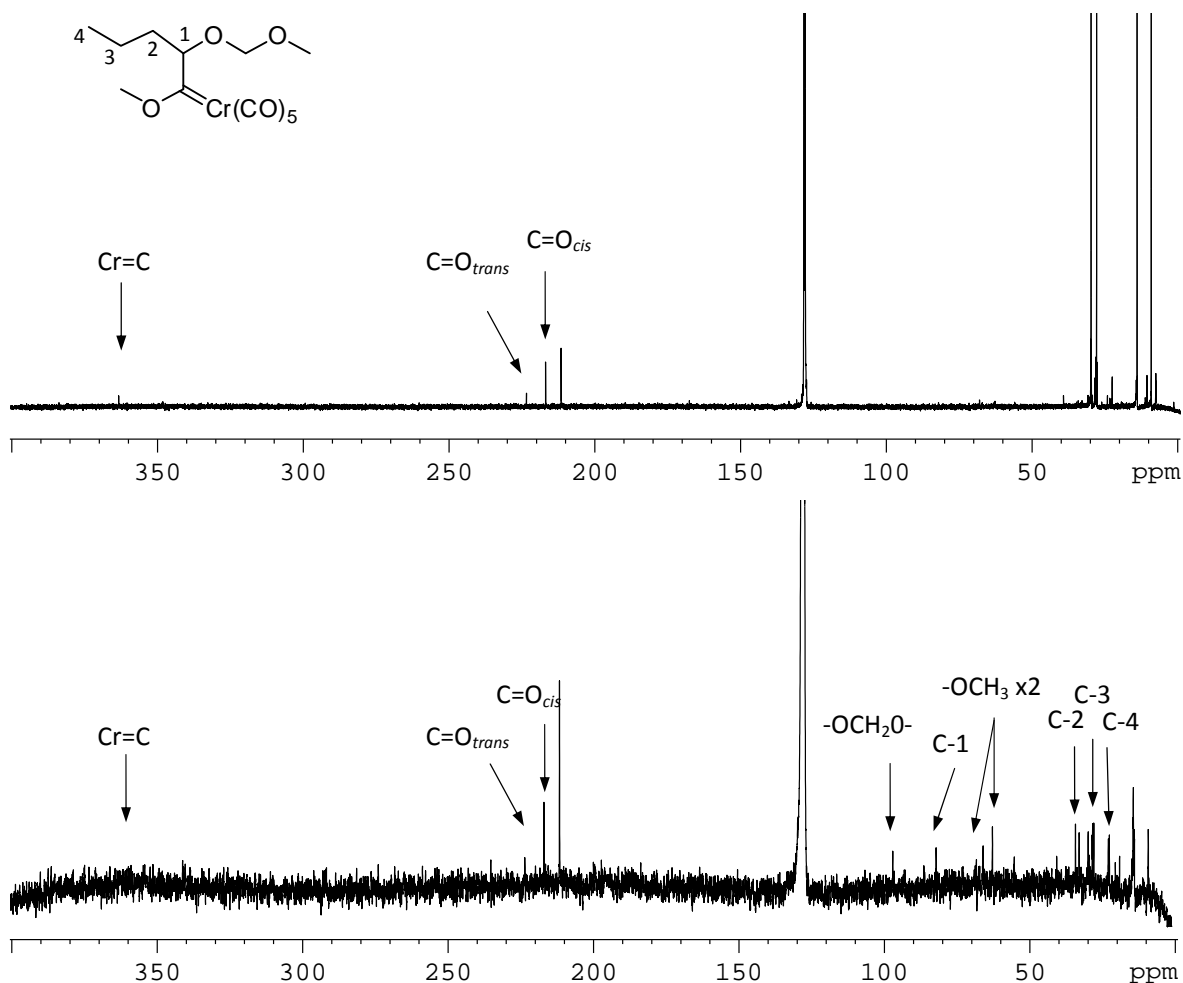


Figure 26: ^{13}C NMR (100 MHz, C_6D_6) spectra of carbene **68b** before and after sublimation

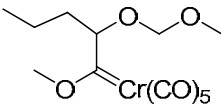
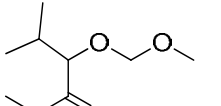
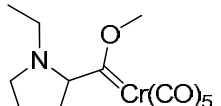
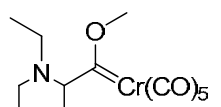
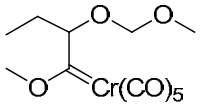
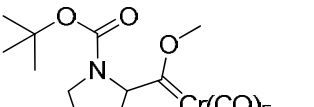
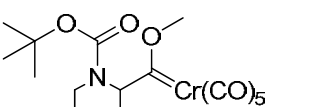
The purification of the N-BOC derivative crude carbene products (**72a** and **b**) using a cold finger sublimation technique failed as the crude product did not sublime and oxidised to form a green oily mixture in both cases.

Column chromatography under an inert atmosphere was also attempted, using a 10% ethyl acetate in hexane solvent system in order to remove the stannous side product. This was attempted for the carbene complex derived from isobutyl α -alkoxystannane (**68c**). Four fractions were collected, of which the first was tetrabutyltin, the second fraction was orange in colour, followed by a colourless fraction before the last fraction eluted as a bright yellow solution. Tetrabutyltin is known to streak on silica, as was evident since all the fractions were still contaminated with the byproduct.

The ^{13}C NMR spectrum of **68c** revealed that the second fraction contained the carbene, as well as the four signals corresponding to tetrabutyltin. All the characteristic resonances of the carbene

moiety appear in the spectrum, however not all the signals of **68c** could be accounted for. This suggested that the compound may have fragmented while eluting from the column and lost the MOM substituent. The MOM protecting group is an acetyl which is prone to acid hydrolysis to give an alcohol.⁵⁸ The prolonged retention time on the column could have lead to an interaction between the acidic silica and the protection group. In summary only two carbenes derived from the α -alkoxystannanes (**68b** and **68c**) and two from the α -aminostannanes (**70a** and **70b**) were characterised successfully (Table 7).

Table 7: Summary of Fischer Chromium Carbenes synthesised and their characteristics

	Crude Mass /g	Expected mass /g	Appearance	δ_c Cr=C / ppm	δ_c C=O / ppm		δ_c [O] ^b ppm
					CO _{trans}	CO _{cis}	
 68b	0.66	1.05	Yellow solid	363.3	223.4	216.8	167.5
 68c	0.34	0.80	Yellow solid	363.3	223.5	216.8	167.5
 70a	0.02	0.60	Dark yellow solid	360.5	224.8	214.3	-
 70b	1.06	0.61	Pale yellow solid	361.0	220.1	210.1	169.1
 68a	- ^a	0.75	Pale yellow solid	-	-	-	-
 72a	- ^a	1.74	Dark yellow oil	-	-	-	167.5
 72b	0.41	1.46	Yellow oil	-	-	-	-

^a The mass was not obtained due to prior decomposition

^b A signal corresponding to an ester carbonyl indicated the presence of the oxidation product

3.2.2. NMR Characterisation of carbenes

The ^1H NMR analysis of the carbene complexes proved to be difficult since the strong resonances of the tetrabutyltin in the methylene window (δ_{H} 0 – 40.0 ppm) complicated the elucidation of protons on the alkyl chain. The relative intensity of the protons from the tetrabutyltin in comparison to the proton signals of the carbene also made it difficult to observe the protons situated more down field such as the methoxy signal from the MOM protecting group or the carbene substituent (OMe).

The ^{13}C NMR analysis of the crude products were carried out using a standard Waltz 16 decoupling pulse with an increased sweep width of 400 ppm. The stability of the carbene in solution was not known; therefore consecutive ^{13}C NMR experiments were set up, each 3 h long.

The ^{13}C NMR spectrum of the carbene (**68c**) derived from the isobutyl α -alkoxystannane (Figure 27) showed the characteristic carbene peak at 363.3 ppm and the carbonyl signals at 223.5 ppm and 216.8 ppm which was similar to the chemical shifts for these functional groups found in the methyl carbene **66**. The resonance of the $\text{C}=\text{O}_{\text{trans}}$ was inverted (δ_{C} 223.5 ppm), most probably due to a mismatch between recycle delay and the spin lattice relaxation time (T_1) of the *trans* carbonyl. The spin system is disturbed by irradiating at the resonance frequency and then allowing the nuclei to relax and reach equilibrium before being irradiated again. If the delay time is not long enough between the pulses the nuclei will not reach equilibrium and the signal may appear inverted. This problem can be resolved by changing the delay time or the pulse length, once the relaxation time is known for the nucleus in question. The relaxation time (T_1) can be investigated by an inversion recovery experiment.⁷⁶

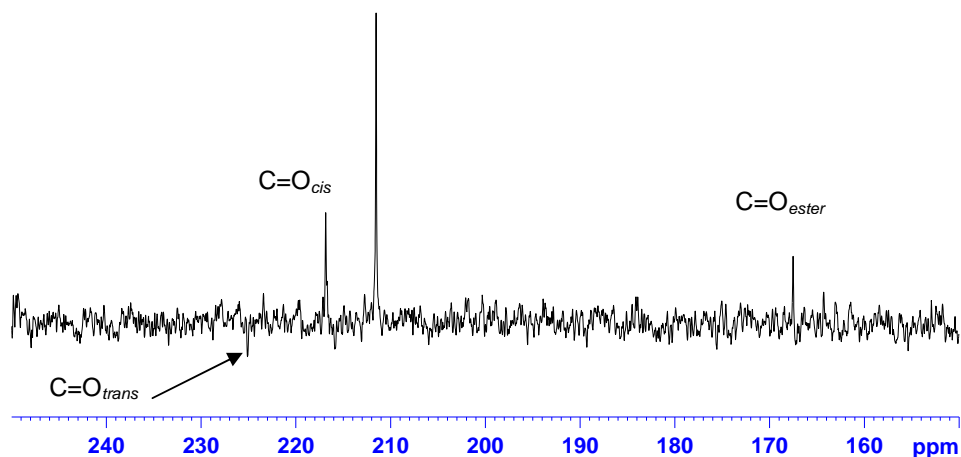


Figure 27: ^{13}C NMR region (100 MHz, C_6D_6 250-150 ppm) of isobutyl carbene **68c** illustrating the inverted $\text{C}=\text{O}_{\text{trans}}$ signal

It was clear that decomposition of the carbene had taken place after three hours, and even more after six hours, since the intensity of some of the signals had decreased and the presence of a green precipitate at the end of the three NMR experiments indicated that the chromium had been oxidized from oxidation state (0) to oxidation state (III) which is green in colour.¹⁵¹ This is also confirmed by the signal at 167.5 ppm, which is in the region common for ester carbonyls, further illustrating the oxidation of the carbene which was discussed previously in more detail (Figure 28). The suggested oxidation product of the carbene (**68c**) derived from isobutyl α -alkoxystannane is the corresponding ester (**73**), illustrated in the accompanying scheme, however this oxidation product was not isolated.

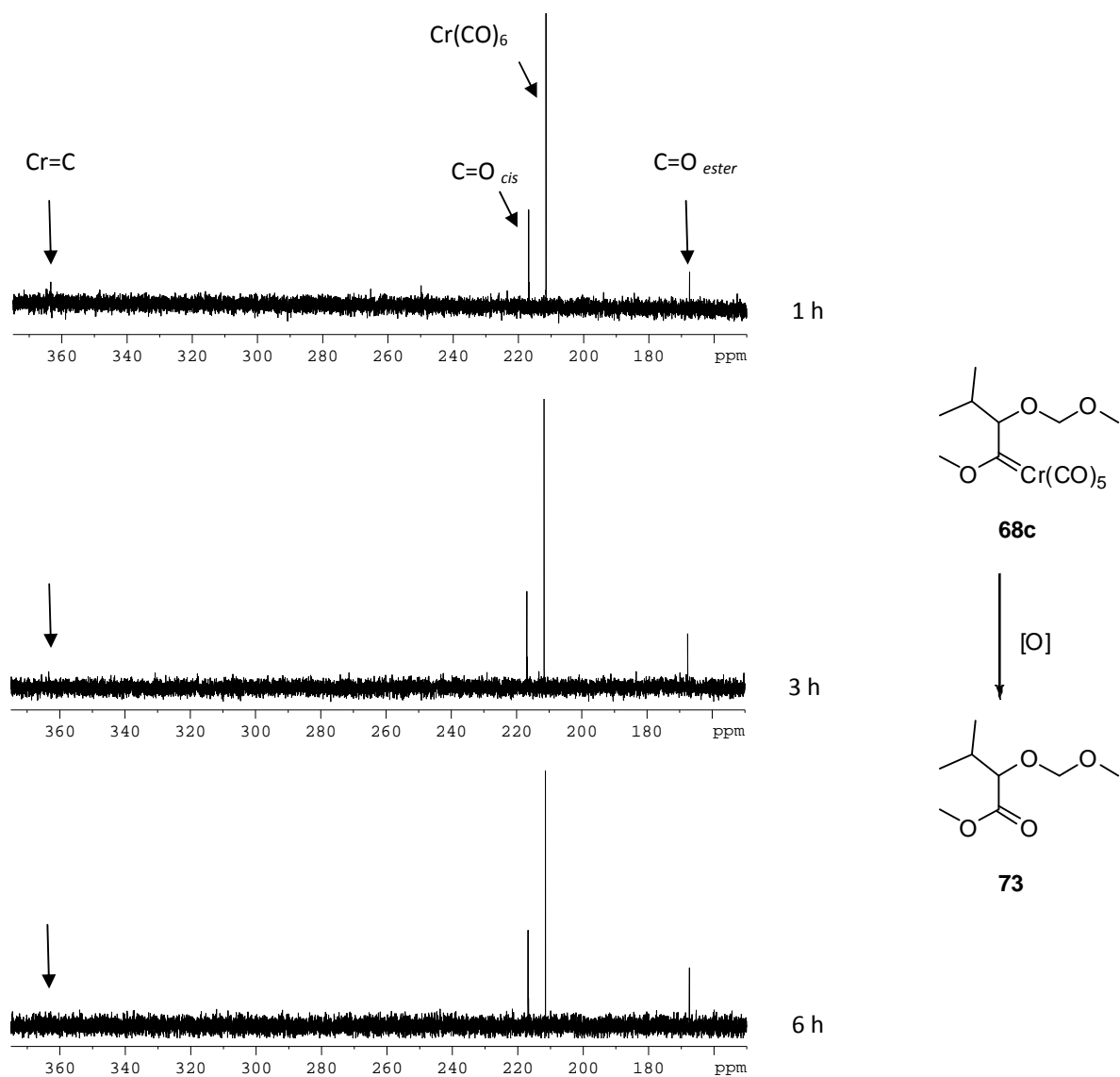


Figure 28: ^{13}C NMR region (100 MHz, C_6D_6 380-150 ppm) of isobutyl carbene **68c** showing the presence of oxidation products ($\text{C}=\text{O}_{\text{ester}}$) and the decrease in the carbene signal ($\text{Cr}=\text{C}$)

The structure of the carbene complex **68c** was elucidated from the ^{13}C NMR spectrum of the crude mixture (Figure 28) and by analogy to the stannane **37c** taking into consideration the effect of the electron withdrawing strength of the pentacarbonyl chromium moiety (Table 8). Thus all the resonances from the alkyl chain and the MOM group were accounted for, including the new methoxy signal at 68.0 ppm from the methoxy directly attached to the carbene carbon. The presence of the single carbonyl resonance at 211.5 ppm for chromium hexacarbonyl is an indication that it was in excess.

Table 8: ^{13}C NMR (C_6D_6 , 100 MHz) acquired for **37c** and **68c**

Carbon	37c δ_{C} /ppm	68c δ_{C} /ppm
C=Cr		363.3
C=O _{trans}		223.5
C=O _{cis}		216.8
OCH ₂	97.3	97.7
C-1	82.4	87.8
OCH ₃		68.0
OCH ₃	55.4	62.7
C-2	33.3	39.2
C-2'	29.7	29.8
C-3'	28.0	27.9
C-3	21.5	24.2
C-4	20.2	23.4
C-4'	13.9	14.0
C-1'	10.4	9.1

The carbene signal was not observed in the ^{13}C NMR spectrum of the carbene derived from N-Boc piperidine α -aminostannane (**72b**), yet the presence of two signals in the region 210 – 215 ppm showed that there may have been limited conversion to the carbene. Nonetheless these results were not conclusive due to the presence of many impurities and the full structure could not be elucidated. An alternative pulse program was used to investigate if the carbene signal would be revealed, using broad-band ^1H decoupling in place of the composite decoupling pulse applied originally. This is a more simple pulse program than Waltz 16 decoupling program. In addition, the delay time in between acquisitions was changed from 2 seconds to 6 seconds.⁷⁶ No visible change to the new spectrum acquired was noted, as the carbene signal around 360 ppm was still not observed.

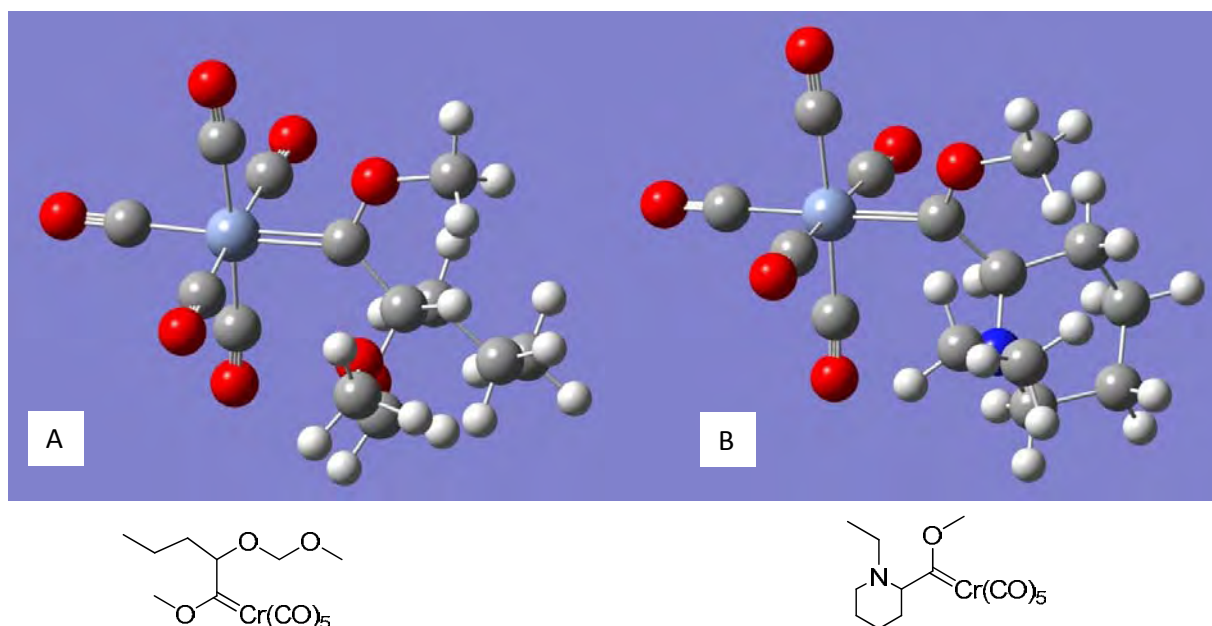
3.2.3. Molecular modelling and Infra-red spectroscopy

An energy minimisation and frequency analysis analogous to those for the stannanes was performed for each of the carbenes using the Gaussian 03 program.⁸² The level of theory used was DFT with unrestricted B3LYP (uB3LYP) functional sets used. Although the carbene is a metal, it is in the first row of transition elements and it is not considered a 'heavy atom' and so there was no need to use the effective core potential approximation. Recently, Fernandez *et al.*¹⁵² carried out a DFT study using the effective core potential approximation for metals chromium, scandium and tungsten while investigating the mechanism for 1,3-dipolar cycloaddition reaction of alkynyl Fischer carbenes and they found that the calculations were in agreement with experimental data.¹⁵² Although, this parameter was not used in the DFT calculations for the novel Fischer carbenes, the results obtained for the bond lengths showed a close correlation to previously reported bond lengths for Fischer carbenes.

The bond lengths in α -alkoxy Fischer carbene complexes have been found to be smaller than their counterparts, amino carbenes, due to the greater π -donation from the amino group which contributes more to the resonance structure.^{153, 154} A heteroatom such as an oxygen atom or nitrogen atom is known to stabilize the carbene carbon atom by its electron pair donation. The stabilization results in a partial double bond character between the carbene carbon and the heteroatom and this is evident from the shortening of the bond length.¹⁵³ A summary of the bond lengths obtained from the optimized models of each of the Fischer carbenes is shown in Table 9. Clearly the Cr=C carbene bond length is longer than the Cr-CO bond lengths in all cases, which is in agreement with previous DFT studies and crystallographic data obtained for known Fischer carbenes.^{153, 154} There is little to no change for the Cr=C carbene bond length in all the compounds modelled resulting from the methoxy group as the π -donor substituent being present in all cases and the change in the other substituent does not seem to have a major effect on the bonding of the chromium and carbene carbon. This is similar to the effect observed in the ¹³C NMR analysis of the carbene carbon, with the chemical shift having a slight difference between the compounds (Table 7). The carbenes derived from α -alkoxystannanes have a chemical shift of 363.3 ppm, while the carbenes derived from α -aminostannanes resonate at 360 ppm.

Table 9: DFT calculated bond lengths of novel chromium Fischer carbenes synthesized in this study

		C=Cr / Å	C-CO _{cis} / Å	C-CO _{trans} / Å
Methyl carbene	66	2.0149	1.9058	1.9040
Derived from α -alkoxystannanes	68a	2.0290	1.9055	1.9020
	68b	2.0299	1.9067	1.8971
	68c	2.0298	1.9066	1.9004
Derived from α -aminostannanes	70a	2.0331	1.9044	1.9002
	70b	2.0376	1.9062	1.8990
	72a	2.0488	1.9029	1.8960
	72b	2.0833	1.9032	1.8864

**Figure 29:** A geometry optimised model of (A) butyl carbene **68b** and (B) *N*-ethyl piperidine carbene **70b**

The optimised models of the butyl carbene and the *N*-ethyl piperidine carbene represent the carbenes derived from different stannanes (Figure 29). It is clear that there are only slight changes in the bond lengths and torsion angles of the pentacarbonyl chromium moiety between the two different carbenes.

The characterisation of the carbenes was facilitated by the calculated vibrational spectra obtained from the computational analysis. For example, the IR spectra of *N*-ethyl piperidine carbene complex **70b** were a good fit to the calculated IR analysis (Figure 30). The mid IR region showed the broad

carbonyl vibrations of the pentacarbonyl moiety in the region $2032\text{--}1893\text{ cm}^{-1}$ as well as a carbene carbon metal (C=Cr) bend at 672 cm^{-1} . The far IR spectrum clearly showed the Cr-C stretches of the carbonyls attached to the central metal at 471 cm^{-1} and the Cr-C bend at 175 cm^{-1} .

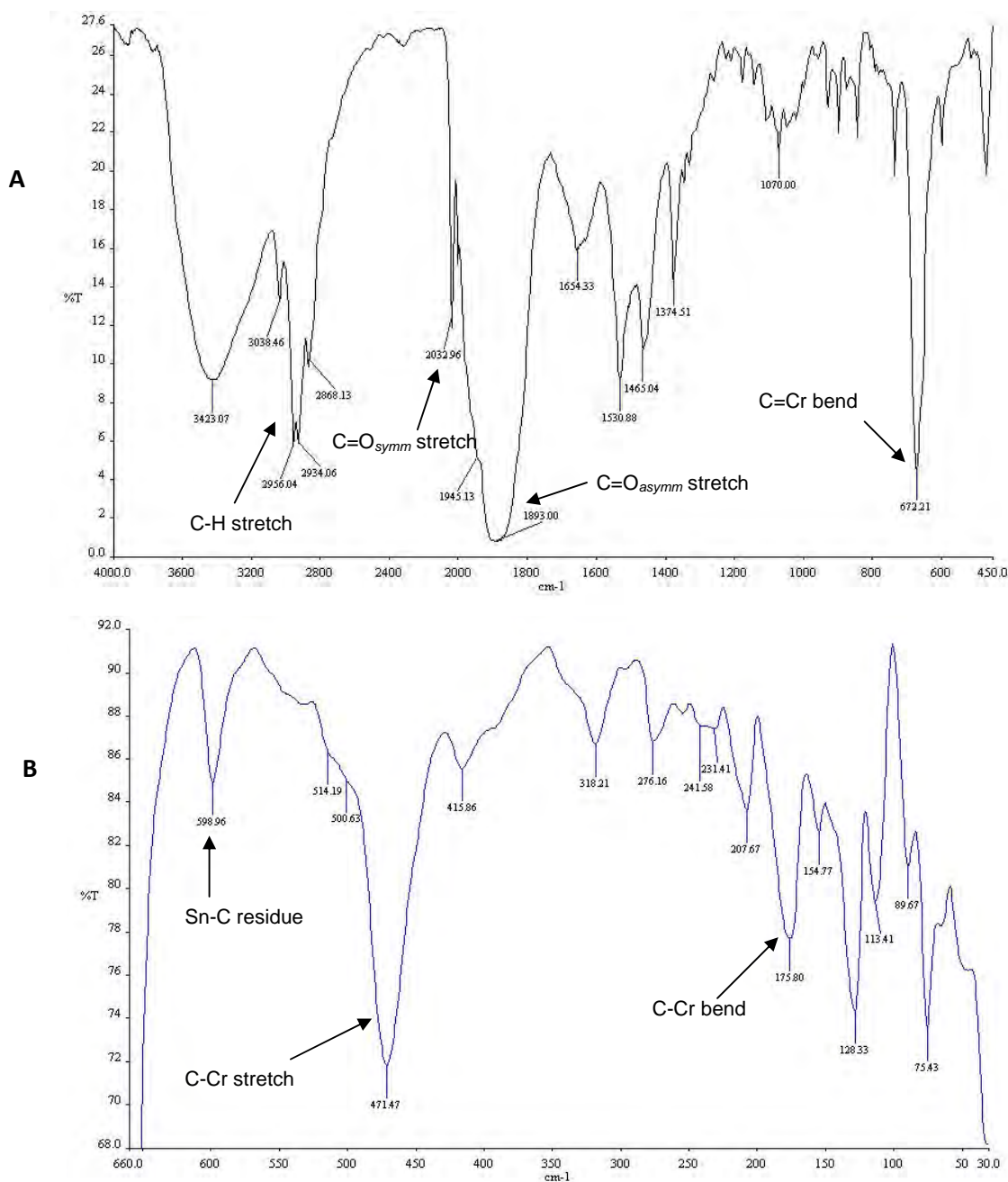


Figure 30: (A) Mid and (B) Far IR region ($4000\text{--}30\text{ cm}^{-1}$) of *N*-ethyl piperidine carbene complex **70b**

Some of the frequencies of the mid IR region were due to the presence of impurities such as the tetrabutyltin, but these were easily identified from a comparison of the calculated IR spectrum of the stannane and the carbene derivative (Figure 31).

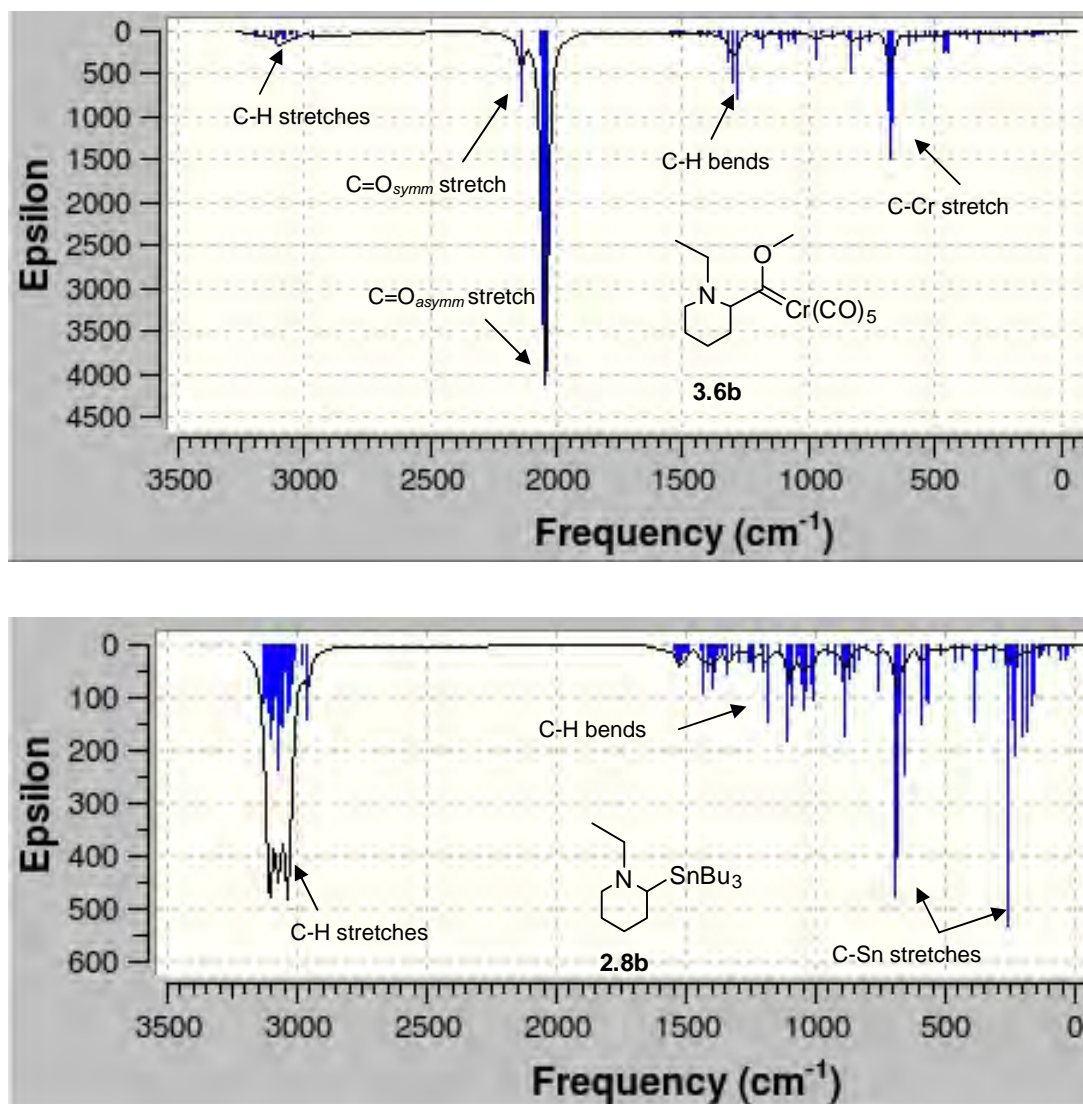


Figure 31: Calculated IR spectra for the *N*-ethyl carbene (**70b**) and the stannane precursor (**45b**)

The two carbenes derived from the α -alkoxystannanes (**68b** and **68c**) and two from the α -aminostannanes (**70a** and **70b**) were modelled and the frequency analysis was used to compare with experimental IR frequencies (Table 10). There is a strong correlation between the calculated and experimental IR analysis. There is a difference of 100-150 units for the carbonyl frequencies, this may be due to the broadness of the band in the experimental data recorded, but this is consistent for all the carbenes analysed and therefore the difference was considered insignificant.

Table 10: Frequency analysis of Fischer carbene complexes **68b**, **68c**, **70a** and **70b**

Bond	68b /cm ⁻¹		68c /cm ⁻¹		70a /cm ⁻¹		70b /cm ⁻¹	
	Calc.	Exp	Calc.	Exp ^a	Calc.	Exp	Calc.	Exp
C=O _{symm}	2141.28	2061.62	2140.83	-	2140.52	1997.25	2139.87	2032.96
C=O _{asymm}	2046.54	1939.64	2048.97	-	2043.94	1868.31	2043.91	1893.00
C-Cr bend	683.49	653.92	682.86	-	682.04	655.75	678.50	672.21
C-Cr stretch	457.96	433.71	455.80	444.69	461.90	449.35	467.87	471.47

^a Mid IR spectrum was not measured.

3.3. Concluding remarks

The α -alkoxy and α -aminostannanes provided stable precursors to the organolithiums required for the synthesis of the novel Fischer chromium carbenes. The organolithiums were obtained *via* tin-lithium exchange at low temperatures, followed by the addition of chromium hexacarbonyl to form the acylpentacarbonyl-chromate salt. Alkylation of this intermediate using a Meerwein salt, Me₃OBF₄, gave rise to the novel Fischer chromium carbene complexes. Fischer carbenes **68b,c** derived from two isomers, butyl and isobutyl stannane were successfully synthesised and characterised using NMR and IR spectroscopic techniques. N-BOC and *N*-ethyl aminostannanes were used to synthesise the Fischer carbene derivatives. Only the *N*-ethyl pyrrolidine **70a** and *N*-ethyl piperidine **70b** derivatives were successfully characterized. The difficulty encountered in the purification of the Fischer carbene complexes hindered the full characterisation, due to the presence of a by-product, tetrabutyltin. Future work will include an improved method of purification in order to isolate and use these compounds in further reactions such as cycloaddition reactions to access novel biologically active heterocycles. A detailed spectroscopic study is already underway to determine the effect of the alkyl substituents in longitudinal relaxation (T_1) of the various carbon nuclei.

Chapter Four: Experimental Details

4.1. General Experimental Procedures

The reagents used were supplied by Sigma Aldrich® and used without further purification unless indicated otherwise. All reactions involving organometallic compounds made use of Schlenk techniques, and all procedures were carried out under an inert atmosphere as outlined by Jordaan.⁷⁰ Solvents were dried and purified according to the methods described by Perrin and Armarego.¹⁵⁵ Hence, tetrahydrofuran (THF) and diethyl ether were distilled from sodium/benzophenone under nitrogen; dichloromethane and hexane were distilled from calcium hydride. *N,N,N',N'*-Tetramethylethylenediamine (TMEDA) was distilled from calcium hydride at atmospheric pressure. Reactions requiring an inert atmosphere were run under argon or nitrogen atmosphere in flame dried glassware. All cold baths at -78°C refer to a dry ice/isopropanol slurry. Melting points of the carbene complexes were not recorded because of their decomposition on heating and due to the presence of impurities. *n*-Butyllithium was titrated before use with 1,3-diphenylacetic acid as the acid and indicator. All chiral compounds are racemic.

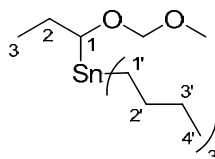
Thin layer chromatography (TLC) was carried out using Merck TLC silica gel 60 PF₂₅₄ plates and viewed under ultraviolet (UV) light or developed using phosphomolybdic acid (20% ethanol solution as supplied by Sigma Aldrich®) followed by gentle heating with a heat gun. Flash column chromatography was carried out using Merck silica gel 60 (particle size 0.063-0.200 mm) and Sigma Aldrich® aluminum oxide (Al₂O₃, activated, basic Brockmann I, standard grade, ca. 150 mesh, 58 Å). Radial thin layer chromatography was carried out using silica gel 60 PF₂₅₄ containing gypsum on a Harrison Research Chromatotron™.

NMR spectra were recorded on a Bruker 400 MHz AVANCE and a Bruker 600 MHz AVANCE II spectrometer. Chemical shifts are reported in ppm and referenced to residual solvent resonances (δ_{H} : 7.26 ppm for CDCl₃ and 7.15 ppm for C₆D₆; δ_{C} : 77.0 ppm for CDCl₃ and 128.02 ppm for C₆D₆). IR spectra were recorded as thin films on a Perkin-Elmer FT-IR Spectrum 2000 spectrometer using KBr and polyethylene discs.

4.2. Synthesis of Stannanes

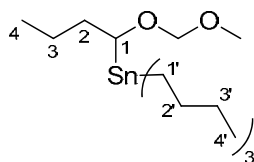
4.2.1. Synthesis of α -alkoxystannanes

a) Synthesis of Tributyl(1-(methoxymethoxy)propyl)stannane (**37a**)



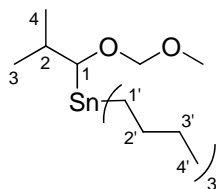
Diisopropylamine (3.4 mL, 24.0 mmol) was dissolved in dry THF (50 mL) at 0°C. nBuLi in hexane (17.2 mL, 1.4 M, 24.0 mmol) was added dropwise over 30 min *via* cannula. After 30 min tributyltin hydride (6.4 mL, 24.0 mmol) was added and the solution turned dark orange during the addition. After 1 h, the mixture was cooled to -78°C, and a solution of propionaldehyde (1.09 mL, 15.0 mmol) in THF (2 mL) was added and left to stir for 5 h while maintaining the low temperature bath. The mixture was quenched with sat. NH₄Cl solution (3 x 20 mL), washed with water (3 x 20 mL) and extracted with petroleum ether (2 x 30 mL). The combined organic layers were dried over anhydrous MgSO₄, filtered and evaporated to afford 1-tributylstannyl-propan-1-ol **36a** as a colourless oil, which was used in the next step without further purification.

N,N-Dimethylaniline (3.81 mL, 30 mmol) was added to a solution of 1-tributylstannyl-propan-1-ol dissolved in CH₂Cl₂ (30 mL) at 0°C. α -Chloromethylmethylether (2.28 mL, 30.0 mmol) was added slowly and left to stir for 5 h. The mixture was washed with ice cold 0.5N HCl (3 x 30 mL), water (3 x 30 mL) and sat. NaHCO₃ (3 x 30 mL). The organic layer was dried over anhydrous MgSO₄, filtered and evaporated. The oil was purified by column chromatography. The byproduct, tetrabutyltin, was eluted using 10% dichloromethane in hexane, followed by elution with 10% ethyl acetate in hexane to afford tributyl(1-(methoxymethoxy)propyl)stannanes (**37a** 3.40 g, 57.6%); IR (film) $\nu_{\text{max}}/\text{cm}^{-1}$ 2956, 2923, 1462, 1358, 1078 cm^{-1} ; δ_{H} NMR (400 MHz, CDCl₃) 4.61 (1H, d, $J = 6.7$ Hz, O-CH^AH^B), 4.55 (1H, d, $J = 6.7$ Hz, O-CH^AH^B), 3.99 (1H, t, $J = 6.5$ Hz, 1-CH), 3.34 (3H, s, OCH₃), 1.95-1.75 (2H, m, 2-CH₂), 1.60-1.41 [6H, m, (2'-CH₂)₃], 1.36-1.27 [6H, m, (3'-CH₂)₃], 0.96 (2H, t, $J = 7.2$ Hz, 3-CH₂), 0.91-0.81 [15H, m, (1'-CH₂, 4'-CH₃)₃]; δ_{C} NMR (100 MHz, CDCl₃) 96.4 (OCH₂), 75.7 (C-1), 55.3 (OCH₃), 29.2 (C-2'), 27.9 (C-2), 27.5 (C-3'), 13.6 (C-4'), 12.3 (C-3), 9.2 (C-1')

b) Synthesis of tributyl(1-(methoxymethoxy)butyl)stannane (**37b**)

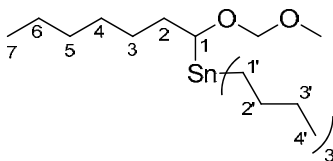
Diisopropylamine (1.7 mL, 12.0 mmol) was dissolved in dry THF (50 mL) at 0°C. *n*BuLi in hexane (8.6 mL, 1.4M, 12.0 mmol) was added dropwise over 30 min *via* cannula. After 30 min tributyltin hydride (3.2 mL, 12.0 mmol) was added. The solution turned light pink/orange during the addition. After 1 h, the mixture was cooled to -78°C, and a solution of butyraldehyde (0.7 mL, 7.5 mmol) in THF (2 mL) was added and left to stir for 5 h, while maintaining the low temperature bath. The solution turned yellow. The mixture was quenched with sat. NH₄Cl solution (3 x 20 mL), washed with water (3 x 20 mL) and extracted with petroleum ether (2 x 30 mL). The combined organic layers were dried over anhydrous MgSO₄, filtered and evaporated to afford (tributylstannyl)butan-1-ol **36b** as a colourless oil, which was used in the next step without further purification.

N,N-Dimethylaniline (1.91 mL, 15 mmol) was added to a solution of (tributylstannyl)butan-1-ol in CH₂Cl₂ (30 mL) at 0°C. α -Chloromethylmethylether (1.14 mL, 15.0 mmol) was added slowly and left to stir for 5 h. The mixture was washed with ice cold 0.5N HCl (3 x 30 mL), water (3 x 30 mL) and sat. NaHCO₃ (3 x 30 mL). The organic layer was dried over anhydrous MgSO₄, filtered and evaporated. The colourless oil was purified by column chromatography. The byproduct, tetrabutyltin was eluted with 10% dichloromethane in hexane, followed by the elution with 10% ethyl acetate in hexane to afford tributyl(1-(methoxymethoxy)butyl)stannanes (**37b**, 1.42 g, 46.4%); IR (film) $\nu_{\max}/\text{cm}^{-1}$ 2957, 2925, 1463, 1378, 1147 cm^{-1} ; δ_{H} NMR (400 MHz, C₆D₆) 4.59-4.57 (2H, m, OCH₂), 4.21 (1H, t, *J* = 6.4 Hz, 1-CH), 3.21 (3H, s, OCH₃), 1.99-1.82 (2H, m, 2-CH₂), 1.73-1.58 [6H, m, (2'-CH₂)₃], 1.54-1.47 (2H, m, 3-CH₂), 1.44-1.35 [6H, m, (3'-CH₂)₃], 1.10-1.00 [6H, m, (1'-CH₂)₃], 0.97-0.93 [12H, m, 4-CH₃ and (4'-CH₃)₃]; δ_{C} NMR (100 MHz, CDCl₃) 96.9 (OCH₂), 74.1 (C-1), 55.4 (OCH₃), 38.1 (C-2) 29.9 (C-2'), 28.1 (C-3'), 21.8 (C-3), 14.4 (C-4), 13.9 (C-4'), 9.7 (C-1')

c) Synthesis of tributyl(1-(methoxymethoxy)-2-methylpropyl)stannanes (**37c**)

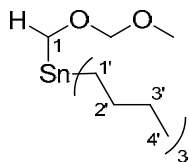
Diisopropylamine (1.7 mL, 12.0 mmol) was dissolved in dry THF (50 mL) at 0°C. *n*BuLi in hexane (8.6 mL, 1.4 M, 12.0 mmol) was added dropwise over 30 min *via* cannula. After 30 min tributyltin hydride (6.4 mL, 24.0 mmol) was added. The solution turned light pink/orange during the addition. After 1 h, the mixture was cooled to -78°C, and a solution of isobutyraldehyde (1.08 mL, 12.0 mmol) in THF (2 mL) was added and left to stir for 5 h while maintaining the low temperature bath. The solution turned yellow. The mixture was quenched with sat. NH₄Cl solution (3 x 20 mL), washed with water (3 x 20 mL) and extracted with petroleum ether (2 x 30 mL). The combined organic layers were dried over anhydrous MgSO₄, filtered and evaporated to afford a pale yellow oil, 2-methyl-1-(tributylstannyl)propan-1-ol **36c**, which was used in the next step without further purification.

N,N-Dimethylaniline (1.91 mL, 15 mmol) was added to a solution of 2-methyl-1-(tributylstannyl)propan-1-ol in CH₂Cl₂ (30 mL) at 0°C. α -Chloromethylmethylether (1.14 mL, 15.0 mmol) was added slowly and left to stir for 5 h. The mixture was washed with ice cold 0.5N HCl (3 x 30 mL), water (3 x 30 mL) and sat. NaHCO₃ (3 x 30 mL). The organic layer was dried over anhydrous MgSO₄, filtered and evaporated. The opaque oil was purified by column chromatography. The byproduct, tetrabutyltin was eluted with 10% dichloromethane in hexane, followed by the elution with 10% ethyl acetate in hexane to afford tributyl(1-(methoxymethoxy)-2-methylpropyl) stannane (**37c**, 1.61 g, 26.4%); IR (film) $\nu_{\text{max}}/\text{cm}^{-1}$ 2956, 2923, 1462, 1374, 1070 cm^{-1} ; δ_{H} NMR (400 MHz, C₆D₆) 4.56-4.54 (1H, m, O-CH₂), 4.05 (1H, d, *J* = 4.5 Hz, 1-CH), 3.21 (3H, s, OCH₃), 2.28-2.13 (2H, m, 2-CH₂), 1.73-1.56 [6H, m, (2'-CH₂)₃], 1.43-1.37 [6H, m, (3'-CH₂)₃], 1.10-1.01 [9H, m, (3-CH₃ and (1'-CH₂)₃], 0.98-0.84 [12H, m, 4-CH₃ and (4'-CH₃)₃]; δ_{C} NMR (100 MHz, CDCl₃) 97.3 (OCH₂), 82.4 (C-1), 55.4 (OCH₃), 33.3 (C-2) 29.7 (C-2'), 28.0 (C-3'), 21.5 (C-3), 20.2 (C-4), 13.9 (C-4'), 10.4 (C-1')

d) Attempted synthesis of tributyl(1-(methoxymethoxy)heptyl)stannane (**37d**)

Diisopropylamine (3.4 mL, 24.0 mmol) was dissolved in dry THF (50 mL) at 0°C. nBuLi in hexane (12.0 mL, 2.0 M, 24.0 mmol) was added dropwise over 20 min *via* cannula. After 30 min tributyltin hydride (6.4 mL, 24.0 mmol) was added and the solution turned dark orange during the addition. After 30 minutes the mixture was cooled to -78°C. A solution of heptaldehyde (1.37 mL, 15.0 mmol) in THF (2 mL) was added and left to stir for 2 h, while maintaining the low temperature bath. The mixture was quenched with sat. NH₄Cl solution (3 x 20 mL), washed with water (3 x 20 mL) and extracted with petroleum ether (2 x 30 mL). The combined organic layers were dried over anhydrous MgSO₄, filtered and evaporated. The colourless oil was used in the next step without further purification.

N,N-Dimethylaniline (3.81 mL, 30 mmol) was added to a solution of the colourless oil in CH₂Cl₂ (30 mL) at 0°C. α-Chloromethylmethylether (2.28 mL, 30.0 mmol) was added slowly and left to stir for 1 h. The mixture was washed with ice cold 0.5N HCl (3 x 30 mL), water (3 x 30 mL) and sat. NaHCO₃ (3 x 30 mL). The organic layer was dried over anhydrous MgSO₄, filtered and evaporated. The oil was purified by column chromatography. The byproduct, tetrabutyltin was eluted with 10% dichloromethane in hexane, followed by elution with 10% ethyl acetate in hexane to obtain several fractions. ¹H and ¹³C NMR analysis of the fractions showed the presence of the desired product. Upon further purification using the Chromatotron™, the product decomposed and therefore not isolated.

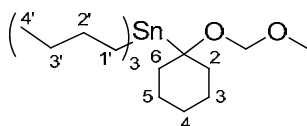
e) Attempted synthesis of tributyl((methoxymethoxy)methyl)stannane (**37e**)

Diisopropylamine (1.7 mL, 12.0 mmol) was dissolved in dry THF (50 mL) at 0°C. nBuLi in hexane (8.6 mL, 1.4 M, 12.0 mmol) was added dropwise over 30 min *via* cannula. After 30 min tributyltin hydride (3.2 mL, 12.0 mmol) was added. The solution turned light pink/orange during the addition. After 1 h the mixture was cooled to -78°C. In a separate flask paraformaldehyde (0.23 g, 7.5 mmol) was

crushed into a fine powder and suspended in dry THF (5 mL). The tributylstannyl lithium was added to the paraformaldehyde solution *via* a syringe. The organolithium solution turned dark brown during the addition. The mixture was left to stir for 5 h, while maintaining the low temperature bath. The solution turned dark brown. The mixture was quenched with sat. NH_4Cl solution (3 x 20 mL), washed with water (3 x 20 mL) and extracted with petroleum ether. The organic layers were dried over anhydrous MgSO_4 , filtered and solvent was removed to obtain a yellow oil that was used in the next step without further purification.

N,N-Dimethylaniline (1.91 mL, 15 mmol) was added to a solution of the yellow oil in CH_2Cl_2 (30 mL) at 0°C . α -Chloromethylmethylether (1.14 mL, 15.0 mmol) was added slowly and left to stir for 5 h. The mixture was washed with ice cold 0.5N HCl (3 x 30 mL), water (3 x 30 mL) and sat. NaHCO_3 (aq) (3 x 30 mL). The organic layer was dried over anhydrous MgSO_4 , filtered and the solvent was evaporated. TLC analysis of the crude material indicated the presence of the starting material paraformaldehyde and many side products such as tetrabutyltin.

f) Attempted synthesis of tributyl(1-(methoxymethoxy)cyclohexyl)stannane (37f)

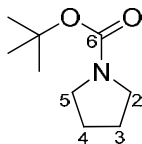


Diisopropylamine (3.4 mL, 24.0 mmol) was dissolved in dry THF (50 mL) at 0°C . *n*BuLi in hexane (17.2 mL, 1.4 M, 24.0 mmol) was added dropwise over 30 min *via* cannula. After 30 min tributyltin hydride (6.4 mL, 24.0 mmol) was added, the solution turned dark orange during the addition. After 1 h, the mixture was cooled to -78°C , and a solution of cyclohexanone (1.56 mL, 15.0 mmol) in THF (2 mL) was added. The mixture was left to stir for 5 h, while maintaining the low temperature bath, and then left to stir overnight for a total of 16 h. The mixture was quenched with sat. NH_4Cl solution (3 x 20 mL), followed by water (3 x 20 mL). The organic layers were dried over anhydrous MgSO_4 , filtered and evaporated to obtain a pale yellow oil which was used in the next step without further purification.

N,N-Dimethylaniline (3.81 mL, 30 mmol) was added to a solution of the pale yellow in CH_2Cl_2 (30 mL) at 0°C . α -Chloromethylmethylether (2.28 mL, 30.0 mmol) was added slowly and left to stir for 1 h. The mixture was washed with ice cold 0.5N HCl (3 x 30 mL), water (3 x 30 mL) and sat. NaHCO_3 (3 x 30 mL). The organic layer was dried over anhydrous MgSO_4 , filtered and the solvent was evaporated. TLC analysis of the crude material showed only starting material and side products.

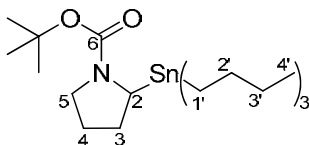
4.2.2. Synthesis of α -aminostannanes

a) Synthesis of *tert*-Butyl pyrrolidine-1-carboxylate (**42a**)



Pyrrolidine (7.94 mL, 96.01 mmol) was dissolved in CH_2Cl_2 (50 mL) at 0°C . Di-*tert*-butyl dicarbonate (19.64 g, 89.99 mmol) was added slowly over 10 min. The reaction mixture was allowed to warm to room temperature, and stirred for 12 h. The mixture was quenched with sat. NH_4Cl solution (2 x 40 mL). The organic layers were dried over anhydrous MgSO_4 , filtered and the solvent was evaporated. The opaque oil was purified by vacuum distillation to afford *tert*-butyl pyrrolidine-1-carboxylate **42a** as a colourless oil (11.09 g, 72.0%); IR (film) $\nu_{\text{max}}/\text{cm}^{-1}$ 2978, 2890, 1695(C=O), 1391 (C-N), 1253 (C-O) cm^{-1} ; δ_{H} NMR (400 MHz, CDCl_3) 3.33-3.28 (4H, m, 5- CH_2 and 2- CH_2), 1.83 (4H, br s, 3- CH_2 and 4- CH_2), 1.46 [9H, s, $(\text{CH}_3)_3$]; δ_{C} NMR (100 MHz, CDCl_3) 154.7 (C=O), 78.9 (C-8), 45.9 (C-2), 45.6 (C-5), 28.6 (3 x CH_3), 25.8 (C-3), 25.0 (C-4)

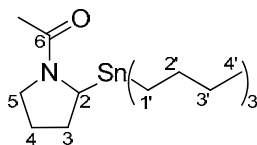
b) Synthesis of *tert*-Butyl 2-(tributylstannyl)pyrrolidine-1-carboxylate (**43a**)



sec-Butyllithium (0.9 M) in cyclohexane (60 mL, 53.14 mmol) was added dropwise over 45 min *via* cannula to a solution of TMEDA (7.9 mL, 53.14 mmol) in dry Et_2O (100 mL) at -78°C . After 20 min, *tert*-butyl pyrrolidine-1-carboxylate (**42a**, 7.20 g, 42.0 mmol) was added. The mixture turned milky yellow during the addition and stirred for 4 h. Tri-*n*-butyltin chloride (22.13 mL, 81.6 mmol) was added and the mixture warmed to room temperature while being stirred for 15 h. The mixture was washed with water (2 x 50 mL) and then with 50 mL of 2% $\text{H}_3\text{PO}_4(\text{aq})$. The aqueous layer was extracted with petroleum ether (2 x 10 mL). The combined organic layers were dried over anhydrous MgSO_4 , filtered evaporated and purified by column chromatography eluting with 10% ethyl acetate in hexane, to give *tert*-butyl 2-(tributylstannyl)pyrrolidine-1-carboxylate **43a** as a colourless oil (8.94 g, 46.2%); IR (film) $\nu_{\text{max}}/\text{cm}^{-1}$ 2923, 2875, 1675 (C=O), 1427 (C-N), 1270 (C-O) cm^{-1} ; δ_{H} NMR (400 MHz, C_6D_6) 3.27-3.21 (1H, m, 5- $\text{CH}^{\text{A}}\text{H}^{\text{B}}$), 3.15-3.11 (1H, m, 2-CH), 3.07-3.01 (1H, m, 5- $\text{CH}^{\text{A}}\text{H}^{\text{B}}$), 1.89-1.78 (2H, m, 3- CH_2), 1.74-1.56 [12H, m, (2'- CH_2)₃ and (3'- CH_2)₃], 1.42 (9H, s, 3 CH_3),

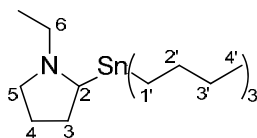
1.40-1.35 (2H, m, 4-CH₂), 1.03-0.98 [6H, m, (1'-CH₂)₃], 0.94 [9H, t, *J* = 7.3 Hz, (4'-CH₃)₃];
 δ_c NMR (100 MHz, C₆D₆) 154.5 (C=O), 78.4 (C-8), 46.7 (C-2), 46.5 (C-5), 30.8 (C-3), 29.8 (C-2'),
 28.7 (3 x CH₃), 28.1 (C-3'), 27.7 (C-4), 14.1 (C-4'), 10.9 (C-1')

c) Synthesis of *N*-acetyl-2-tributylstannylpyrrolidine (**44a**)



tert-Butyl 2-(tributylstannyl)pyrrolidine-1-carboxylate (**43a**, 1.45 g, 3.15 mmol) was dissolved in 20 mL of dry CH₂Cl₂. The flask was capped with a rubber septum and flushed with nitrogen. Iodotrimethylsilane (0.701 mL, 1.5 equiv) was added to the reaction by syringe in a single portion. The colourless solution immediately turned orange. As the reaction was stirred for 30 min the colour slowly changed to a faint yellow solution. A TLC (silica gel, 10% ethyl acetate in hexane) showed that all the starting material had been consumed. A 2.5 M solution of NaOH (20 mL) and acetyl chloride (0.8 mL, 10.5 mmol) was added. After 16 h, the two layers were separated and the aqueous layer was extracted with CH₂Cl₂ (3x 20 mL). The combined organic layers were dried over anhydrous MgSO₄, filtered, evaporated and purified by chromatography on silica gel, eluting with 20% ethyl acetate in hexane, to give *N*-acetyl-2-tributylstannylpyrrolidine **44a** as a colourless oil (0.80 g, 63.1%); IR (film) $\nu_{\max}/\text{cm}^{-1}$ 2954, 2927, 2854, 1627 (C=O), 1444 (C-N) cm⁻¹; δ_H NMR (400 MHz, CDCl₃) 3.49-3.44 (1H, m, 5-CH^AH^B), 3.35-3.27 (2H, m, 5-CH^AH^B and 2-CH), 2.17-2.11 (1H, m, 3-CH^AH^B), 2.00 (3H, s, COCH₃), 1.97-1.83 (3H, m, 3-CH^AH^B, 4-CH₂), 1.63-1.37 [6H, m, (2'-CH₂)₃], 1.32-1.23 [6H, m, (3'-CH₂)₃], 0.91-0.77 [15H, m, (1'-CH₂, 4'-CH₃)₃]; δ_c NMR (100 MHz, CDCl₃) 167.2 (C=O), 47.9 (C-5), 46.7 (C-2), 29.8 (C-3), 29.1 (C-2'), 27.5 (C-3' and C-4), 21.9 (C-7), 13.7 (C-4'), 10.4 (C-1')

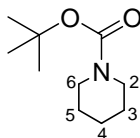
d) Synthesis of *N*-ethyl-2-(tributylstannyl)pyrrolidine (**45a**)



N-acetyl-2-tributylstannylpyrrolidine (**44a**, 0.80 g, 1.99 mmol) in Et₂O (5 mL) was added to a suspension of LiAlH₄ (0.1927 g, 5.51 mmol) in Et₂O (10 mL) at 0°C. The solution was stirred for 20 min, a TLC (silica gel, 20% ethyl acetate in hexane) showed that the starting material was consumed.

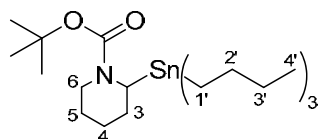
The reaction was quenched with methanol (1 mL) added dropwise and the mixture was adsorbed onto basic alumina. Elution with 20% ethyl acetate in hexane, gave *N*-ethyl-2-(tributylstannyl)pyrrolidine **45a** as a colourless oil (0.69 g, 89.4%); IR (film) $\nu_{\max}/\text{cm}^{-1}$ 2959, 2927, 2872, 1464 (C-N) cm^{-1} ; δ_{H} NMR (400 MHz, CDCl_3) 2.89-2.84 (1H, m, 5- $\text{CH}^{\text{A}}\text{H}^{\text{B}}$), 2.80-2.72 (1H, m, 6- $\text{CH}^{\text{A}}\text{H}^{\text{B}}$), 2.50-2.42 (1H, m, 2-CH), 2.12-1.83 (4H, series of multiplets, 6- $\text{CH}^{\text{A}}\text{H}^{\text{B}}$, 5- $\text{CH}^{\text{A}}\text{H}^{\text{B}}$ and 3- CH_2), 1.81-1.71 (2H, m, 4- CH_2), 1.64-1.41 [6H, m, (2'- CH_2)₃], 1.35-1.26 [6H, m, (3'- CH_2)₃], 1.10 (3H, t, *J* 7.1, 7- CH_3), 0.98-0.79 [15H, m, (1'- CH_2 and 4'- CH_3)₃]; δ_{C} NMR (100 MHz, CDCl_3) 57.8 (C-2), 53.7 (C-5), 50.8 (C-6), 29.4 (C-3), 29.3 (C-2'), 27.5 (C-3'), 24.3 (C-4), 14.2 (C-7), 13.7 (C-4'), 9.2 (C-1')

e) Synthesis of *tert*-Butyl piperidine-1-carboxylate (**42b**)



Di-*tert*-butyl dicarbonate (11.8 g, 54.0 mmol) was dissolved in CH_2Cl_2 (50 mL) at 0°C. Piperidine (4.71 mL, 47.5 mmol) was added slowly over 30 min. The ice bath was removed and the mixture was allowed to warm to room temperature, and stirred for 12h. The mixture was quenched with sat. NH_4Cl solution (2 x 40 mL). The organic layers were dried over anhydrous MgSO_4 , filtered evaporated and purified chromatography on silica gel, eluting with 10% ethyl acetate in hexane, to afford *tert*-butyl piperidine-1-carboxylate (**42b**) as a colourless oil (7.21 g, 81.9%); IR (film) $\nu_{\max}/\text{cm}^{-1}$ 2934, 2857, 1692(C=O), 1421 (C-N), 1268 (C-O) cm^{-1} ; δ_{H} NMR (400 MHz, C_6D_6) 3.29 (4H, br s, 2- CH_2 and 6- CH_2), 1.46 (9H, s, 3 CH_3), 1.20-1.18 (6H, m, 3- CH_2 , 4- CH_2 and 5- CH_2); δ_{C} NMR (100 MHz, C_6D_6) 154.7 (C=O), 78.7 (C-9), 44.7 (C-2 and C-6), 28.6 (3 x CH_3), 26.0 (C-4), 24.7 (C-3 and C-5)

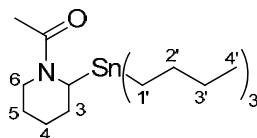
f) Synthesis of *tert*-butyl 2-(tributylstannyl)piperidine-1-carboxylate (**43b**)



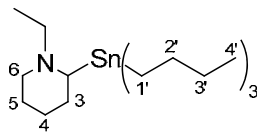
sec-Butyllithium (1.3 M) in cyclohexane (33.0 mL, 42.75 mmol) was added dropwise over 45 min *via* cannula to a solution of TMEDA (6.3 mL, 42.75 mmol) in dry Et_2O (100 mL) at -78°C. After 20 min, *tert*-butyl piperidine-1-carboxylate (**42b**, 6.11 g, 33.0 mmol) was added. The mixture turned milky yellow during the addition and stirred for 6 h. Tri-*n*-butyltin chloride (17.9 mL, 33.0 mmol) was added and the mixture warmed to room temperature while being stirred for 15 h. The mixture was

washed with water (2 x 50 mL) and then with 50 mL of 2% H₃PO₄(aq). The aqueous layer was extracted with petroleum ether (2 x 10 mL). The combined organic layers were dried over anhydrous MgSO₄, filtered evaporated and purified by column chromatography eluting with 10% ethyl acetate in hexane, to give *tert*-butyl 2-(tributylstannyl)piperidine-1-carboxylate **43b** as a colourless oil (9.55g, 61.0%); IR (film) $\nu_{\max}/\text{cm}^{-1}$ 2924, 2875, 1672 (C=O), 1427 (C-N), 1270 (C-O) cm^{-1} ; δ_{H} NMR (400 MHz, C₆D₆) 3.82-3.80 (1H, m, 6-CH^AH^B), 3.02-3.01 (2H, m, 2-CH₂), 2.88-2.85 (1H, m, 6-CH^AH^B), 1.78-1.69 [7H, m, 3-CH^AH^B and (2'-CH₂)₃], 1.67-1.57 (1H, m, 3-CH^AH^B), 1.56-1.44 [7H, m, 5-CH^AH^B and (3'-CH₂)₃], 1.39 (3H, s, COCH₃), 1.38-1.18 (3H, m, 4-CH₂ and 5-CH^AH^B), 1.16-1.05 [6H, m, (1'-CH₂)₃], 1.00 [9H, t, J 7.3 (4'-CH₃)₃]; δ_{C} NMR (100 MHz, C₆D₆) 156.2 (C=O), 79.2 (C-9), 47.5 (C-6), 47.3 (C-2), 31.1 (C-3), 29.9 (C-2'), 28.4 (3 x CH₃), 28.2 (C-3'), 27.1 (C-5), 26.7 (C-4), 14.1 (C-4'), 12.1 (C-1')

g) Synthesis of *N*-acetyl-2-(tributylstannyl)piperidine (**44b**)



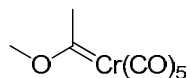
tert-Butyl 2-(tributylstannyl)piperidine-1-carboxylate (**43b**, 1.50 g, 3.16 mmol) was dissolved in 20mL of dry CH₂Cl₂. The flask was capped with a rubber septum and flushed with nitrogen. Iodotrimethylsilane (0.703 mL, 1.5 equiv) was added to the reaction by syringe in a single portion. The colourless solution immediately turned orange. As the reaction was stirred for 30 min the colour slowly changed to a clear solution. A TLC (silica gel, 10% ethyl acetate in hexane) showed that all the starting material had been consumed. A 2.5 M solution of NaOH (20 mL) and acetyl chloride (0.8 mL, 10.5 mmol) was added. After 16 h, the two layers were separated and the aqueous layer was extracted with CH₂Cl₂ (3x 20 mL). The combined organic layers were dried over anhydrous MgSO₄, filtered, evaporated and purified by chromatography on silica gel, eluting with 20% ethyl acetate in hexane, to give *N*-acetyl-2-tributylstannylpiperidine **44b** as a colourless oil (0.85 g, 64.6%); IR (film) $\nu_{\max}/\text{cm}^{-1}$ 2956, 2923, 2868, 1624 (C=O), 1451 (C-N) cm^{-1} ; δ_{H} NMR (400 MHz, CDCl₃) 3.48-3.45 (1H, m, 6-CH^AH^B), 3.38-3.32 (2H, m, 6-CH^AH^B and 2-CH), 2.05 (3H, s, COCH₃), 1.80-1.75 (1H, m, 3-CH), 1.71-1.54 [5H, m, 3-CH, 4-CH₂ and 5-CH₂], 1.52-1.39 [6H, m, (2'-CH₂)₃], 1.34-1.25 [6H, m, (3'-CH₂)₃], 0.91-0.79 [15H, m, (1'-CH₂, 4'-CH₃)₃]; δ_{C} NMR (100 MHz, CDCl₃) 168.4 (C=O), 49.0 (C-6), 45.0 (C-2), 30.38 (C-3), 29.2 (C-2'), 27.6 (C-3'), 26.9 (C-5), 26.2 (C-4), 21.4 (C-8), 13.7 (C-4'), 11.3 (C-1')

h) Synthesis of *N*-ethyl-2-(tributylstannyl)piperidine (**45b**)

N-acetyl-2-tributylstannylpiperidine (**44b**, 0.85 g, 2.04 mmol) in Et₂O (5 mL) was added to a suspension of LiAlH₄ (0.1801 g, 5.16 mmol) in Et₂O (10 mL) at 0°C. Stirred for 20 min, a TLC (silica gel, 20% ethyl acetate in hexane) showed that the starting material was consumed. The reaction was quenched with methanol (1 mL) added dropwise and the mixture was adsorbed onto basic alumina. Elution with 20% ethyl acetate in hexane, gave *N*-ethyl-2-(tributylstannyl)piperidine **45b** as a colourless oil (0.69 g, 84.1%); IR (film) $\nu_{\text{max}}/\text{cm}^{-1}$ 2950, 2923, 2868, 1462 (C-N) cm^{-1} ; δ_{H} NMR (400 MHz, CDCl₃) 3.29 (1H, br s, 2-CH), 2.65-2.62 (1H, m, 6-CH^AH^B), 2.44-2.31 (1H, m, 7-CH^AH^B), 2.30-2.18 (1H, m, 7-CH^AH^B), 2.09-1.95 (2H, m, 6-CH^AH^B and 3-CH^AH^B), 1.84-1.73 (1H, m, 3-CH^AH^B), 1.66-1.56 (2H, m, 5-CH₂), 1.52-1.40 [6H, m, (2'-CH₂)₃], 1.36-1.15 [8H, m, (3'-CH₂)₃ and 4-CH₂], 1.07 (3H, t, *J* = 14.3 Hz, 8-CH₃), 0.95-0.79 [15H, m, (1'-CH₂, 4'-CH₃)₃]; δ_{C} NMR (100 MHz, CDCl₃) 60.7 (C-2), 53.7 (C-6), 53.6 (C-7), 31.0 (C-3), 29.4 (C-2'), 27.6 (C-3'), 26.2 (C-5), 25.4 (C-4), 13.6 (C-4'), 12.6 (C-8), 11.3 (C-1')

4.3. Synthesis of Fischer Carbenes

Synthesis of [(methyl)(methoxy)carbene]pentacarbonyl chromium (0) (**66**) adapted from Hegedus *et al.*¹¹¹



Chromium hexacarbonyl (0.45 g, 2.05 mmol, 1 eq) was suspended in Et₂O (50 mL) under argon. Methylolithium (4.1 mL, 1.0M, 2 eq) was added *via* cannula dropwise over 15 min and stirred at room temperature for 1 h. The solution turned from yellow to dark brown. The solvent was removed under reduced pressure and the brown residue was dissolved in degassed water (10 mL). Trimethyloxonium tetrafluoroborate (1.35 g, 9.13 mmol, 4 eq) was added gradually and left to stir for 2 h. The mixture was extracted with 5 mL portions of Et₂O and collected. The solvent was removed under reduced pressure to give bright yellow crystals.

Methyl carbene (**66**) was obtained as a yellow crystalline solid (1.61g, 56.4%); IR (film) $\nu_{\text{max}}/\text{cm}^{-1}$ 2060, 1923, 1451, 1259; δ_{H} NMR (400 MHz, CDCl₃) 4.73 (3H, br s, OCH₃), 2.96 (3H, s, CH₃); δ_{C} NMR (100 MHz, CDCl₃) 360.5 (Cr=C), 223.3 (CO_{trans}), 216.4 (CO_{cis}), 67.5 (OCH₃), 49.8 (CH₃)

The remaining carbenes were synthesized from their respective stannanes following Method A or Method B as outlined below.

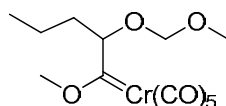
Method A¹¹¹

A stannane (2.74 mmol, 1 eq) was dissolved in dry Et₂O (20 mL) at 0°C. TMEDA (2.74 mmol, 1 eq) was added to the cold solution, followed by the drop wise addition of nBuLi in hexane (2.74 mmol, 2.0 M, 1 eq). The solution was left to stir for 20 min. Chromium hexacarbonyl (2.46 mmol, 0.9 eq) was crushed into a fine powder and added in small portions over 10 min and left to stir for ½ h in the cold and then a further 3 h at room temperature. The solvent was removed *in vacuo* and degassed water (20 mL) added to the residue. A freeze pump thaw method with liquid nitrogen was used to remove all the gas from the water. Trimethyloxonium tetrafluoroborate (10.95 mmol, 4 eq) was added then left to stir for 30 min at room temperature. The carbene was extracted from the aqueous layer with dry Et₂O in small portions (5 x 5 mL) and placed into a Schlenk flask, where the solvent was removed *in vacuo* to afford the carbene product.

Method B¹⁴⁹

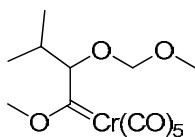
A stannane (3mmol, 1 eq) was dissolved in dry Et₂O (50 mL) at 0°C. TMEDA (2.06 mmol, 1 eq) was added to the cold solution, followed by dropwise addition of nBuLi in hexane (6.4 mmol, 2.0 M, 2.13 eq). The solution was left to stir for 20 min and then the temperature of the bath was cooled to -40°C. Chromium hexacarbonyl (6.00 mmol, 2 eq) was crushed into a fine powder and added in small portions over 15 min. The solution turned yellow and was stirred for 30 min. The cold bath was removed and the yellow/brown solution was stirred at rt for 1 h. The solvent was removed under reduced pressure and the residue was dissolved in dry dichloromethane (10 mL) and cooled again to -30°C. Trimethyloxonium tetrafluoroborate (6.4 mmol, 2.13 eq) was added then left to stir for 30 min in the cold and for a further 1 h at room temperature. The solvent was removed under pressure to afford the carbene product.

a) Synthesis of [(1-methoxy-2-(methoxymethoxy)pentyl carbene] pentacarbonyl chromium (0) (**68b**)



Method A was used with the following quantities of reagents; tributyl(1-(methoxymethoxy)butyl)stannane (**37b**, 1.06 g, 3.0 mmol, 1 eq) and TMEDA (0.45 mL, 3.0 mmol, 1 eq) in dry Et₂O (20 mL), followed by the addition of nBuLi in hexane (1.5 mL, 3.0 mmol, 2.0 M, 1 eq) and chromium hexacarbonyl (0.66 g, 3.0 mmol, 1 eq). Trimethyloxonium tetrafluoroborate (1.33 g, 9.0 mmol, 3 eq) was added to the aqueous mixture. The carbene was extracted from the aqueous layer with dry Et₂O in small portions (5 x 5 mL) and placed into a Schlenk flask, where the solvent was removed *in vacuo* to afford the product **68b** obtained as a component of a yellow slurry (0.66 g crude mass); δ_c NMR (100 MHz, C₆D₆) 363.3 (Cr=C), 223.4 (CO_{trans}), 216.8 (CO_{cis}), 95.2 (OCH₂), 82.0 (CH), 68.0 (OCH₃), 62.7 (OCH₃), 39.2 (CH₂), 22.8 (CH₂), 14.3 (CH₃)

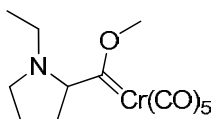
b) Synthesis of [(1-methoxy-2-(methoxymethoxy)-3-methylbutyl) carbene] pentacarbonyl chromium (0) (**68c**)



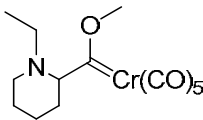
Method A was used with the following quantities of reagents; tributyl(1-(methoxymethoxy)-2-methylpropyl) stannane (**37c**, 1.03 g, 2.3 mmol, 1 eq) and TMEDA (0.34 mL, 2.3 mmol, 1 eq) in dry Et₂O (20 mL), followed by the addition of *n*BuLi in hexane (1.14 mL, 2.3 mmol, 2.0 M, 1 eq) and chromium hexacarbonyl (0.45 g, 2.1 mmol, 0.9 eq). Trimethyloxonium tetrafluoroborate (1.35 g, 9.1 mmol, 4 eq) was added to the aqueous mixture. The carbene was extracted from the aqueous layer with dry Et₂O in small portions (5 x 5 mL) and placed into a Schlenk flask, where the solvent was removed *in vacuo* to afford the product **68c** obtained as a component of a yellow slurry (0.34 g crude mass); δ_c NMR (100 MHz, C₆D₆) 363.3 (Cr=C), 224.8 (CO_{trans}), 216.8 (CO_{cis}), 97.7 (OCH₂), 87.8 (CH), 68.0 (OCH₃), 62.7 (OCH₃), 39.2 (CH), 24.2 (CH₃), 23.4 (CH₃)

Method B was attempted, however ¹³C NMR analysis of the crude material was inconclusive.

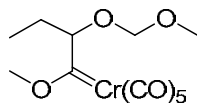
c) Synthesis of [(1-ethylpyrrolidin-2-yl)(methoxy)carbene]pentacarbonyl chromium (0) (**70a**)



Method A was used with the following quantities of reagents; *N*-ethyl-2-(tributylstannyl)pyrrolidine (**45a**, 0.69 g, 1.8 mmol, 1 eq) and TMEDA (0.54 mL, 3.6 mmol, 2 eq) in dry Et₂O (20 mL), followed by the addition of *n*BuLi in hexane (1.8 mL, 3.6 mmol, 2.0 M, 2 eq) and chromium hexacarbonyl (0.39 g, 1.8 mmol, 1 eq). Trimethyloxonium tetrafluoroborate (0.80 g, 5.4 mmol, 3 eq) was added to the aqueous mixture. The carbene was extracted from the aqueous layer with dry Et₂O in small portions (5 x 5 mL) and placed into a Schlenk flask, where the solvent was removed *in vacuo* to afford the product **70a** obtained as a component of a dark yellow slurry (0.02 g crude mass); δ_c NMR (100 MHz, C₆D₆) 360.5 (Cr=C), 224.8 (CO_{trans}), 214.3 (CO_{cis}), 85.9 (OCH₃), 59.8 (CH₂), 55.7 (CH), 49.8 (CH₂), 27.4 (CH₂), 22.9 (CH₂), 11.0 (CH₃)

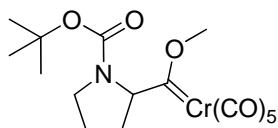
d) Synthesis of [(1-ethylpiperidin-2-yl)(methoxy)carbene]pentacarbonyl chromium (0) (**70b**)

Method A was used with the following quantities of reagents; *N*-ethyl-2-(tributylstannyl)piperidine (**45b**, 0.69 g, 1.8 mmol, 1 eq) and TMEDA (0.54 mL, 3.6 mmol, 2 eq) in dry Et₂O (20 mL), followed by the addition of *n*BuLi in hexane (1.8 mL, 3.6 mmol, 2.0 M, 2 eq) and chromium hexacarbonyl (0.39 g, 1.8 mmol, 1 eq). Trimethyloxonium tetrafluoroborate (0.80 g, 5.4 mmol, 3 eq) was added to the aqueous mixture. The carbene was extracted from the aqueous layer with dry Et₂O in small portions (5 x 5 mL) and placed into a Schlenk flask, where the solvent was removed *in vacuo* to afford the product **70b** obtained as a component of a light yellow slurry (1.06 g crude mass); δ_C NMR (100 MHz, C₆D₆) 361.0 (Cr=C), 220.1 (CO_{trans}), 210.1 (CO_{cis}), 85.8 (OCH₃), 62.6 (CH₂), 59.9 (CH₂), 55.8 (CH), 35.5 (CH₂), 26.4 (CH₂), 23.3 (CH₂), 10.3 (CH₃)

e) Attempted synthesis of [(1-methoxy-2-(methoxymethoxy)butylcarbene]pentacarbonyl chromium (0) (**68a**)

Method B was used with the following quantities of reagents; tributyl(1-(methoxymethoxy)-2-methylpropyl) stannane (**37a**, 1.18 g, 3.0 mmol, 1 eq) and TMEDA (0.93 mL, 6.2 mmol, 2.1 eq) in dry Et₂O (20 mL), followed by the addition of *n*BuLi in hexane (3.2 mL, 6.4 mmol, 2.0 M, 2.1 eq) and chromium hexacarbonyl (1.3 g, 6.0 mmol, 2 eq). The solvent was removed and the residue was dissolved in dry dichloromethane (20 mL) to which trimethyloxonium tetrafluoroborate (0.95 g, 6.4 mmol, 2.1 eq) was added. The solvent was removed to give the crude pale yellow solid residue. ¹H and ¹³C NMR analysis of the crude mixture showed the absence of diagnostic signals hence the carbene was not isolated.

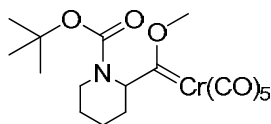
f) Attempted synthesis of [(1-(*tert*-butoxycarbonyl)pyrrolidin-2-yl)(methoxy)carbene] pentacarbonyl chromium (0) (**72a**)



Method A was used with the following quantities of reagents; *tert*-butyl 2-(tributylstannyl)pyrrolidine-1-carboxylate (**43a**, 1.26 g, 2.7 mmol, 1 eq) and TMEDA (0.41 mL, 2.7 mmol, 1 eq) in dry Et₂O (20 mL), followed by the addition of *n*BuLi in hexane (1.4 mL, 2.7 mmol, 2.0 M, 1 eq) and chromium hexacarbonyl (0.58 g, 2.5 mmol, 0.9 eq). Trimethyloxonium tetrafluoroborate (1.62 g, 10.9 mmol, 4 eq) was added to the aqueous mixture. The carbene was extracted from the aqueous layer with dry Et₂O in small portions (5 x 5 mL) and placed into a Schlenk flask, where the solvent was removed *in vacuo* to give a dark yellow oil. ¹H and ¹³C NMR analysis of the crude mixture showed only starting material such as chromium hexacarbonyl and byproducts such as tetrabutyltin, hence the carbene was not isolated.

Method B was used with the following quantities of reagents; *tert*-butyl 2-(tributylstannyl)pyrrolidine-1-carboxylate (**43a**, 1.13 g, 2.5 mmol, 1 eq) and TMEDA (0.73 mL, 5.0 mmol, 2.0 eq) in dry Et₂O (20 mL), followed by the addition of *n*BuLi in hexane (2.5 mL, 5.09 mmol, 2.0 M, 2.0 eq) and chromium hexacarbonyl (0.5 g, 2.5 mmol, 1 eq). The solvent was removed and the residue was dissolved in dry dichloromethane (20 mL) to which trimethyloxonium tetrafluoroborate (0.91 g, 6.1 mmol, 2.5 eq) was added. The solvent was removed to give the crude yellow residue. ¹H and ¹³C NMR analysis of the crude mixture showed the absence of diagnostic signals hence the carbene was not isolated.

g) Attempted synthesis of [(1-(*tert*-butoxycarbonyl)piperidine-2-yl)(methoxy)carbene] pentacarbonyl chromium (0) (**72b**)



Method A was used with the following quantities of reagents; *tert*-butyl 2-(tributylstannyl)piperidine-1-carboxylate (**43b**, 0.61 g, 1.3 mmol, 1 eq) and TMEDA (0.19 mL, 1.3 mmol, 1 eq) in dry Et₂O (20 mL), followed by the addition of *n*BuLi in hexane (0.65 mL, 1.3 mmol, 2.0 M, 1 eq) and chromium hexacarbonyl (0.30 g, 1.2 mmol, 0.9 eq). Trimethyloxonium tetrafluoroborate (0.77 g, 5.2 mmol, 4 eq) was added to the aqueous mixture. The carbene was extracted from the aqueous layer with dry Et₂O in small portions (5 x 5 mL) and placed into a Schlenk flask, where the solvent was removed *in vacuo* to give a dark yellow oil (0.41 g crude mass). ¹H and ¹³C NMR analysis of the crude mixture showed only starting material such as chromium hexacarbonyl and byproducts such as tetrabutyltin, hence the carbene was not isolated.

References

- (1) Kauffman, G. B., *Journal of Chemical Education* **1983**, *60*, 185-186.
- (2) Laszlo, P.; Hoffmann, R., *Angew. Chem., Int. Ed* **2000**, *39*, 123-124.
- (3) Wilkinson, G.; Rosenblum, M.; Whiting, M. C.; Woodward, R. B., *J. Am. Chem. Soc.* **1952**, *74*, 2125-2126.
- (4) Kitamura, M.; Oka, H.; Suga, S.; Noyori, R., *Org. Synth.* **2002**, *79*, 139-142.
- (5) Clayden, J.; Greeves, N.; Warren, S.; Wothers, P., In *Organic Chemistry*; Oxford University Press: New York, United States, 2001; Vol. 1, pp 1513.
- (6) Nobelprize.org http://nobelprize.org/nobel_prizes/chemistry/laureates/ (accessed 03/25/ 2011)
- (7) Britovsek, G. J. P.; Gibson, V. C.; Wass, D. F., *Angew. Chem., Int. Ed* **1999**, *38*, 428-447.
- (8) Cotton, F. A., *Chem. Rev.* **1955**, *55*, 551-594.
- (9) Clayden, J., In *Organolithiums: Selectivity for Synthesis*; Tetrahedron Organic chemistry Series; Elsevier Science Ltd: Oxford, **2002**; Vol. 23, pp 383.
- (10) Cotton, F. A., *J. Am. Chem. Soc.* **1968**, *90*, 6230-6232.
- (11) Lloyd, N. C.; Morgan, H. W.; Nicholson, B. K.; Ronimus, R. S., *Angew. Chem., Int. Ed* **2005**, *44*, 941-944.
- (12) Sato, T., In *Tin*; Edward W. Abel, F. Gordon A. Stone and Geoffrey Wilkinson, Eds.; Comprehensive Organometallic Chemistry II; Elsevier: Oxford, **1995**; pp 355-387.
- (13) Davies, A. G., In *Organotin Chemistry*; Wiley-VCH Verlag GmbH & Co. KGaA Weinheim: Germany, **2004**; Vol. 1, pp 438.
- (14) Braunstein, P.; Morise, X., *Chem. Rev.* **2000**, *100*, 3541-3552.
- (15) Molloy, K. C.; Purcell, T. G.; Hahn, E.; Schumann, H.; Zuckerman, J. J., *Organometallics* **1986**, *5*, 85-89.
- (16) van der Kerk, G. J. M., In *Organotin Chemistry: Past, Present and Future*; Organotin Compounds: New Chemistry and Applications; American Chemical Society: **1976**; pp 1-25.
- (17) Wakabayashi, K.; Yorimitsu, H.; Shinokubo, H.; Oshima, K., *Org. Lett.* **2000**, *2*, 1899-1901.
- (18) Kamiura, K.; Wada, M., *Tetrahedron Lett.* **1999**, *40*, 9059-9062.
- (19) Lamandé-Langle, S.; Abarbri, M.; Thibonnet, J.; Duchêne, A., *J. Organomet. Chem.* **2009**, *694*, 2368-2374.
- (20) Li, C., *Chem. Rev.* **2005**, *105*, 3095-3166.

-
- (21) Hamze, A.; Le Menez, P.; Provot, O.; Morvan, E.; Brion, J. D.; Alami, M., *Tetrahedron* **2010**, *66*, 8698-8706.
- (22) Rasolofonjatovo, E.; Provot, O.; Hamze, A.; Bignon, J.; Thoret, S.; Brion, J.; Alami, M., *Eur. J. Med. Chem.* **2010**, *45*, 3617-3626.
- (23) Tanpure, R. P.; Harkrider, A. R.; Strecker, T. E.; Hamel, E.; Trawick, M. L.; Pinney, K. G., *Bioorg. Med. Chem.* **2009**, *17*, 6993-7001.
- (24) Holt, M. S.; Wilson, W. L.; Nelson, J. H., *Chem. Rev.* **1989**, *89*, 11-49.
- (25) Chinchilla, R.; Nájera, C.; Yus, M., *Chem. Rev.* **2004**, *104*, 2667-2722.
- (26) Brenner, M.; Mayer, G.; Terpin, A.; Steglich, W., *Chemistry - A European Journal* **1997**, *3*, 70-74.
- (27) Wolf, C.; Lerebours, R., *J. Org. Chem.* **2003**, *68*, 7551-7554.
- (28) Canovese, L.; Visentin, F.; Levi, C.; Santo, C., *J. Organomet. Chem.* **2008**, *693*, 3324-3330.
- (29) Espinet, P.; Echavarren, A. M., *Angew. Chem., Int. Ed* **2004**, *43*, 4704-4734.
- (30) Paterson, I.; Man, J., *Tetrahedron Lett.* **1997**, *38*, 695-698.
- (31) Durham, T. B.; Blanchard, N.; Savall, B. M.; Powell, N. A.; Roush, W. R., *J. Am. Chem. Soc.* **2004**, *126*, 9307-9317.
- (32) Evano, G.; Blanchard, N.; Toumi, M., *Chem. Rev.* **2008**, *108*, 3054-3131.
- (33) Flöistrup, E.; Goede, P.; Strömberg, R.; Malm, J., *Tetrahedron Lett.* **2011**, *52*, 209-211.
- (34) Ye, J.; Bhatt, R. K.; Falck, J. R., *J. Am. Chem. Soc.* **1994**, *116*, 1-5.
- (35) Goli, M.; He, A.; Falck, J. R., *Org. Lett.* **2011**, *13*, 344-346.
- (36) Fagnoni, M.; Dondi, D.; Ravelli, D.; Albin, A., *Chem. Rev.* **2007**, *107*, 2725-2756.
- (37) Campari, G.; Fagnoni, M.; Mella, M.; Albin, A., *Tetrahedron Asymmetry* **2000**, *11*, 1891-1906.
- (38) Whitfield, D. M.; Ogawa, T., *Glycoconjugate J.* **1998**, *15*, 75-78.
- (39) Thibaud, S.; Moine, L.; Degueil, M.; Maillard, B., *Eur. Polym. J.* **2006**, *42*, 1273-1283.
- (40) Gastaldi, S.; Stien, D., *Tetrahedron Lett.* **2002**, *43*, 4309-4311.
- (41) Curran, D. P.; Hadida, S.; Kim, S.-Y.; Luo, Z., *J. Am. Chem. Soc.* **1999**, *121*, 6607-6615.
- (42) Light, J.; Breslow, R., *Tetrahedron Lett.* **1990**, *31*, 2957-2958.
- (43) Clive, D. L. J.; Wang, J., *J. Org. Chem.* **2002**, *67*, 1192-1198.
- (44) Cokley, T. M.; Harvey, P. J.; Marshall, R. L.; McCluskey, A.; Young, D. J., *J. Org. Chem.* **1997**, *62*, 1961-1964.
-

-
- (45) Kells, K. W.; Nielsen, N. H.; Armstrong-Chong, R. J.; Michael Chong, J., *Tetrahedron* **2002**, *58*, 10287-10291.
- (46) Peterson, D. J., *J. Organomet. Chem.* **1970**, *21*, 63-64.
- (47) Peterson, D. J., *J. Am. Chem. Soc.* **1971**, *93*, 4027-4031.
- (48) Hoppe, D.; Hense, T., *Angew. Chem., Int. Ed* **1997**, *36*, 2282.
- (49) Santiago, M.; Low, E.; Chambournier, G.; Gawley, R. E., *J. Org. Chem.* **2003**, *68*, 8480-8484.
- (50) Ashweek, N. J.; Brandt, P.; Coldham, I.; Dufour, S.; Gawley, R. E.; Hæffner, F.; Klein, R.; Sanchez-Jimenez, G., *J. Am. Chem. Soc.* **2005**, *127*, 449-457.
- (51) Grana, P.; Paleo, M. R.; Sardina, F. J., *J. Am. Chem. Soc.* **2002**, *124*, 12511-12514.
- (52) Beak, P.; Zajdel, W. J.; Reitz, D. B., *Chem. Rev.* **1984**, *84*, 471-523.
- (53) Sawyer, J. S.; Kucerovy, A.; Macdonald, T. L.; McGarvey, G. J., *J. Am. Chem. Soc.* **1988**, *110*, 842-853.
- (54) Still, W. C., *J. Am. Chem. Soc.* **1978**, *100*, 1481-1487.
- (55) Coldham, I.; Adams, H.; Ashweek, N. J.; Barker, T. A.; Reeder, A. T.; Skilbeck, M. C., *Tetrahedron Lett.* **2010**, *51*, 2457-2460.
- (56) Coldham, I.; Fernández, J.-C.; Snowden, D. J., *Tetrahedron Lett.* **1999**, *40*, 1819-1822.
- (57) Chen, Z.; Trudell, M. L., *Chem. Rev.* **1996**, *96*, 1179-1193.
- (58) Danheiser, R. L.; Romines, K. R.; Koyama, H.; Gee, S. K.; Johnson, C. R.; Medich, J., *Org. Syn.* **1993**, *71*, 133-138.
- (59) Kells, K. W.; Chong, J. M., *Org. Lett.* **2003**, *5*, 4215-4218.
- (60) Linderman, R. J.; Griedel, B. D., *J. Org. Chem.* **1991**, *56*, 5491-5493.
- (61) Still, W. C.; Sreekumar, C., *J. Am. Chem. Soc.* **1980**, *102*, 1201-1202.
- (62) Linderman, R. J.; Cusack, K. P.; Jaber, M. R., *Tetrahedron Lett.* **1996**, *37*, 6649-6652.
- (63) Beak, P.; Kerrick, S. T.; Wu, S.; Chu, J., *J. Am. Chem. Soc.* **1994**, *116*, 3231-3239.
- (64) Gawley, R. E.; Zhang, Q.; McPhail, A. T., *Tetrahedron: Asymmetry* **2000**, *11*, 2093-2106.
- (65) Gawley, R. E.; Narayan, S.; Vicic, D. A., *J. Org. Chem.* **2005**, *70*, 328-329.
- (66) Coeffard, V.; Beaudet, I.; Evain, M.; Le Grogneec, E.; Quintard, J.-P., *Eur. J. Org. Chem.* **2008**, 3344-3351.
-

- (67) Quintard, J.-P.; Degueil-Castaing, M.; Barbe, B.; Petraud, M., *J. Organomet. Chem.* **1982**, *234*, 41-61.
- (68) Cintrat, J.-C.; Léat-Crest, V.; Parrain, J.-L.; Le Grogneq, E.; Beaudet, I.; Toupet, L.; Quintard, J.-P., *Eur. J. Org. Chem.* **2004**, 4268-4279.
- (69) Snieckus, V., *Chem. Rev.* **1990**, *90*, 879-933.
- (70) Jordaan, M., PhD Thesis North West University **2007**.
- (71) Hoye, T. R.; Kabrhel, J. E.; Hoye, R. C., *Org. Lett.* **2005**, *7*, 275-277.
- (72) Lipton, M.F.; M. Sorensen, C.; C. Sadler, A.; H. Shapiro, R., *J. Organomet. Chem.* **1980**, *186*, 155-158.
- (73) Behling, J. R.; Ng, J. S.; Babiak, K. A.; Campbell, A. L.; Elsworth, E.; Lipshutz, B. H., *Tetrahedron Lett.* **1989**, *30*, 27.
- (74) Farina, V.; Farina, V., *J. Org. Chem.* **1991**, *56*, 4985.
- (75) Still, W., *J. Org. Chem.* **1978**, *43*, 2923.
- (76) Friebolin, H., *Basic One-Dimensional and Two-Dimensional NMR Spectroscopy*; WILEY-VCH Verlag GmbH & Co. KGaA, Weinheim: Germany, **2005**
- (77) Clark, H. C.; Kwon, J. T.; Reeves, L. W.; Wells, E. J., *Can. J. Chem.* **1963**, *41*, 3005-3012.
- (78) Martins, J. C.; Biesemans, M.; Willem, R., *Prog. Nucl. Magn. Reson. Spectrosc.* **2000**, *36*, 271-322.
- (79) Kuivila, H. G.; Considine, J. L.; H. Sarma, R.; J. Mynott, R., *J. Organomet. Chem.* **1976**, *111*, 179-196.
- (80) Al-Allaf, T. A. K., *J. Organomet. Chem.* **1986**, *306*, 337-346.
- (81) Wrackmeyer, B., *J. Magn. Reson.* **1981**, *42*, 287-297.
- (82) Frish, M. J.; Trucks, G. W.; Schlegel, H. B.; Scuseria, M. A.; Robb, J. R.; Cheeseman, J. A.; Montgomery, J.; Vreven, T.; Kudin, J. C.; Burant, J. C.; Millam, J. M.; Iyengar, S. S.; Tomasi, J.; Barone, V.; Mennucci, B.; Cossi, M.; Scalmani, G.; Rega, N.; Petersson, G. A.; Nakatsuji, H.; Hada, M.; Ehara, M.; Toyota, K.; Fukuda, R.; Hasegawa, J.; Ishida, M.; Nakajima, T.; Honda, Y.; Kitao, O.; Nakai, H.; Klene, M.; Li, X.; Knox, J. E.; Hratchian, H. P.; Cross, J. B.; Bakken, V.; Adamo, C.; Jaramillo, J.; Gomperts, R.; Stratmann, R. E.; Yazyev, O.; Austin, A. J.; Cammi, R.; Pomelli, C.; Ochterski, J. W.; Ayala, P. Y.; Morokuma, K.; Voth, G. A.; Salvador, P.; Dannenberg, J. J.; Zakrzewski, V. G.; Dapprich, S.; Daniels, A. D.; Strain, M. C.; Farkas, O.; Malick, K.; Rabuck, A. D.; Raghavachari, K.; Foresman, J. B.; Ortiz, J. V.; Cui, Q.; Baboul, A. G.; Clifford, S.; Cioslowski, J.; Stefanov, B. B.; Liu, G.; Liashenko, A.; Piskorz, P.; Komaromi, I.; Martin, R. L.; Fox, D. J.; Keith, T.; Al-Laham, M. A.; Peng, C. Y.; Nanayakkara, A.; Challacombe, M.; Gill, P. M. W.; Johnson, B.; Chen, W.; Wong, M. W.; Gonzalez, C.; Pople, J. A., *Gaussian 03* [Computer Program]. Gaussian, Inc.: Wallingford CT, **2004**.

-
- (83) Cramer, C. J., In *Essentials of Computational Chemistry: Theories and Models*; John Wiley & Sons: England, **2002**; pp 542-556.
- (84) Wakamatsu, K.; Orita, A.; Otera, J., *Organometallics* **2008**, *27*, 1092-1097.
- (85) Beak, P.; Lee, W. K., *J. Org. Chem.* **1993**, *58*, 1109-1117.
- (86) Beak, P.; Lee, W., *Tetrahedron Lett.* **1989**, *30*, 1197-1200.
- (87) Meyers, A. I.; Edwards, P. D.; Rieker, W. F.; Bailey, T. R., *J. Am. Chem. Soc.* **1984**, *106*, 3270-3276.
- (88) Wakefield, B. J., *Organolithium Methods*; Best Synthetic Methods; Academic Press, London, **1988**
- (89) Doddrell, D.; Burfitt, I.; Kitching, W.; Bullpitt, M.; Lee, C.-H.; Mynott, R. J.; Considine, J. L.; Kuivila, H. G.; Sarma, R. H., *J. Am. Chem. Soc.* **1974**, *96*, 1640-1642.
- (90) Kitching, W.; Olszowy, H.; Waugh, J.; Doddrell, D., *J. Org. Chem.* **1978**, *43*, 898-906.
- (91) Pedretti, A.; Villa, L.; Vistoli, G., *J. Mol. Graph. Model.* **2002**, *21*, 47-49.
- (92) Pedretti, A.; Villa, L.; Vistoli, G., *Theor. Chem. Acc.* **2003**, *109*, 229-232.
- (93) Bourissou, D.; Guerret, O.; Gabbai, F. P.; Bertrand, G., *Chem. Rev.* **2000**, *100*, 39-92.
- (94) Herndon, J. W., *Coord. Chem. Rev.* **2010**, *254*, 103-194.
- (95) de Frémont, P.; Marion, N.; Nolan, S. P., *Coord. Chem. Rev.* **2009**, *253*, 862-892.
- (96) Dötz, K. H.; Stendel Jr., J., *Chem. Rev.* **2009**, *109*, 3227-3274.
- (97) Barluenga, J.; Fernández-Rodríguez, M. A.; Aguilar, E., *J. Organomet. Chem.* **2005**, *690*, 539-587.
- (98) Butler, W. M.; Enemark, J. H.; Parks, J.; Balch, A. L., *Inorg. Chem.* **1973**, *12*, 451-457.
- (99) Fischer, E. O.; Maasböl A., *Angew. Chem., Int. Ed* **1964**, *3*, 580.
- (100) Wanzlick, H. W.; Fjedor, E.; Jerg, H. J., *Chem. Ber.* **1963**, *96*, 1208.
- (101) Wanzlick, H.-W.; Schönherr, H.-J., *Angew. Chem., Int. Ed* **1968**, *7*, 141-142.
- (102) Arduengo, A. J.; Harlow, R. L.; Kline, M., *J. Am. Chem. Soc.* **1991**, *113*, 361-363.
- (103) Schrock, R. R., *J. Am. Chem. Soc.* **1974**, *96*, 6796-6797.
- (104) Hartley, R. C.; Li, J.; Main, C. A.; McKiernan, G. J., *Tetrahedron* **2007**, *63*, 4825-4864.
- (105) Petasis, N. A.; Bzowej, E. I., *J. Am. Chem. Soc.* **1990**, *112*, 6392-6394.
- (106) Meurer, E. C.; Santos, L. S.; Pilli, R. A.; Eberlin, M. N., *Org. Lett.* **2003**, *5*, 1391-1394.

-
- (107) Tebbe, F. N.; Parshall, G. W.; Reddy, G. S., *J. Am. Chem. Soc.* **1978**, *100*, 3611-3613.
- (108) Schrock, R. R., *Chem. Rev.* **2002**, *102*, 145-180.
- (109) Jacobsen, H.; Ziegler, T., *J. Am. Chem. Soc.* **1994**, *116*, 3667-3679.
- (110) Truscott, B. J.; Klein, R.; Kaye, P. T., *Tetrahedron Lett.* **2010**, *51*, 5041-5043.
- (111) Hegedus, L. S.; McGuire, M. A.; Schultze, L. M., *Org. Synth.* **1987**, *65*, 140-144.
- (112) Semmelhack, M. F.; Lee, G. R., *Organometallics* **1987**, *6*, 1839-1844.
- (113) Imwinkelried, R.; Hegedus, L. S., *Organometallics* **1988**, *7*, 702-706.
- (114) Dötz, K. H.; Tomuschat, P., *Chem. Soc. Rev.* **1999**, *28*, 187-198.
- (115) Matsuyama, H.; Nakamura, T.; Iyoda, M., *J. Org. Chem.* **2000**, *65*, 4796-4803.
- (116) Hahn, F. E., *Angew. Chem., Int. Ed.* **1993**, *32*, 650-665.
- (117) Rendina, L. M.; Vittal, J. J.; Puddephatt, R. J., *Organometallics* **1995**, *14*, 1030-1038.
- (118) Moss, R. A.; Fede, J.-M.; Yan, S., *J. Am. Chem. Soc.* **2000**, *122*, 9878-9879.
- (119) Fischer, E. O.; Beck, H.-J., *Angew. Chem., Int. Ed.* **1970**, *9*, 72-73.
- (120) Liu, S.-T.; Reddy, K. R., *Chem. Soc. Rev.* **1999**, *28*, 315-322.
- (121) Lage, M. L.; Fernández, I.; Mancheño, M. J.; Sierra, M. A., *Inorg. Chem.* **2008**, *47*, 5253-5258.
- (122) Hegedus, L. S., *Tetrahedron* **1997**, *53*, 4105-4128.
- (123) Nakatsuji, H.; Ushio, J.; Han, S.; Yonezawa, T., *J. Am. Chem. Soc.* **1983**, *105*, 426-434.
- (124) Taylor, T. E.; Hall, M. B., *J. Am. Chem. Soc.* **1984**, *106*, 1576-1584.
- (125) Cundari, T. R., *Chem. Rev.* **2000**, *100*, 807-818.
- (126) Gómez-Gallego M.; Mancheño M. J.; Sierra, M. A., *Acc. Chem. Res.* **2005**, *38*, 44.
- (127) Fernández, I.; Cossío, F. P.; Arrieta, A.; Lecea, B.; Mancheño, M. J.; Sierra, M. A., *Organometallics* **2004**, *23*, 1065-1071.
- (128) Sierra, M. A., *Chem. Rev.* **2000**, *100*, 3591-3638.
- (129) Barluenga, J.; Flórez, J.; Fañanás, F. J., *Journal of Organometallic Chemistry* **2001**, *624*, 5-17.
- (130) Fischer, E. O.; Kreis, G.; Kreiter, C. G.; Müller, J.; Huttner, G.; Lorenz, H., *Angew. Chem., Int. Ed.* **1973**, *12*, 564-565.
- (131) Amin, S. R.; Sarkar, A., *Organometallics* **1995**, *14*, 547-550.
- (132) Andersen, B. A.; Wulff, W. D.; Rahm, A., *J. Am. Chem. Soc.* **1993**, *115*, 4602-4611.
-

- (133) Wang, H.; Hsung, R. P.; Wulff, W. D., *Tetrahedron Lett.* **1998**, *39*, 1849-1852.
- (134) Wulff, W. D.; Bax, B. M.; Brandvold, T. A.; Chan, K. S.; Gilbert, A. M.; Hsung, R. P.; Mitchell, J.; Clardy, J., *Organometallics* **1994**, *13*, 102-126.
- (135) Boger, D. L.; Hüter, O.; Mbiya, K.; Zhang, M., *J. Am. Chem. Soc.* **1995**, *117*, 11839-11849.
- (136) Louie, J.; Grubbs, R. H., *Organometallics* **2002**, *21*, 2153-2164.
- (137) McGuire, M. A.; Hegedus, L. S., *J. Am. Chem. Soc.* **1982**, *104*, 5538-5540.
- (138) Hegedus, L. S.; McGuire, M. A.; Schultze, L. M.; Yijun, C.; Anderson, O. P., *J. Am. Chem. Soc.* **1984**, *106*, 2680-2687.
- (139) Doyle, K. O.; Gallagher, M. L.; Pryce, M. T.; Rooney, A. D., *J. Organomet. Chem.*, **2001**, *617-618*, 269-279
- (140) Fernández-Rodríguez, M. A.; García-García, P.; Aguilar, E., *Chemical Communications* **2010**, *46*, 7670-7687.
- (141) Zheng, Z.; Chen, J.; Yu, Z.; Han, X., *J. Organomet. Chem.* **2006**, *691*, 3679-3692.
- (142) Nandi, B.; Sinha, S., *Tetrahedron* **2011**, *67*, 106-113.
- (143) Licandro, E.; Maiorana, S.; Papagni, A.; Hellier, P.; Capella, L.; Persoons, A.; Houbrechts, S., *J. Organomet. Chem.* **1999**, *583*, 111-119.
- (144) Barluenga, J.; Fernández-Marí, F.; Viado, A. L.; Aguilar, E.; Olano, B., *J. Chem. Soc., Perkin Trans. 1*, **1997**, 2267-2268.
- (145) Barluenga, J.; Andina, F.; Fernández-Rodríguez, M. A.; García-García, P.; Merino, I.; Aguilar, E., *J. Org. Chem.* **2004**, *69*, 7352-7354.
- (146) Ezquerro, J.; Pedregal, C.; Merino, I.; Flórez, J.; Barluenga, J.; García-Granda, S.; Llorca, M.-A., *J. Org. Chem.* **1999**, *64*, 6554-6565.
- (147) Perdicchia, D.; Licandro, E.; Maiorana, S.; Vandoni, B.; Baldoli, C., *Org. Lett.* **2002**, *4*, 827-830.
- (148) Crause, C.; Helmar Görls, H.; Lotz, S., *Dalton Trans.* **2005**, 1649-1657.
- (149) Lotz, S.; Crause, C.; Olivier, A. J.; Liles, D. C.; Górls, H.; Landman, M.; Bezuidenhout, D. I., *Dalton Trans.* **2009**, 697-710.
- (150) Hoye, T. R.; Chen, K.; Vyvyan, J. R., *Organometallics* **1993**, *12*, 2806-2809.
- (151) Ebbing, D. D.; Gammon, S. D., *General Chemistry*; Stratton, R., Ed.; Houghton Mifflin Company: Boston, USA, **1999**
- (152) Andrada, D. M.; Granados, A. M.; Solà, M.; Fernández, I., *Organometallics* **2011**, *30*, 466-476.
- (153) Wang, C.-C.; Wang, Y.; Liu, H.-J.; Lin, K.-J.; Chou, L.-K.; Chan, K.-S., *J. Phys. Chem. A* **1997**, *101*, 8887-8901.

- (154) Reinheimer, E. W.; Kantardjieff, K. A.; Ouyang, X.; Herron, S. R.; Lu, T.; Casalnuovo, J. A., *J. Chem. Cryst.* **2007**, *37*, 507-515.
- (155) Armarego, W. L. F.; Perrin, D. D., *Purification of Laboratory Chemicals*; 4th Ed Butterworth-Heinemann: **1997**